Report Documentation Page Information

Title and Subtitle: Cold Work Embrittlement of Interstitial Free Steel

Authors: Pierre Martin and John T. Bowker

Performing Organization Names, Addresses:

Materials Technology Laboratories (MTL)
Canada Centre for Mineral and Energy Technology (CANMET)
568 Booth Street
Ottawa, Ontario K1A 0G1
Canada

Abstract:

This work addresses the issues of measurement of secondary cold work embrittlement (SCWE) of an IF steel in deep-drawn parts using laboratory tests, and its correlation with real part fracture. It aimed at evaluating the influence of the steel chemistry and processing condition, microstructure, and test conditions on SCWE as well as the effect of SCWE on fatigue properties. 6-in. cups produced with various draw ratios or trimmed at different heights were tested to determine the ductile-to-brittle-transition temperature (DBTT) as a function of strain. The 2-in. cup/expansion test, bend test and fracture of notched specimens were also used to generate information complementary to that provided by the 6-inch cup/expansion test. The relationship between laboratory tests and fracture in real parts was established by testing large-scale parts. The fatigue behavior was investigated in the as-rolled and deep drawn (high strain) conditions, using prestrained specimens taken from the wall of a formed part.

From the work presented in this report, the following conclusions were drawn:

- A good relationship was found between the cup test and the bend test. However the bend test DBTT was significantly higher than cup test DBTT.
- A linear relationship was found between DBTT and fraction of intergranular (IG) fracture in unstrained interstitial-free (IF) steel.
- In general straining increased the fraction of IG and DBTT.
- No significant effect of sheet thickness was found when testing reduced-wall thickness cups.
- Impact speed increased DBTT slightly.
- The presence of pre-machined or pre-cracks at the edge of cups did not significantly influence DBTT.
- Significant difference in DBTT was observed between the 2-inch and 6-inch bend test when comparing DBTT in trimmed cup, flanged cup and cups with different draw ratios or cup heights.
- The data generated using laboratory cup tests to predict the behavior of the large scale parts used in this study showed that the cup tests were conservative.
- The strain-life behavior of the as-rolled condition is consistent with other IF and non-IF sheet steel grades.
- The stress – strain behavior showed cyclic hardening for the as-rolled condition and cyclic softening for the deep drawn condition.
- It is not clear that SCWE has an effect on fatigue performance in deep drawn IF sheet steels.

Table 1. Steels selected for the project CWE of IF Steel

Material				TEST SPECIMENS										
				Oil Pan	Shock Tower	Suspension component	2-inch Cup Expansion		Bend test	6-inch cup exapansion				
Steel	Steel Type	Expected DBTT	Thickness (mm)	Fatigue Tests	Part Geometry effect	Part Geometry effect	Steel chemistry DR=2.0	Thickness Effect DR=2.0	CWE Steel ranking (1)	Draw ratio (3 levels)	Steel chemistry	Edge effect (3 levels)	Impact speed (2 levels)	
S1	BH, BA , Rephos., EG	L	0.79				√		√		√			
S2	Rephos IF with B, GA	ML	0.74				√		√		√			
S3	Rephos IF , GA	H	0.74				√		√	√	√	√	√	
S4a	Ti-sta. batch annealed, CR	MH	0.77				√	√	√		√			
S4b	Ti-sta. batch annealed, CR	MH	1.0				√	√						
S4c	Ti-sta. batch annealed, CR	MH	1.26				√	√						
S4d	Ti-sta. batch annealed, CR	MH	1.45				√	√	√					
S5a	Ti-sta CA, GA	L	0.98			√	√							
S5b	Ti/Nb CA, GI	L	1.14		√		√							
S6a	Ti-sta. batch annealed, EG	MH	1.03		√		√							
S6b	Ti-sta. batch annealed, CR	MH	1.75	√			√							
S7	Rephos IF, GI	H	0.93			√	√			√				

BH : bake hardenable, BA : batch anneal, CR : cold rolled, GA : hot dip galvanneal, CA : continuous anneal, GI : hot dip galvanized, EG: electrogalvanized

Table 2. Chemistry (wt %) of the steels investigated in the parametric study [1]

Steel Type	Code	Thick-ness (mm)	C	N	Ti	Nb	Mn	P
BH batch annealed ELC, with P EG	S1[2,3,4]	0.79	0.010	0.0061			0.14	0.056
Rephopshorized IF withB GA	S2[3, 6]	0.74	0.0029	0.0037	0.019	0.029	0.36	0.040
Rephophorized IF GA	S3[3]	0.74	0.0039	0.0048	0.021	0.033	0.39	0.042
Batch Annealed ULC, Ti-sta., CR	S4a[4,7]	0.77	0.0077	0.0064	0.084		0.15	
Batch Annealed ULC, Ti-sta., CR	S4b[4,7]	1.0	0.0050	0.0042	0.077		0.21	
Batch Annealed ULC, Ti-sta., CR	S4c[4,7]	1.26	0.0038	0.0023	0.068		0.17	
Batch Annealed ULC, Ti-sta., CR	S4d[4,7]	1.45	0.0036	0.0023	0.064		0.13	
Ti/Nb w/o B, GA,	S5a	0.98	0.0031	0.0027	0.071	0.0073	0.14	
Ti-sta. with B, GI	S5b[5,6]	1.14	0.0050	0.0024	0.071		0.13	
Ti- sta. BA, EG	S6a[4,5]	1.03	0.0057	0.0066	0.062		0.11	
Ti-sta. BA, CR	S6b[4]	1.75	0.0045	0.0065	0.015	0.035	0.23	
Rephos IF, GI	S7[3]	0.93	0.0026	0.0019	0.038	0.0073	0.11	0.053

Note:

1) All analyses were performed at MTL/CANMET on sheet material.

2) Steel S1 is not stabilized.

3) Steels S1, S2, S3 and S7 are rephosphorized grades.

4) Steels S1, S4a, S4b, S4c, S4d, S6a and S6b were produced by batch annealing.

5) Steels S5b and S6a used for the shock towers have a similar composition, except that continuous annealing was used for steel S5b and batch annealing for steel S6a.

6) According to the steel suppliers steels S2 and S5b contain B but it could not be analyzed because the level was lower than the detection limit.

7) Steels S4a, S4b, S4c and S4d used for the effect of thickness showed minor variations in the chemistry. Steels S4b, S4c and S4d have similar P content, however P content is extremely low in S4a.

Table 3. Mechanical Properties

Materials	Orientation	Yield Strength (MPA)	Ultimate Strength (MPa)	Elongation (%)	r-value	n-value
S1	0°	215	326	41.6	2.96	0.15
	90°	224	322	43.2	3.16	0.13
	45°	230	336	40.9	1.98	0.14
					$\in \underline{r} = 1.07$ $\bar{r} = 2.51$	
S2	0°	191	345	40.5	1.59	0.19
	90°	200	346	41.6	2.69	0.18
	45°	197	336	43.1	2.53	0.18
					$\in \underline{r} = -0.40$ $\bar{r} = 2.34$	
S3	0°	180	330	42.6	1.88	0.19
	90°	191	331	41.3	3.11	0.18
	45°	186	331	44.9	2.19	0.18
					$\in \underline{r} = 0.31$ $\bar{r} = 2.35$	
S4a	0°	128.5	283	52.8	2.4	0.23
	90°	131	286	50.3	2.93	0.23
	45°	133	292	52.8	2.38	0.23
					$\in \underline{r} = 0.79$ $\bar{r} = 2.77$	
S7	0°	241	362	39.0	NA	0.208
	90°	263	360	39.5	NA	0.202

$\in \underline{r} = r^0 + r^{90} - 2\,r^{45}$

$\bar{r} = r^0 + 2\,r^{45} + r^{90}$

ASTM Tensile specimen: 0.500 inch wide x 2.25 inch long reduced section.

Table 4. Trim height and strain
for 6-inch cups

Draw Ratio	Trim Height, (mm)	Strain at Cup Edge, %	
		minor	major
1.8	82	-40	+52
2.0	105	-45	+65
2.1	120	-49	+69
2.2	125	-50	+99
2.3	105	-49	+100
2.3	70	-36	+65

Table 5. 2-inch cup/expansion test transition temperature (° C).

Steel Type	Code	Thickness (mm)	DBTT 2-inch cups
BH, batch annealed, rephosphorised ELC, EG	S1	0.79	-70
Rephopshorised IF, with B GA	S2	0.74	-40
Rephophorised IF GA	S3	0.74	0
Batch Annealed ULC, Ti-sta., CR	S4a	0.77	-25
Batch Annealed ULC, Ti-sta., CR	S4b	1.0	-45
Batch Annealed ULC, Ti-sta., CR	S4C	1.26	-45
Batch Annealed ULC, Ti-sta., CR	S4d	1.45	-10
Ti/Nb w/o B, GA,	S5a	0.98	< -70
Ti-sta. w/ B, GI	S5b	1.14	-50
Ti- sta. BA, EG	S6a	1.03	-15
Ti-sta. BA, CR	S6b	1.75	-20
Rephos IF w/o B, GI	S7	0.93	-30

Table 6. DBTT obtained by 2-inch and 6-inch cup/expansion tests.

Cup Test	S1	S2	S3	S4a
2-inch	-70°C	-40°C	0°C	-25°C
6-inch	-55°C	-30°C	10°C	-15°C

Table 7. Comparison of DBTT obtained with notched specimen test and cup/expansion test for S3 steel

Major Strain	Notched specimens test	6-inch cup/expansion test
40%	-100°C	-----
52%	-----	-10°C
56%	-88°C	-----
65%	-72°C	+10°C

Table 8. Trim height, strain and transition temperatures for 6-inch and 2-inch cups for steel S3

Draw Ratio	Trim Height, mm	Strain at Cup Edge, %		Transition Temperature, °C
		minor	major	
(6" cup)				
1.8	82	-40	+52	-10
2.0	105	-45	+65	+10
2.1	120	-49	+69	+10
2.2	125	-50	+99	+10
2.3	105	-49	+100	-5
2.3	70	-36	+65	-40
(2" cup)				
2.0	31	-40	+55	0

Table 9. Strain gauge data

Draw Ratio	Height	Major Strain	DBTT	Position	Position
2.0	105 mm	65%	+10°C	0°	1320
				120°	1306
				240°	1355
2.3	105 mm	100%	-5°C	0°	785
				120°	1140
				240°	1150
2.3	70 mm	65%	-40°C	0°	511
				120°	686
				240°	-----

Table 10. DBTT cup/expansion results obtained in series S4 steels.

Temperature (Degree C)	**Steel S4a**	**Steel S4b**	**Steel S4c**	**Steel S4d**	
	Original wall Thickness 0.77 mm	Original wall Thickness 1.0 mm	Original wall Thickness 1.26 mm	Original wall Thickness 1.42 mm	Reduce- wall cups
-55		2P, 3F			
-50		2P, 2F	2F		
-45		7P, 1F √	7P, 1F √	2F	
-40				2F	
-35	3F	4P			
-30	3F			2F	
-25	6P, 2F √	4P			
-20				2F	
-15	4P				1F (2)
-10				4P, 2F	2P (2), 1F(1)
-5				8P √	1P (2)

(1) Wall thickness is 0.51 mm
(2) Wall thickness varies in a range 0.72 to 0.79 mm

Table 11. Effect of test speed on DBTT for steel S2

Temperature	**Test Speed**	
	4.34 m/s	**7.41 m/s**
-25°C	2F 1P	1F 4P
-30°C	1F 4P	2F 3P
-35°C	5P	2F

Table 12. Effect of flanges on DBTT (steel S3)

	DR=2.0 Cups		**DR=2.3 Cups**	
Temperature (degree C)	**Flanged Cup**	**Full Cup**	**Flanged Cup**	**Full Cup**
-10	1F	2F	2F	4P, 2F
-5	1F	4F, 1P		5P (*)
0	1F	3F, 2P	3P	4P, 1F
5	2F	3F, 5P		
10	3P-2F	5P (*)		2P
15	1P (*)			
20				2P

(*) Estimate DBTT

Table 13. Effect of edge cracks and notches on DBTT (steel S3)

Brittle precrack	+21°C Ductile +10°C Ductile
Machined notch (2mm)	0°C Ductile 0°C Brittle

Table 14. Shock tower localized test results for steel S6a

2-inch cup test DBTT = -10°C

Test Temperature (°C)	Lower Strain (50 – 60%)	Higher Strain (70 – 80%)
-20	1P	4P, 1F
-30	4P, 1F	2P, 3F
-35	1P, 2F	1F
-40	1P, 2F	1F

Table 15. Shock tower localized test results for steel S5b

2-inch cup test DBTT = -50°C

Test Temperature (°C)	Lower Strain (50 – 60%)	Higher Strain (70 – 80%)
-60	1P	1P
-65		4P, 1F
-70	1P	2F
-80	3P, 3F	
-85	1P, 3F	
-90	1F	

Table 16: Summary Results of Floor Panel Tests

	Impactor	Location	Test Temp., (°C)	Specimen height[2], (mm)	Comments
S7-1	Drop weight	2[1]	-33	100	No fracture
S7-2	Drop weight	3[1]	-45	100	Small (3 mm) ductile tear outside the high strain region
S7-3	Drop weight	Critical region	-65	[3]	No fracture, modified positioning for location 3
S7-4	Sledge hammer	Critical region	-70	n.a.	No fracture
S7-5	Drop weight	1[1]	-50	50	No fracture
S7-6	Hemispherical Punch	Critical region	-73	n.a.	No fracture
S7-7	Conical Punch	Critical region	-88	n.a.	Ductile fracture resulting from punched hole
S7-8	Drop weight	4[1]	-75	125	Specimen supported on 75 mm dia. Rollers, No fracture

(1) see Figure 9

(2) specimens were supported on the base plate. These values are height of the impact location from the base plate.

(3) was placed at an oblique angle accurate height is not available

Table 17. Average grain size of some of the steels investigated.

Steel	Average grain size (μm)
S1	12.75
S2	4.0
S3	3.5
S4	17
S4b	14
S4c	15
S4d	NA
S6b	5

Table 18. Fracture analysis of notched specimens

Sample	DBTT 2.0 DR Cup/expansion Strain: -45%, +65%	Percentage of Intergranular Fracture		
		Prestrained Material Strain: -45%, +65%		Unstrained Material
		LN Orientation	TN Orientation	
S1 Steel	-55°C	12%	2% visual	4%
S2 Steel	-30°C	67%	20% visual	20%
S4a Steel	-15°C	72%	44%	63%
S3 Steel	+10°C	80%	78%	82%

Table 19. Auger analysis of grain boundaries (atomic %)

Sample	Grain	P	Fe3	P/Fe3	C	O	time
S3-spc01	Spot2	2.2	88.3	2.4	0	7.8	40
	Spot3	2.3	86.9	2.6	0	10.9	45
S3-spc02	Spot1	7.1	85	7.7	5.1	2.9	18 min
	Spot1b	7.8	79.6	8.9	6.5	3.7	55 min
	Spot1c	4.2	73.9	5.4	12.2	7.2	75 min
	Spot2	2.7	90.5	2.9	3.2	3.5	25min.
	Spot3	3.9	87.1	4.3	4.5	4.5	33min.
	Spot4	1.3	82.8	1.5	9.4	4.9	46 min
	Spot5	4.6	73.5	5.9	12.2	9.7	58 min.
	Spot6	1.1	84.7	1.3	5.9	8.3	70 min

APPENDIX A

EFFECT OF COLD WORK EMBRITTLEMENT ON THE FATIGUE PROPERTIES OF DEEP DRAWN IF STEELS

CONTENTS

EFFECT OF COLD WORK EMBRITTLEMENT ON THE FATIGUE PROPERTIES OF DEEP DRAWN IF STEELS

by

J.E.M. Braid* and O. Dremailova*[1]

SUMMARY

The fatigue behaviour of an IF steel sensitive to secondary cold work embrittlement (SCWE) was investigated in the as-rolled and deep drawn (high strain) conditions. The strain-life behaviour of the as-rolled condition is consistent with other IF and non-IF sheet steel grades and exhibited a mixed intergranular/transgranular cracking mode at strain amplitudes of 0.3% and lower.

The major strain of the deep drawn condition was estimated from the measurement of elongated grains at 89%. Specimens with the major strain transverse to the loading direction showed a significant reduction in fatigue life compared to the as-rolled condition by a factor ranging from 2 at 0.1% strain amplitude to 4 at 0.3% strain amplitude. Specimens in the longitudinal orientation tested at 0.2% strain amplitude had the same fatigue life as those in the as-rolled condition while those tested at 0.1% strain amplitude had significantly longer lives (run-out).

The stress – strain behaviour showed cyclic hardening for the as-rolled condition and cyclic softening for the deep drawn condition. However, the cyclic stress-strain behaviour of the deep drawn material is significantly above that of the as-rolled material. This is attributed to the differences in high starting prestrain levels and grain elongation in the deep drawn condition. The significant decrease in fatigue life for the deep drawn-transverse condition is thought to be an effect of the orientation of the highly elongated grains. The elongated grain boundaries and their associated surface features are transverse to the loading direction thus increasing the number of favourable initiation sites. Cyclic stress-strain results from other researchers show minor orientation effects at low prestrain levels while at high prestrain levels, the current data suggests that there are no orientation effects due to cyclic stress-strain behaviour.

It is not clear that SCWE has an effect on fatigue performance in deep drawn IF sheet steels. The results for the as-rolled condition support earlier work in that mode of cracking, and not fatigue life, is affected. In the deep drawn condition an orientation effect was observed related the highly elongated grain structure developed during the deep drawing process. Further tests are required in the deep drawn condition in non-SCWE sensitive IF and non-IF steel grades before a definitive statement can be made.

---

* The authors are with Materials Technology Laboratory, Canada Centre for Mineral and Energy Technology (MTL/CANMET), 568 Booth Street, Ottawa, Ontario K1A 0G1, Canada.

INTRODUCTION

There is currently limited information on the relationship between SCWE and fatigue of IF sheet steels. Yan [1] investigated the fatigue life and crack growth rates in the as-rolled condition of a series of four IF sheet steels and a non-IF sheet steel. There was no difference in total life for the steels tested although the IF steel with a high ductile-brittle transition temperature showed both intergranular and transgranular fatigue crack growth modes.

In general, the total fatigue life of steels is relatively insensitive to microstructure for a given strength level. In structural steels it is known that crack propagation rates are similar irrespective of yield strength [2]. However, values of the threshold stress intensity factor, $?K_{th}$, and near threshold growth rates can vary between steels of different strengths and microstructures. Previous work in HY80 structural steel demonstrated variations in near threshold growth rates with variations in grain size [3]. Changes in growth rates were shown to occur when the crack tip plastic zone size reached that of the grain size.

Miller [4] has discussed the two thresholds of fatigue behaviour: the first is related to microstructural texture and the second is mechanically based and is characterized by linear elastic fracture mechanics (LEFM). The LEFM behaviour is strongly dependent on both crack length and stress level, and microstructure plays an insignificant role. However, at initiation, cracks are of the order of the grain size and microstructure plays a dominant role.

In deep drawn components, the sheet material undergoes significant amounts of deformation. Grains that were previously equiaxed become highly elongated giving the component a significant grain texture. The effect of texture on fatigue performance has been studied for a variety of materials including titanium and nickel based alloys. However, there is very little relevant work in sheet steels. Recently, Yan et al. [5] have investigated the effect of forming strain on fatigue life of an IF sheet steel. Prestrain was shown to increase yield strength and fatigue resistance increased in the long life region and decreased in the short life region with increasing yield strength. For non-balanced biaxial prestrains the transverse orientation exhibited higher yield strength than the longitudinal orientation and a slightly higher improvement in fatigue strength in the long life region. However, this study was limited to low prestrain levels, 12% maximum, compared to those present in a deep drawn component, 70 to 100+ %. The grains structure in [5] would still be equiaxed and the observed effect would be attributed solely to dislocation structures that would be significantly lower in magnitude that a deep drawn component.

EXPERIMENTAL

The main thrust of here project was to establish if there is an effect of SCWE on the fatigue performance of IF steels. One IF steel with a demonstrated susceptibility to SCWE, was selected. The basic approach was to carry out fatigue tests on both as-rolled and deep drawn (high forming strain) conditions. In the deep drawn condition, two orientations were investigated, transverse and parallel to the major strain direction. Detailed metallography and fractography was carried out to relate crack formation and appearance with microstructure/forming strain.

The original proposal for this phase was to test strip type samples in tension – tension at an R ratio of approximately 0.1. This approach was chosen to avoid specimen/machine alignment problems, especially for specimens removed from deep drawn components where flatness/straightness was an issue. However, the AISI sponsor group preferred that the fatigue tests be carried out using the Auto/Steel Partnership procedure. This involved testing under strain control with an R ratio of -1. To prevent buckling of the specimen during the compressive part of the load cycle, a significant effort was required to improve the alignment of the servo-hydraulic test system used. This involved the installation of an load train alignment fixture, upgrades to the specimen gripping system, the manufacturing of specimen installation and alignment fixtures, and a significant amount of time aligning the system which included the use of both a strain gauged specimen and an optical stereoscope. Additionally, it was necessary to develop a technique to produce straight samples from deep drawn components without introducing further deformation within the gauge length. This effort was beyond the original proposal plan and resulted in significant delays. To keep the project close to budget and avoid prolonged delays a change in the test plan was made. Fewer tests were carried out in the high strain condition; however, sufficient tests were completed to address the principal thrust of the project - to establish if there is an effect of SCWE on the fatigue performance of IF steels.

MATERIAL

As indicated in the main report, the steel used for this fatigue stdy was steel S6b. The selection of this steel was based on its demonstrated SCWE sensitivity – the appearance of brittle cracking during secondary forming operations in the production of a large diesel engine oil pan. A number of unformed blanks and a set of five (5) oil pans were obtained for this study. The base composition of this low P steel is shown in Table A-1, and Fig. A-1 shows a photograph of one of the oil pans.

An examination of Fig. A-2 shows the cracking of the flange created during secondary forming operations. Using the 2-in. diameter cup/expansion test, the ductile to brittle transition temperature for this steel S6b was determined to be –20°C (as shown in the main report). Although this result is not as high as that for a highly sensitive rephosphorised IF galvannealed grade (0°C), it is still well above other grades that do not exhibit SCWE (DBTT $\leq$ -45°C).

A measurement of the distribution of forming strains in the oil pans was not available. Hence, as part of the metallographic examination (below) the aspect ratio of the deformed grains was established to give an estimate of the major strain in the area from which the fatigue specimens were removed.

METALLOGRAPHIC EXAMINATION

Two samples of steel S6b were used for grain size measurements, one as-received in the unstrained condition with a thickness of 1.76 mm and the other in the prestrained condition taken from the oil pan with a thickness of 1.70 mm. Both samples were ultrasonically cleaned using acetone and chemically polished to reveal the grain structure. Scanning electron microscopy (SEM) with an accelerating voltage of 20 kV was used in the back-scattered-electron (BSE) imaging mode. This produced contrast as a result of grain orientation and was used for grain size and grain aspect ratio measurement.

Ten images were taken from an unstrained sample at an appropriately determined magnification and a standard circle intercept method was used for quantitative grain size measurements. Because of the difficulty in revealing the grain structure in the deformed material it was necessary to take a total of six images from the oil pan sample. This revealed approximately fifteen grains from which accurate measurements of grain size could be made and aspect ratio determined.

FRACTOGRAPHIC EXAMINATION

As-rolled or as-drawn and fracture surfaces of selected test specimens were examined after fatigue testing using a scanning electron microscope with an accelerating voltage of 20 kV. The fracture surfaces were examined to determine the fatigue crack initiation point as well as the fracture mode. The as-rolled or as-drawn surfaces were examined to investigate the relationship between surface features and fatigue cracking.

MONOTONIC TENSION PROPERTIES

Tension tests were carried out for the as-rolled sheet and deep drawn condition in two orientations (transverse and parallel to the major drawing strain direction). Tension tests were conducted according to ASTM E8 on flat, full-sheet thickness specimens. The strain hardening exponent and strength coefficient, n and k, were determined according to ASTM E646.

FATIGUE TESTING

Test Procedure

The test procedure used was based on that of the Auto/Steel Partnership (A/S-P) sheet steel fatigue program [6]. The test method conformed to ASTM E606-92 [7] with specimen design, strain rate, and test termination based on that used by Reemsnyder [8] for A/S-P testing at Bethlehem Steel.

The strain-controlled fatigue tests were conducted using a triangular waveform at a constant strain rate of 0.008/s in a computer controlled, closed-loop servohydraulic test system.

Fatigue tests that resulted in cracking were terminated at 40% drop in maximum load. Thus, the tests were terminated before complete fracture with cracks on the order of 0.5 to 1.5 mm long. Run-outs were defined when a specimen did not fail after five million cycles (10 million reversals).

The computer control system records relevant test data, including cyclic stress-strain hysteresis loops at the beginning of a test and at logarithmic intervals during the test. An idealized hysteresis loop is shown in Fig. A-5. In addition to the total strain range (controlled parameter), the test system measures the plastic component from which the elastic component can be estimated:

$$\Delta\varepsilon_e = \Delta\varepsilon - \Delta\varepsilon_p \qquad \text{Eq 1}$$

The cyclic stress-strain results measured at half-life were used to compute cyclic true stress – true strain curves using:

$$\frac{\Delta\varepsilon}{2} = \varepsilon_a = \frac{\Delta\sigma}{2E} + \left(\frac{\Delta\sigma}{2k'}\right)^{1/n'} \qquad \Delta\sigma \equiv \sigma_a \qquad \text{Eq 2}$$

These were compared to the monotonic true-stress – true strain curves. In addition, the cyclic strength and strain hardening exponents were determined from a regression analysis of the true stress – true plastic strain data. The 0.2% offset cyclic yield strength, S'_y, is computed from:

$$S'_y = k'(0.002)^{n'} \qquad \text{Eq 3}$$

TEST SPECIMENS

Highly strained, deep drawn sheet material exhibits significant grain elongation. Hence, texture, grain orientation, and associated surface effects were considered to be potential factors affecting the fatigue behaviour. The test specimen was thus designed to have as large of an original surface area as possible while having an acceptable resistance to buckling. The test specimen design is shown in Fig. A-6 and closely resembles Reemsnyder's design (Bethlehem) with a slightly longer gauge length of 6.35 mm (0.25 in.) compared to 5.08 mm (0.2 in.). It was recognized that this would increase the unsupported length of the specimen and hence decrease its resistance to inelastic buckling.

For intermediate length columns with stresses above yield the stiffness of the material is no longer represented by the elastic modulus, E, but is given, instantaneously, by the tangent to the stress-strain curve, ds/de, known as the tangent modulus, E_T. The MTL/CANMET, Bethlehem, and A/S-P specimens are all gripped through wedges. Hence, the tangent modulus form of the generalized buckling formula gives the critical buckling stress for the inelastic behaviour for the fixed end condition as

$$\sigma_{cr} = \frac{\pi^2 E_T}{0.25\left(\frac{L}{R}\right)^2} \qquad \text{Eq 4}$$

where L is the unsupported length, r is the radius of gyration (for the specimen cross section a function of I, the second moment of inertia, and A, the cross sectional area) and L/r is the slenderness ratio.

Assuming that the specimens are supported up to where the shoulder radius starts in the grip ends and ignoring the increase in A and I for radius at the ends, the slenderness ratio, L/r, can be calculated and is given in Table A-2. The results show that the small increase in gauge length did not have a significant impact on L/r, and hence buckling resistance, compared to the Bethlehem specimen while providing 25% more surface area over the gauge length. Overall, the MTL design provides improved buckling resistance, a larger width and exposed surface area compared to the A/S-P specimen.

The test specimens for the high strain condition were removed from three areas at the deepest end of the oil pan next to the flange where cracking was observed as shown in Fig. A-7. The specimens were located in these areas such that the unsupported length (distance between shoulders) was in a relatively flat region. The material was carefully clamped in this region and the material in the grip ends was straightened. The deformation from the straightening procedure was sufficiently far away from the gauge length as not to affect the fatigue behaviour during testing. Two orientations were examined: the transverse condition with the specimen length at right angles to the drawing direction and the longitudinal condition with the specimen length parallel to the drawing direction.

EXPERIMENTAL RESULTS

METALLOGRAPHIC ANALYSIS

Chemical polished samples of the as-received material revealed an equiaxed grain structure with an average grain size of 11.5 μm. A typical microstructure of this material is shown in Fig. A-3. Figure A-4 shows the microstructure of highly elongated grains of sample S6b-1b from a fatigue specimen removed from one of the oil pans from a location just above the flange. An attempt was made to measure the width and length of the deformed grains. However, as seen in Fig. A-4, there was a high degree of uncertainty in the measurement of grain length for those grains whose width could be established. Using the average measured width of the deformed grains of 6.59 μm, the average unstrained grain size of 11.5 μm, and the measured thickness reduction the engineering strains in the region of the fatigue specimens was estimated as:

Major strain	$e_1 = 89\%$
Minor strain	$e_2 = -43\%$
Thickness strain (measured)	$e_3 = -7.96\%$

These values are consistent with those measured by Bhat et al. [9] of 100% major and -48% minor strains for an oil pan at a location near the deepest corner close to the flange.

TENSILE PROPERTIES

The monotonic stress strain curves for the as-rolled condition and in the longitudinal and transverse orientation for the high strain condition are shown in Fig. A-8. The yield, tensile, elongation, and strain-hardening exponent are summarized in Table A-3. In the high strain condition there is no real difference between the transverse and longitudinal directions. However, as expected, there is a substantial increase in yield and tensile strength, and decrease in elongation, from the as-received sheet.

FATIGUE TEST RESULTS

The fatigue test results for the as-received material (designated AR) and those for the high strain condition (transverse to major strain – B, parallel to major strain – C) are shown in Fig. A-9. The limited number of test results indicates that at strain amplitudes above 0.1% the fatigue life of high strain samples with orientation transverse to the major drawing strain is significantly less than the as-received condition, 66% less at 0.2% strain amplitude. However, the limited data for the orientation parallel to the major strain indicates there is no difference in life at strain amplitudes above 0.1% while there appears to be a significant increase in life at and below this strain level when compared to the as received and high-strain transverse orientation conditions.

Figure A-10 shows the results for the measured true plastic strain amplitude as a function of true stress amplitude at half-life. The specimens for the as-received condition show a significant decrease in stress amplitude for a given plastic strain amplitude. Given the limited data for the high strain condition, there appears to be no significant difference in plastic strain behaviour as a result of specimen orientation in the high strain condition. Applying linear regression analysis to this data for the as-received and deep drawn conditions the cyclic strength coefficient, k', and strain hardening exponent, n', were determined. Table A-4 summarizes the results including the cyclic yield strength calculated from Eq 3. The cyclic true stress – true strain curves determined from Eq 2 (E = 207 000 MPa) are shown in Fig. A-11 together with the actual test results at half-life. The results show a significant increase in stress amplitude for the deep drawn condition when compared to the as-received condition.

FRACTOGRAPHIC EXAMINATION

Fatigue cracking for all specimens was found to initiate at or near (corner) the as-rolled or as-drawn surface for all specimens. Initiation and propagation in as-rolled material at applied strains of 0.3% and below, shown in Figs. A-12 to A-14 was by an intergranular, mixed intergranular/transgranular mode consistent with that observed by Yan [1]. Fatigue striations were observed along intergranular facets with secondary cracking along grain boundaries (Fig. A-12). Figure A-15 is an example of a final fracture, achieved by cooling a sample in liquid nitrogen followed by impact loading, showing a mixed intergranular/transgranular cleavage mode. Figure A-16 shows the fatigue fracture surface of a specimen tested at 0.4% strain amplitude. Transgranular fatigue striations are evident. The presence of secondary cracking may hint at intergranular failure; however, there is insufficient evidence to support this. This observation is also consistent with those by Yan [1] who did not observe an intergranular mode at applied strain amplitudes of 0.4% and higher.

An intergranular, mixed intergranular/transgranular failure mode was also observed for those specimens tested in the deep drawn condition. Specimens with orientation transverse to the major strain (B), shown in Figs. A-17 to A-19, showed similar features to that of the as-rolled condition, fatigue striations observed along intergranular facets with secondary cracking along grain boundaries. However, unlike the as-rolled condition, fracture surface features highlight the highly elongated nature of the grains for this orientation (Fig. A-19).

Deep drawn condition specimens with orientation longitudinal to the major strain (C), Fig. A-20, show fatigue fracture surfaces similar to the as-rolled condition. The grain boundary facets have an equiaxed appearance consistent with observing the elongated grains "end-on". The highly elongated nature of the grains is evident from the fracture surfaces only from the final fast fracture features that include the presence of splitting as shown in Fig. A-21. Splitting has been observed in transverse fractures in high toughness structural and linepipe steels that have elongated grain structures among other features.

Examination of the specimen surfaces consisting of the as-rolled or as-drawn condition reveals a number of interesting features. Figure A-22 shows the surfaces for representative samples in the as-rolled condition. Qualitatively, it was observed that the number of surface cracks and their lengths increased with increasing strain amplitude. This was also the case for the deep drawn condition with orientation transverse to the major strain, Fig. A-23. However, the surface roughness was higher for the deep drawn condition as a result of both drawing marks and the highly elongated nature of the grains. Cracks tended to follow the resulting surface depressions along the elongated grain boundaries resulting in somewhat longer "straight" sections when compared to the as-rolled or deep drawn - longitudinal orientation conditions.

DISCUSSION

A comparison of fatigue strain – life results for the as-rolled condition with those by Yan [1], Fig. A-24, indicate that the fatigue behaviour of steel S6ba is consistent with other IF and non IF sheet steels. Also, as noted in the previous section, fatigue cracking at applied strain amplitudes of 0.3% and lower occurred by a mixed intergranular/transgranular mode. This too, is consistent with previous observed behaviour that suggests that the appearance of this mode of cracking, and hence SCWE, does not adversely affect fatigue life.

Results for the highly strained, deep-drawn condition, shown in Fig. A-9, suggest that when loading is applied transverse to the drawing direction (direction of major strain), the fatigue life is reduced considerably by factors of about 4 at 0.3% strain amplitude to 2 at 0.1% strain amplitude. However, this is not the case for the longitudinal orientation were limited results indicate no change in fatigue life at 0.2% strain amplitudes while there is a significant improvement at 0.1% (run-out).

Recently, Yan et al. [5] have studied the effect of forming strains on the fatigue behaviour of an interstitial-free (IF) grade steel. In the long-life region they found that prestrain improves fatigue resistance while in the short-life region fatigue resistance is reduced. This is consistent with previous work by Morrow, Manson, and others (see Hertzberg [10]) where decreases in the cyclic strain hardening exponent, n', resulting from forming strains are associated with increases in fatigue life at low strain amplitudes and decreases in fatigue life at high strain amplitudes. Yan et al. [5] also noted an effect of specimen orientation for non-balanced biaxial prestrains where the direction perpendicular to the major strain exhibits a higher monotonic yield strength and slightly better fatigue resistance in the long life region than for the direction parallel to the major strain. The results of this study are somewhat different from those of Yan et al. [5] and indicate that, at very high prestrain levels, there is a significant effect of orientation on fatigue life.

The cyclic strain – life relationship is expressed as the sum of elastic and plastic components:

$$\frac{\Delta\varepsilon}{2} = \varepsilon_a = \frac{\sigma'_f}{E}(2N_f)^b + \varepsilon'_f(2N_f)^c \qquad \text{Eq 5}$$

where s'_f, e'_f, b and c are the fatigue strength coefficient, fatigue ductility coefficient, fatigue strength exponent and fatigue ductility exponent respectively, as defined in ASTM E606 [7]. The plastic components of strain are measured during testing, and the elastic components are derived by subtracting the measured plastic component from the total strain. The parameters for Eq 5 are then determined using a least squares regression analysis. The results for this study are presented in Table A-5 for the as-rolled and deep-drawn – transverse orientation conditions. These are compared with those provided by Yan et al. [5] for as-rolled and 12% equal biaxial prestrained conditions by substituting into Eq 5 and plotting the results in Fig. A-25. Although the trend for the deep-drawn condition in the transverse orientation is similar to that in [5] for the 12% prestrain, the decrease in fatigue life over the range studied is more significant and it is unclear, due to a lack of data, if the fatigue life improves at longer lives.

The cyclic and monotonic stress strain behaviours from Figs. A-8 and A-11 are compared in Fig. A-26. Cyclic softening for the high-prestrained material and cyclic hardening for the as-rolled condition are evident. However, the cyclic stress-strain behaviour of the high-prestrained material is significantly above that of the as-rolled material. The difference is significantly larger than that apparent in Yan et al. [5] where the maximum applied prestrains investigated were 12% compared to the estimated 89% in this study. The amount of cyclic softening and hardening is affected by dislocation mobility and substructure. It is thought that the amount of prestrain investigated in [5] was sufficient to increase yield strength to similar levels as this study but did not produce as high a level of dislocations and dislocation tangles. It is thought that this resulted in similar cyclically stabilized conditions in [5] for prestrained and as-rolled material. The high prestrain levels in the present study would have produced highly dense dislocation structures that would result in different cyclically stabilized conditions.

The analysis of the results in Figs. A-10 and A-11 indicated that there is no real difference in cyclic stress strain behaviour between the transverse and longitudinal orientations for the deep drawn condition. This is also observed for the monotonic tensile results in Fig. A-8. These would tend to indicate that, at very high prestrain levels, one would not expect to observe an effect of orientation.

In the previous section, post-test fractography showed that fatigue cracking initiated at the surface at grain boundaries and showed intergranular failure, a feature consistent with previous work by other researchers. The deep-drawn condition was shown to produce significant grain elongation. Such grain elongation was not reported by Yan et al. [5], nor is it expected at the prestrain levels that they investigated. The orientation transverse to the major strain resulted in the alignment of relatively long lengths of continuous grain boundaries perpendicular to the applied loading and, hence, significantly more initiation sites than in the longitudinal orientation. This resulted in the observation of cracks with somewhat longer "straight" sections that followed the elongated grain boundaries. The formation of these elongated grains would have involved grain rotations and other movement, which, at the surface, would have resulted in the observed local depressions at the grain boundaries [see, for example, Fig. A-23(b)], and hence microstructrurally localized stress concentrations. This, combined with drawing

marks, which would normally have the same orientation, would provide an increased number of favourable initiation sites. The longitudinal orientation, on the other hand, would have produced favourably oriented grain boundaries that were approximately 43% smaller than the as-rolled condition.

It is not clear that secondary cold work embrittlement (SCWE) has an effect on fatigue performance in deep drawn IF sheet steels. The results for the as-rolled condition support earlier work in that fatigue life is not affected but the mode of cracking is affected. In the deep-drawn condition, the results of this study suggest that the effect on cracking mode, a mixed intergranular/transgranular behaviour, persists. The results also suggest that there is no effect on cyclic stress strain behaviour. However, an orientation effect was observed as a result of the highly elongated grain structure developed during the deep drawing process. Further tests are required in the deep-drawn condition in non-SCWE sensitive IF and non-IF steel grades.

CONCLUSIONS

The fatigue behaviour of an IF steel sensitive to secondary cold work embrittlement (SCWE) was investigated in the as-rolled and high strain, deep drawn conditions. Based on the work presented in this report, the following conclusions are drawn.

1. The fatigue strain – life behaviour of the as-rolled condition is consistent with other IF and non-IF sheet steels.

2. Fatigue cracking initiated at the as-rolled or deep drawn surface.

3. Fatigue cracking at strain amplitudes of 0.3% and lower was by a mixed intergranular/transgranular mode consistent with previous work by other researchers for IF steels.

4. The major strain of the deep drawn condition specimens was estimated to be 89% compared to 12% and 30% by other researchers. This resulted in highly elongated grains oriented in the drawing direction.

5. Over the strain amplitude range studied, the fatigue strain – life behaviour of the deep drawn condition showed a significant orientation effect. The life for the transverse orientation was lower than the as-rolled condition by a factor ranging from 2 at 0.1% strain amplitude to 4 at 0.3% strain amplitude. The life for the longitudinal orientation was the same as the as-rolled condition at 0.2% strain amplitude and significantly increased (run-out) at 0.1% strain amplitude.

6. The stress – strain behaviour showed cyclic hardening for the as-rolled condition and cyclic softening for the deep drawn condition. However, the cyclic stress-strain behaviour of the deep drawn material is significantly above that of the as-rolled material. This is attributed to the differences in high starting prestrain levels and grain elongation in the deep-drawn condition compared to the as-rolled condition that would result in different cyclically stabilized conditions.

7. The observed results indicate that there is no real difference in the monotonic or cyclic stress – strain behaviour for the transverse and longitudinal orientations for the deep-drawn condition.

8. The significant decrease in fatigue life for the deep drawn condition in the transverse orientation is thought to be an effect of the orientation of the highly elongated grains. This orients the elongated grain boundaries and their associated surface features transverse to the loading direction thus increasing the number of favourable initiation sites. Cyclic stress-strain results show minor orientation effects at low prestrain levels [6] while at high prestrain levels, the current data suggests that there are no orientation effects due to cyclic stress-strain behaviour.

9. It is not clear that SCWE has an effect on fatigue performance in deep drawn IF sheet steels. The results for the as-rolled condition support earlier work in that fatigue life is not affected but the mode of cracking is affected. In the deep drawn condition, the results of this study suggest that the effect on cracking mode persists but there is no effect on cyclic stress strain behaviour. However, an orientation effect was observed related the highly elongated grain structure developed during the deep drawing process. Further tests are required in the deep drawn condition in non-SCWE sensitive IF and non-IF steel grades before a definitive statement can be made.

REFERENCES

1. Yan, B., "Intergranular fracture of interstitial free steels under cyclic loading and its effect on fatigue life", Proc. 37th Metal Working and Steel Processing Conf., ISS, Vol. 33, pp 101-114, 1996.

2. Braid, J.E.M., "Fatigue of welded, high strength steels for rail car application – Phase 1: Literature Review", Prepared for AISI Railcar Market Task Group, Materials Technology Laboratory, Report MTL 96-01(CF), Ottawa, February 1996.

3. Braid, J.E.M., "Fatigue crack propagation in residual stress fields". Ph.D. thesis, University of Cambridge, August 1982.

4. Miller, K.J., "The two thresholds of fatigue behaviour", Fatigue Fract. Eng. Mater. Struct., Vol. 16, No. 9, pp. 931-939, 1993.

5. Yan, B., Belanger, P. and Citrin, K., "Effect of forming strain on fatigue performance of a mild automotive steel", New Sheet Steel Products and Sheet Metal Stamping, SP-1614, Society of Automotive Engineers, Warrendale, PA, pp 61-70, March 2001.

6. "Testing procedures for strain controlled fatigue test – Supplementary instructions for A/S P Fatigue program", Auto/Steel Partnership Fatigue Program, June 25, 1997.

7. ASTM Standard E606-92, "Standard practice for strain-controlled fatigue testing", American Society for Testing and Materials, West Conshohocken, PA, 1998.

8. Reemsnyder, H.G., "Strain controlled fatigue tests of Auto/Steel Partnership IF sheet grade 701-2", Bethlehem Steel Report BSC 701-2, AIZ-73-96020, 1999.

9. Bhat, S.P., Yan, B., Chintamani, J.S. and Bloom, T.A., "Secondary work embrittlement (SWE) of stabilized steels: Test methods and applications", Proc. Symposium on high strength sheet steels for the automotive industry, Ed. R. Pradham,

10. Hertzberg, R.W., "Deformation and Fracture Mechanics of Engineering Materials", John Wiley & Sons, New York, 1976.

C	Ti	Nb	Mn	P
0.0045	0.015	0.035	0.11	0.012

Table A-1. Chemical composition of Steel S6b.

Table A-2. Comparison of slenderness ratios of MTL/CANMET, Bethlehem, and A/S-P specimen designs for 1.7 mm thick material.

	L, mm	Width, mm	Surface area*, mm^2	A, mm^2	I, mm^4	$r = \sqrt{\frac{I}{A}}$, mm	L/r
MTL/CANMET	16	3.18	20.1930	5.4060	1.3019	0.4907	32.6033
Bethlehem	15	3.18	16.1544	5.4060	1.3019	0.4907	30.5686
A/S-P	21	2.03	15.4838	3.4544	0.8319	0.4907	42.7918

* Area of original sheet surface within specimen gauge length, one side only.

Table A-3. Monotonic tensile properties.

	Yield strength, MPa	Tensile strength, MPa	Elongation, %	Strain-hardening exponent, n
As-received	140.1	311.7	64.48	0.28
	141.2	311.6	63.54	0.28
High-strain longitudinal	461.3	520.1	32.16	0.06
High-strain transverse	456.7	515.7	34.47	0.08
	470.8	509.6	31.88	0.06

Table A-4. Cyclic stress – strain properties.

	Cyclic strength coefficient, k'	Cyclic strain hardening exponent, n'	0.2% Cyclic yield strength, S'_y, MPa
As-received	1567.978	0.318888	216
Deep drawn	940.1778	0.14874	373

Table A-5. Fatigue life relationship parameters for as-received and deep-drawn conditions.

	As received (AR)	Deep-drawn (transverse to major strain – B)
Fatigue strength coefficient, S'_f(MPa)	938.51	1070.29
Fatigue ductility coefficient, e'_f	0.2227	8.0240
Fatigue strength exponent, b	-0.15245	-0.12981
Fatigue ductility exponent, c	-0.47392	-0.98765

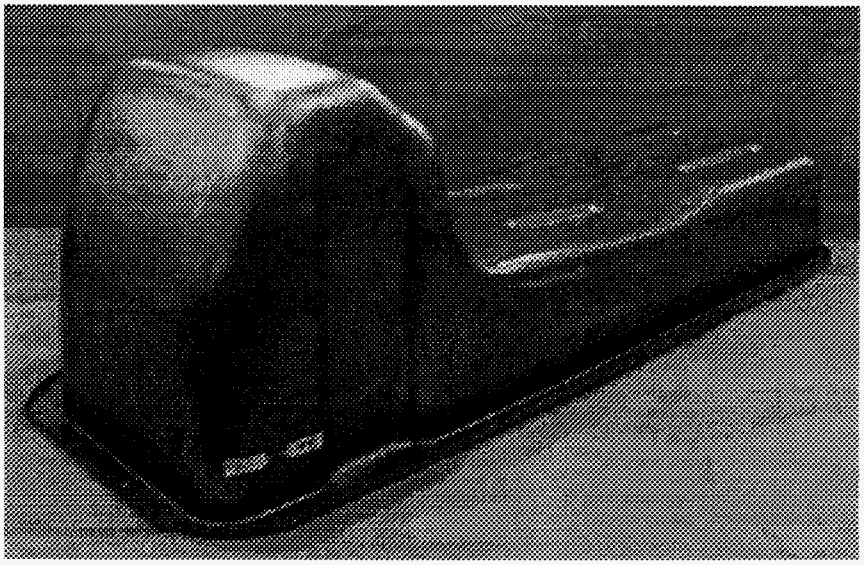

Fig. A-1. General view of oil pan in steel S6b showing general location of fatigue specimens.

Fig. A-2. View of oil pan showing cracking of flange created during secondary forming operations.

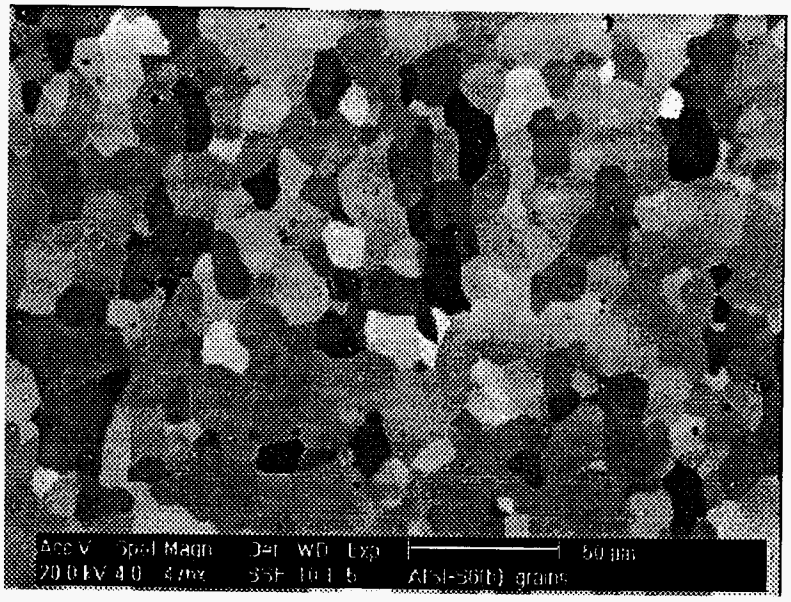

Fig. A-3. Grain structure of as-received steel S6b revealed using SEM back scattered electron imaging.

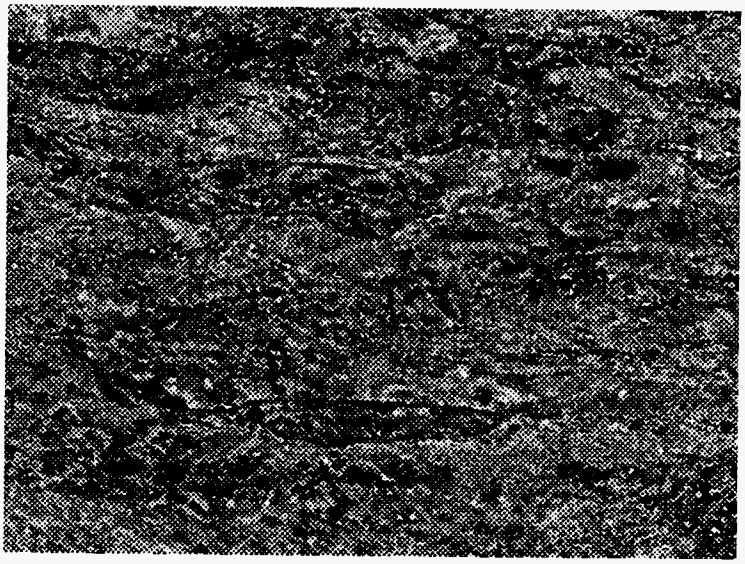

Fig. A-4. Grain structure of steel S6b in the deep-drawn condition revealed using SEM back-scattered electron imaging.

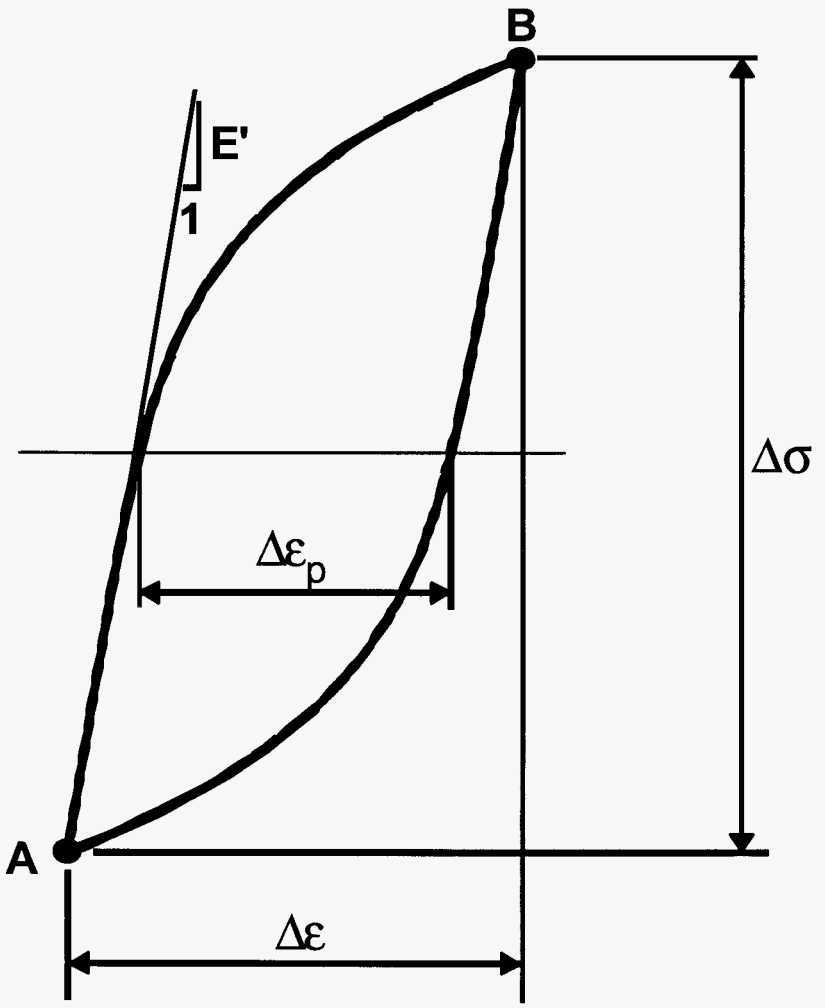

Fig. A-5. Idealized cyclic stress-strain hysteresis loop showing elastic and plastic strain components.

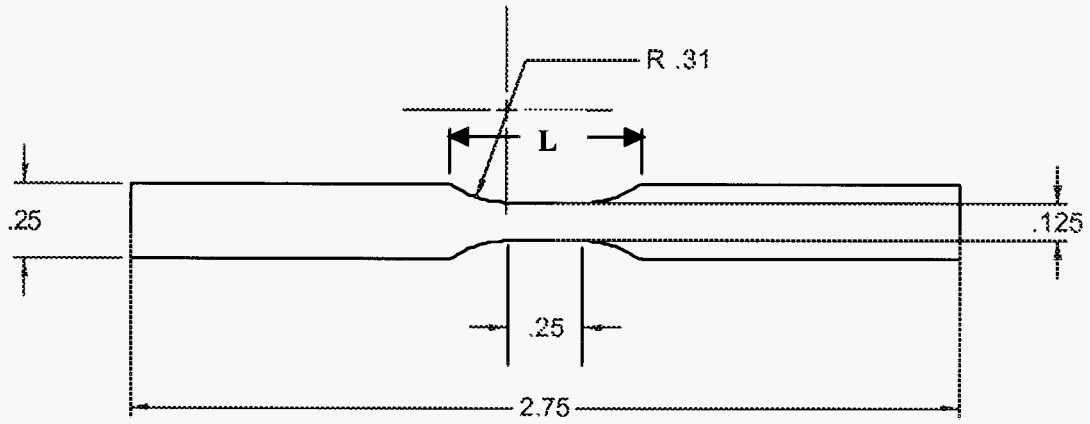

MTL/CANMET

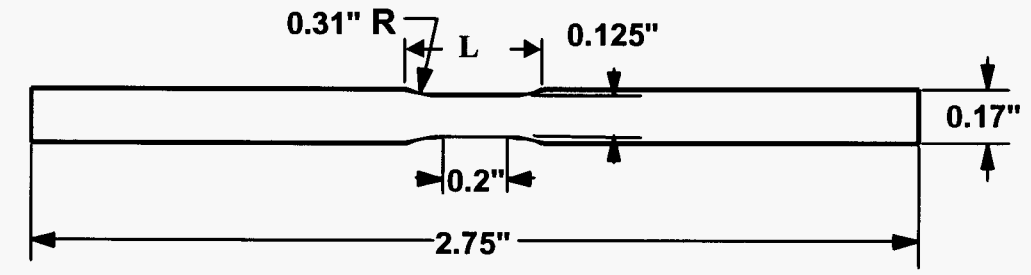

Bethlehem

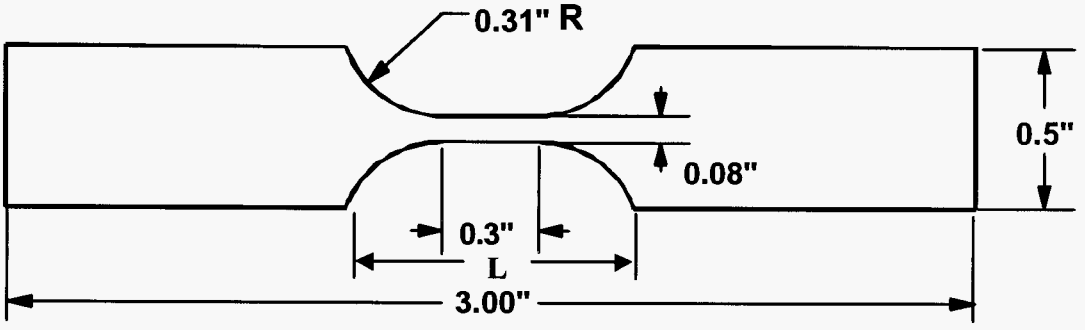

A/S-P

Fig. A-6. Design of fatigue test specimen used in this program (MTL/CANMET) compared to Reemsnyder's specimen (Bethlehem) and the specimen used in the Auto/Steel Partnership fatigue program (A/S-P). The dimension L is the unsupported length.

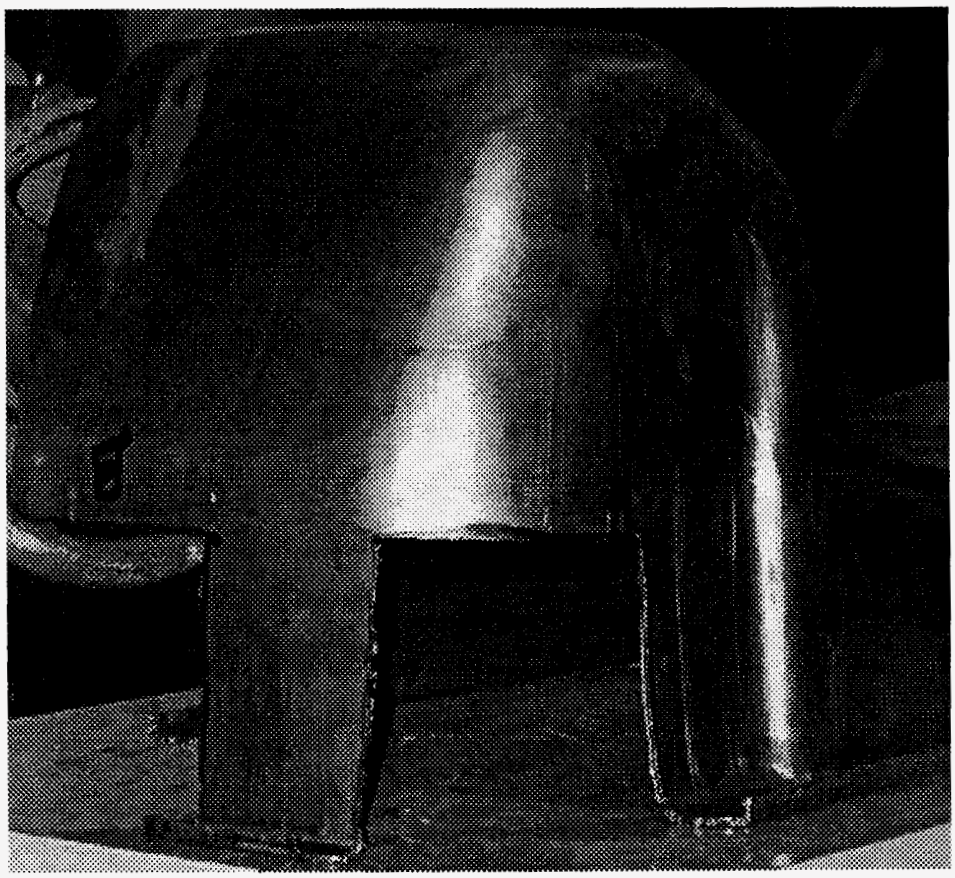

Fig. A-7. Photograph of oil pan showing sections removed for high strain fatigue specimens.

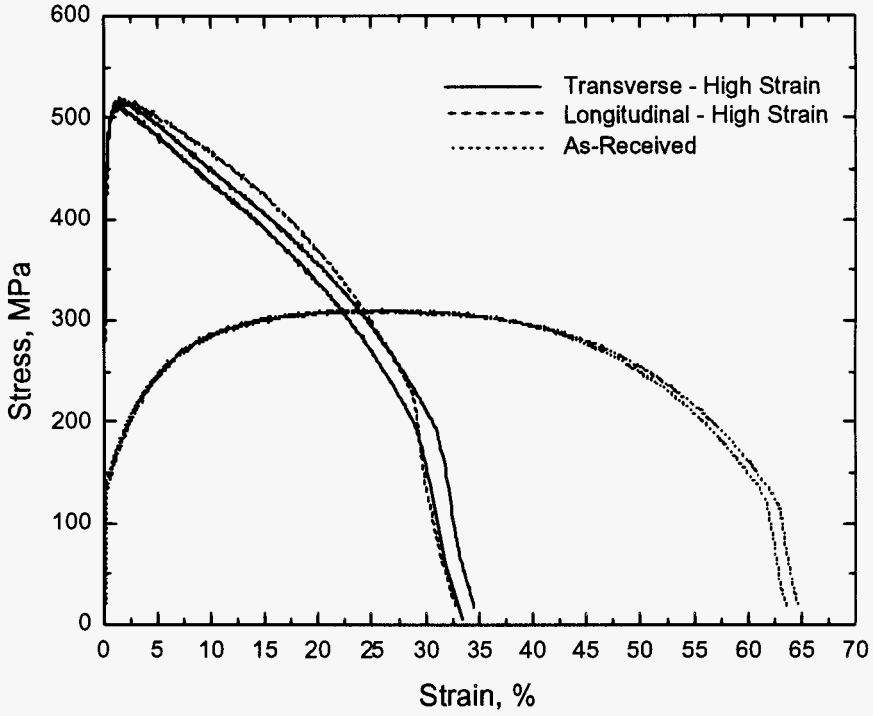

Fig. A-8. Monotonic stress-strain results for as-received sheet and high strain condition (transverse and longitudinal direction).

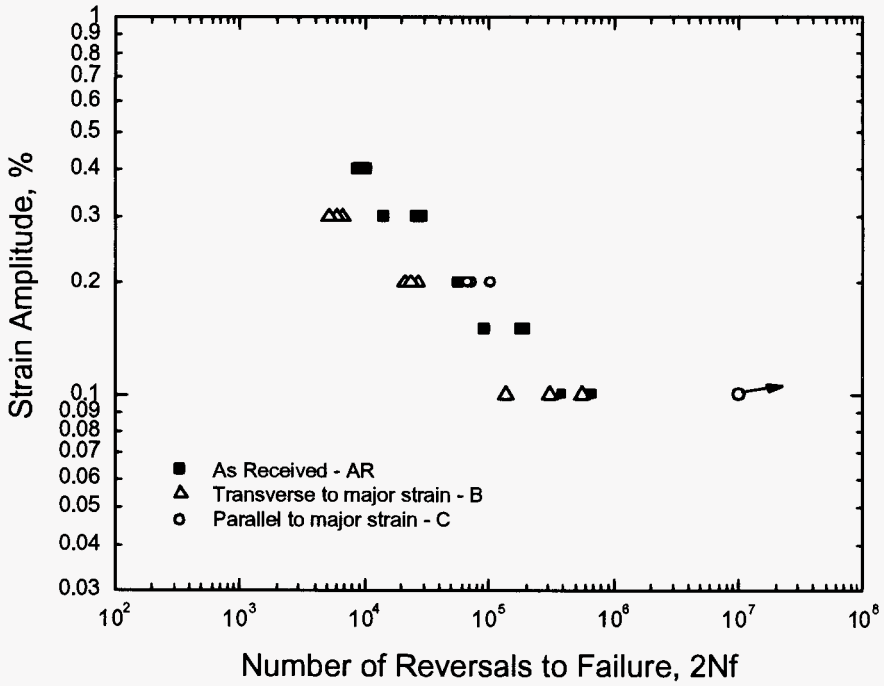

Fig. A-9. Strain amplitude vs. reversals to failure fatigue test results.

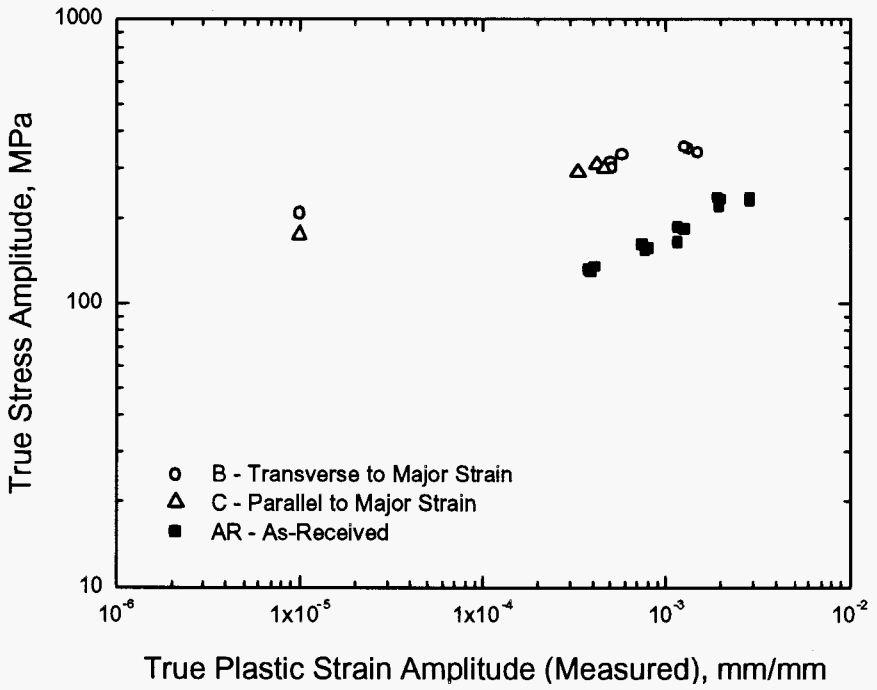

Fig. A-10. Measured true plastic strain amplitude as a function of true stress amplitude at half-life.

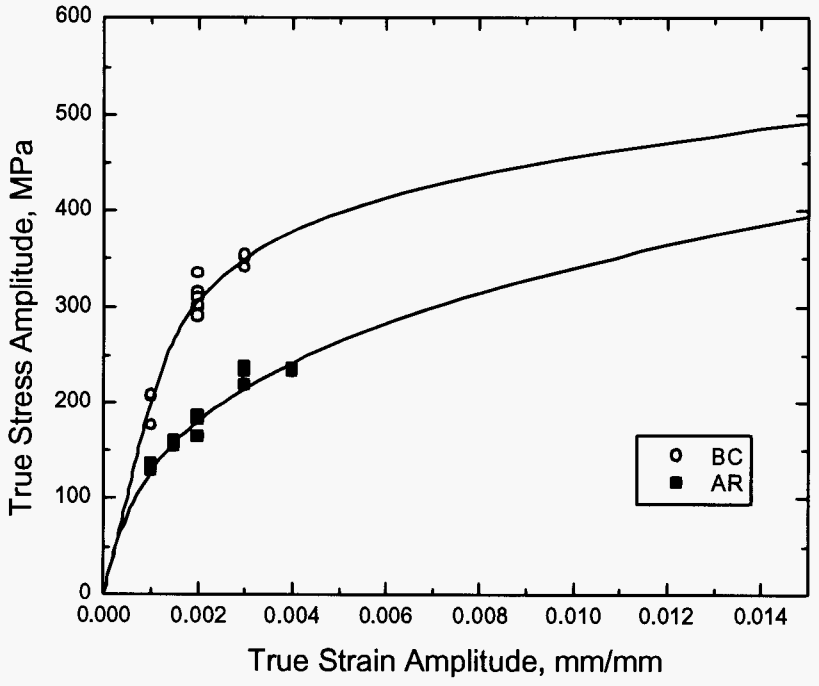

Fig. A-11. Cyclic true stress – true strain behaviour of as-received and deep-drawn conditions.

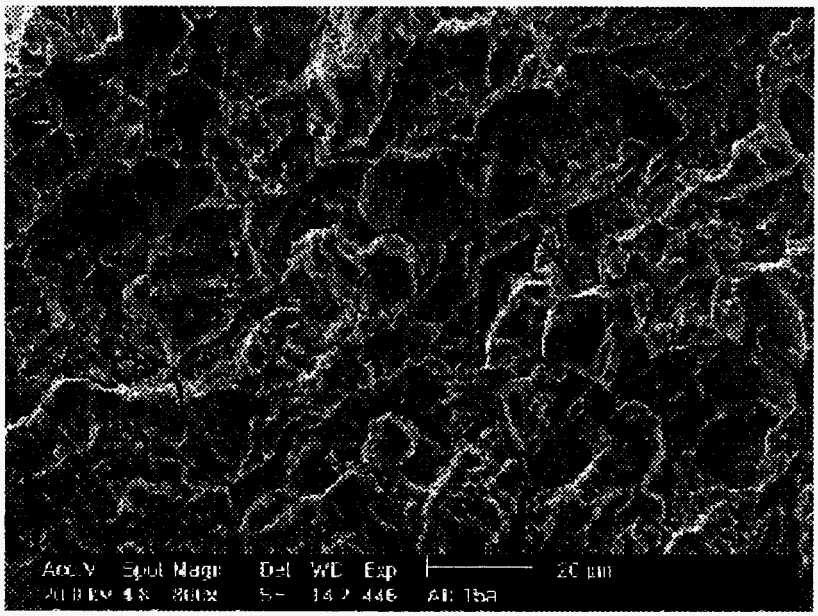

Fig. A-12. Fatigue fracture surface showing mixed intergranular/transgranular crack growth with secondary cracking – as-rolled condition at 0.2% applied strain amplitude (specimen AR15).

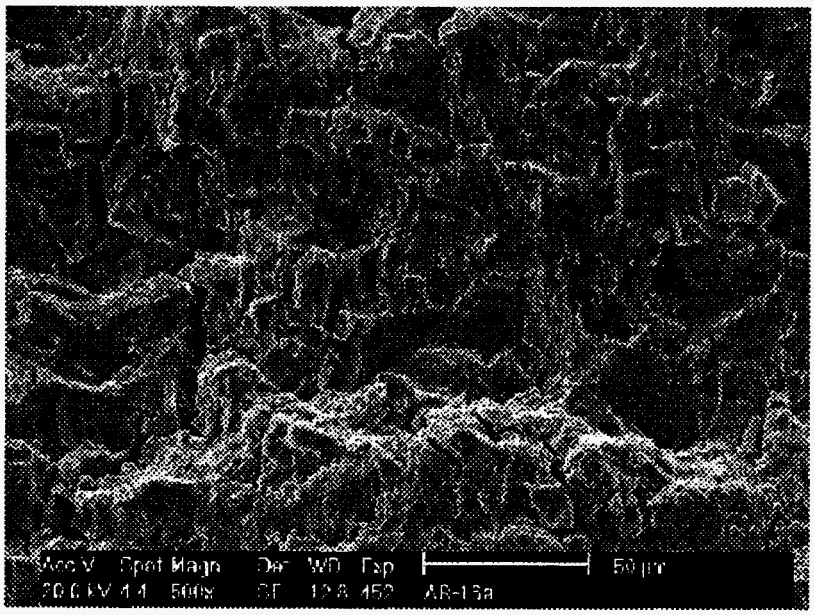

Fig. A-13. Fatigue fracture surface showing mixed intergranular/transgranular crack growth with secondary cracking – as-rolled condition at 0.3% applied strain amplitude (specimen AR16).

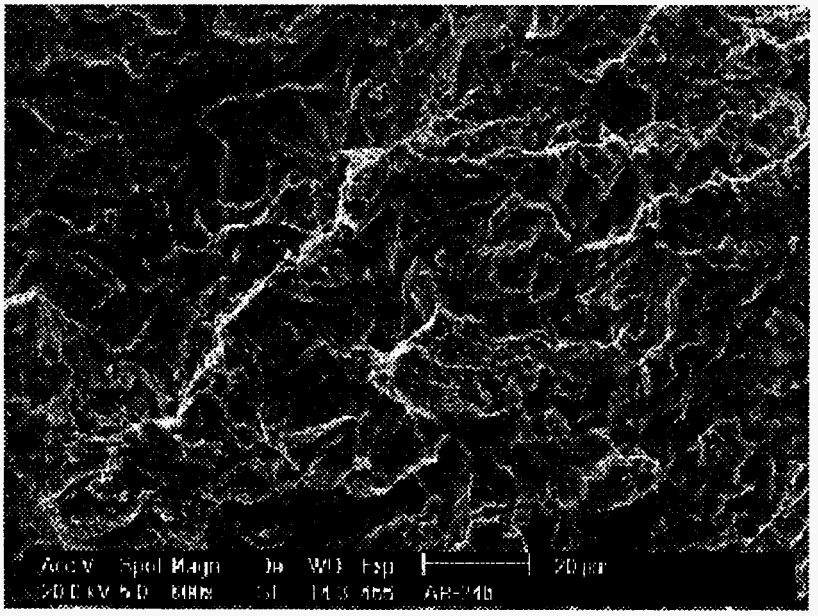

Fig. A-14. Fatigue fracture surface showing mixed intergranular/transgranular crack growth with secondary cracking– as-rolled condition at 0.15% applied strain amplitude (specimen AR24).

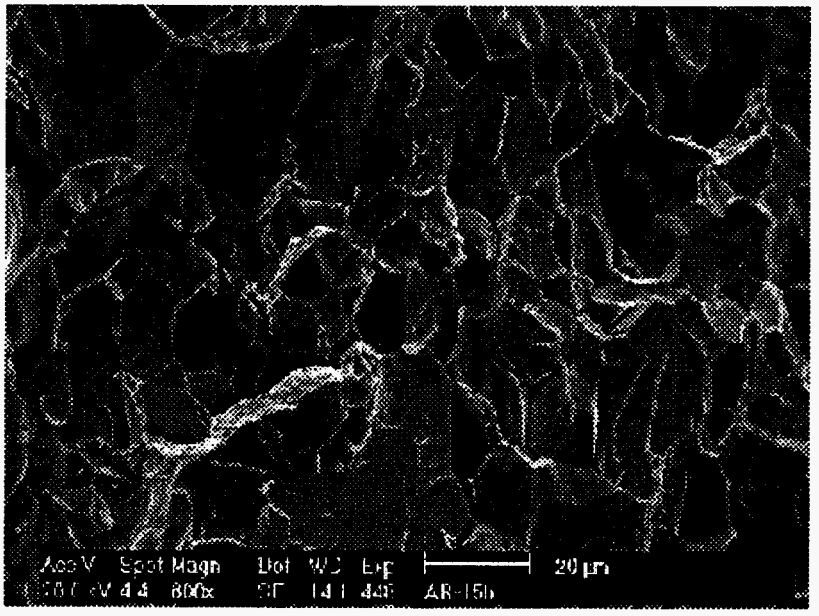

Fig. A-15. Final fracture surface showing mixed intergranular/transgranular cleavage – as-rolled condition (specimen AR15).

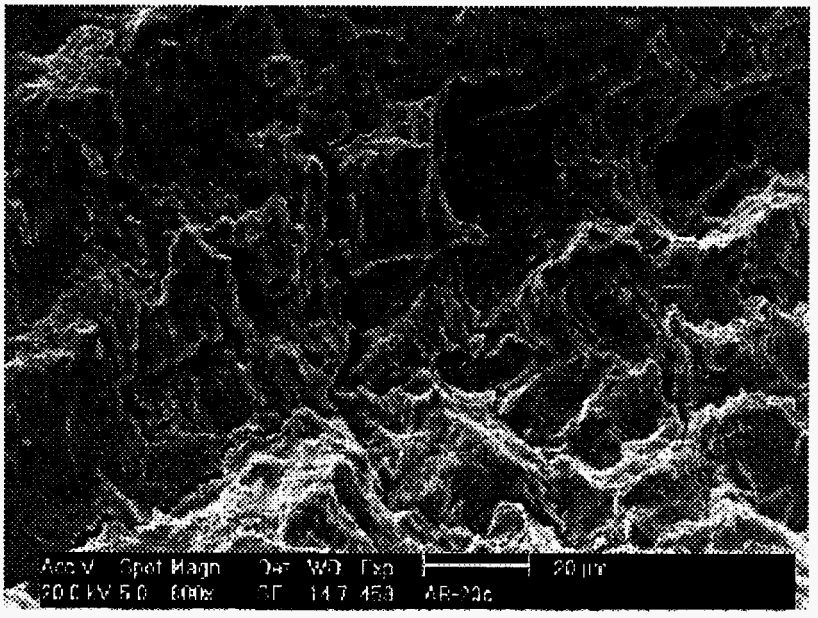

Fig. A-16. Fatigue fracture surface showing transgranular crack growth with secondary cracking – as-rolled condition at 0.4% applied strain amplitude (specimen AR20).

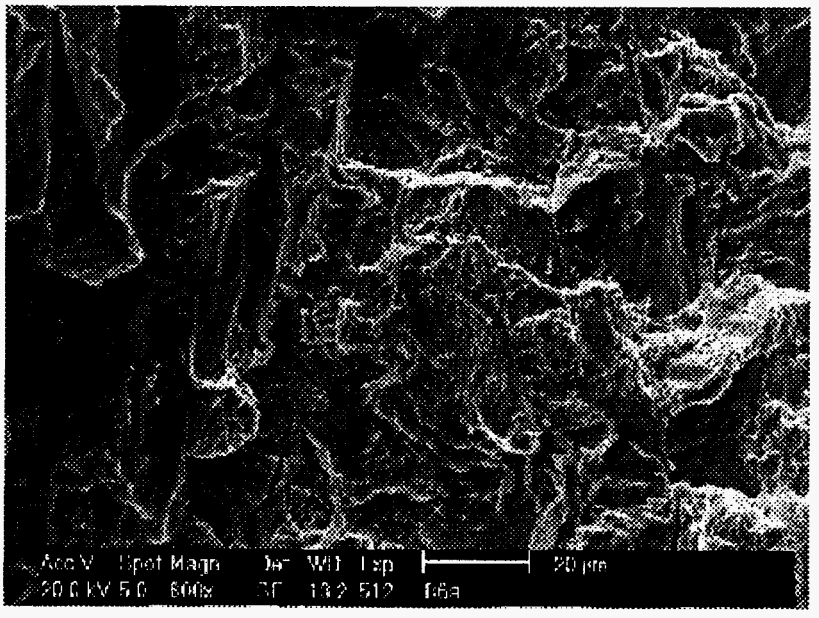

Fig. A-17. Fatigue fracture surface showing mixed intergranular/transgranular crack growth with secondary cracking – deep-drawn condition – transverse orientation at 0.2% applied strain amplitude (specimen B6).

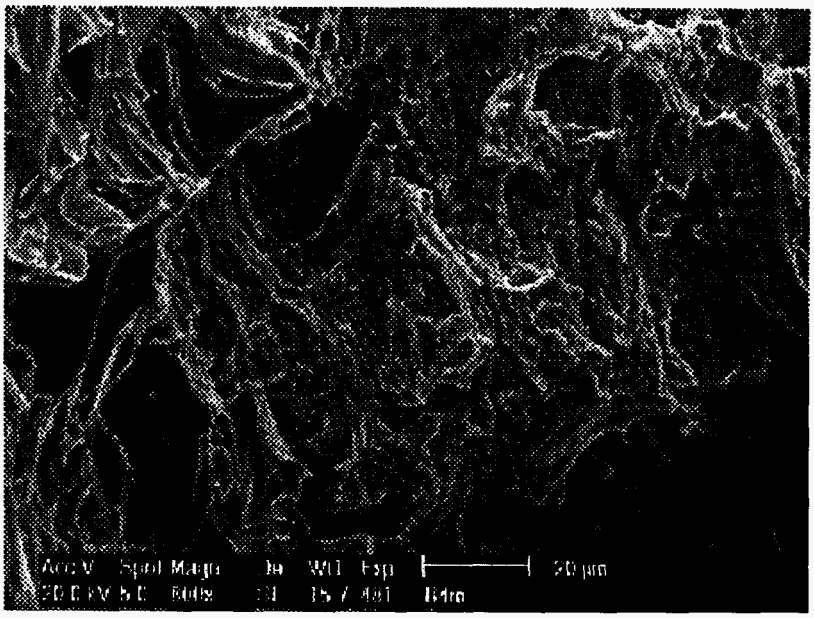

Fig. A-18. Fatigue fracture surface showing mixed intergranular/transgranular crack growth with secondary cracking – deep-drawn condition – transverse orientation at 0.3% applied strain amplitude (specimen B4).

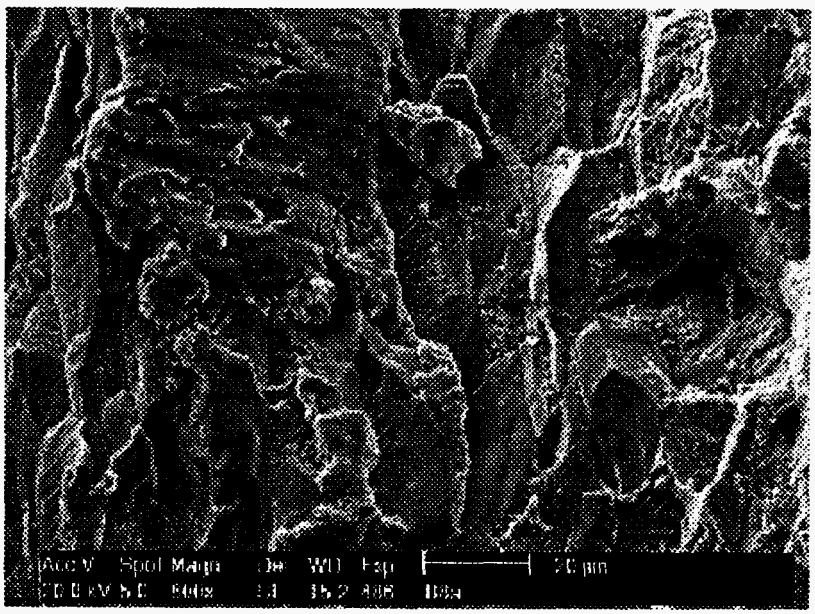

Fig. A-19. Fatigue fracture surface showing mixed intergranular/transgranular crack growth with secondary cracking – deep-drawn condition – transverse orientation at 0.1% applied strain amplitude (specimen B8).

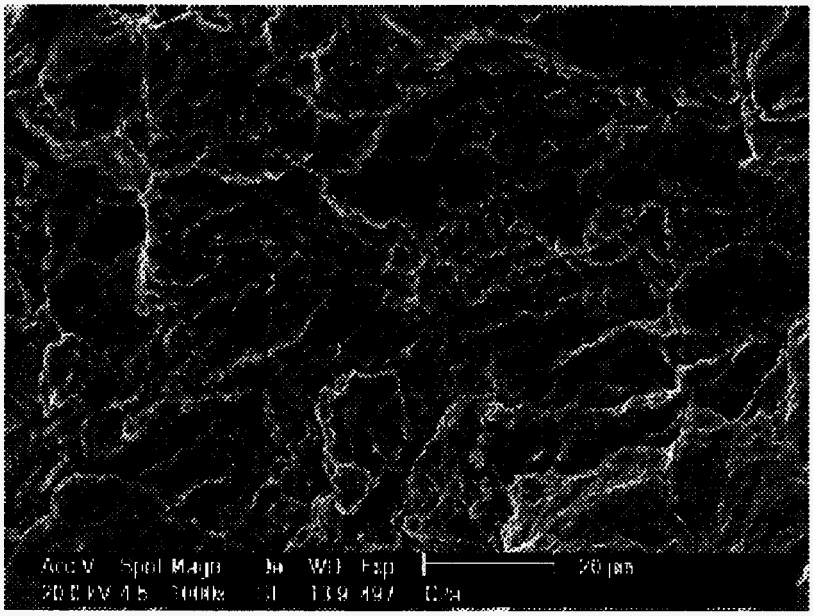

Fig. A-20. Fatigue fracture surface showing mixed intergranular/transgranular crack growth with secondary cracking – deep-drawn condition – longitudinal orientation at 0.2% applied strain amplitude (specimen C2).

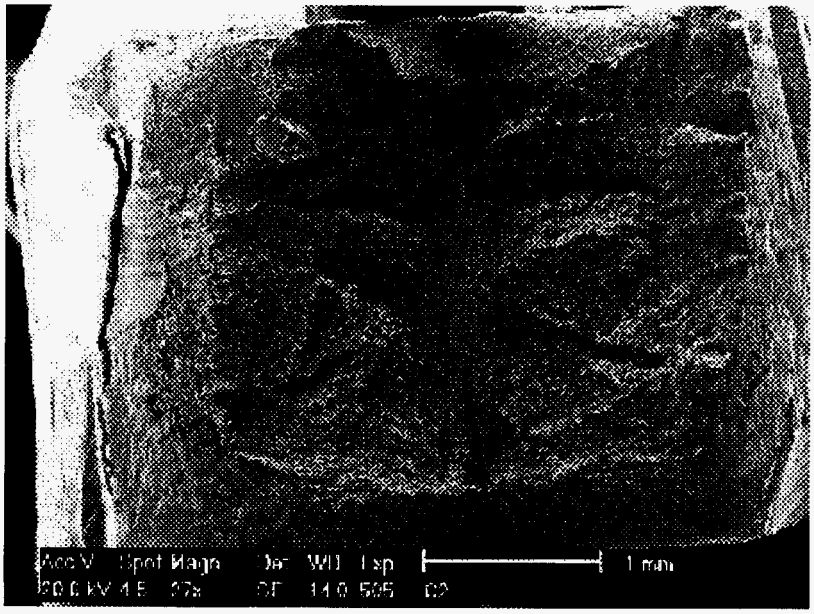

Fig. A-21. Specimen fracture surface showing splitting – deep-drawn condition – longitudinal orientation at 0.2% applied strain amplitude (specimen C2).

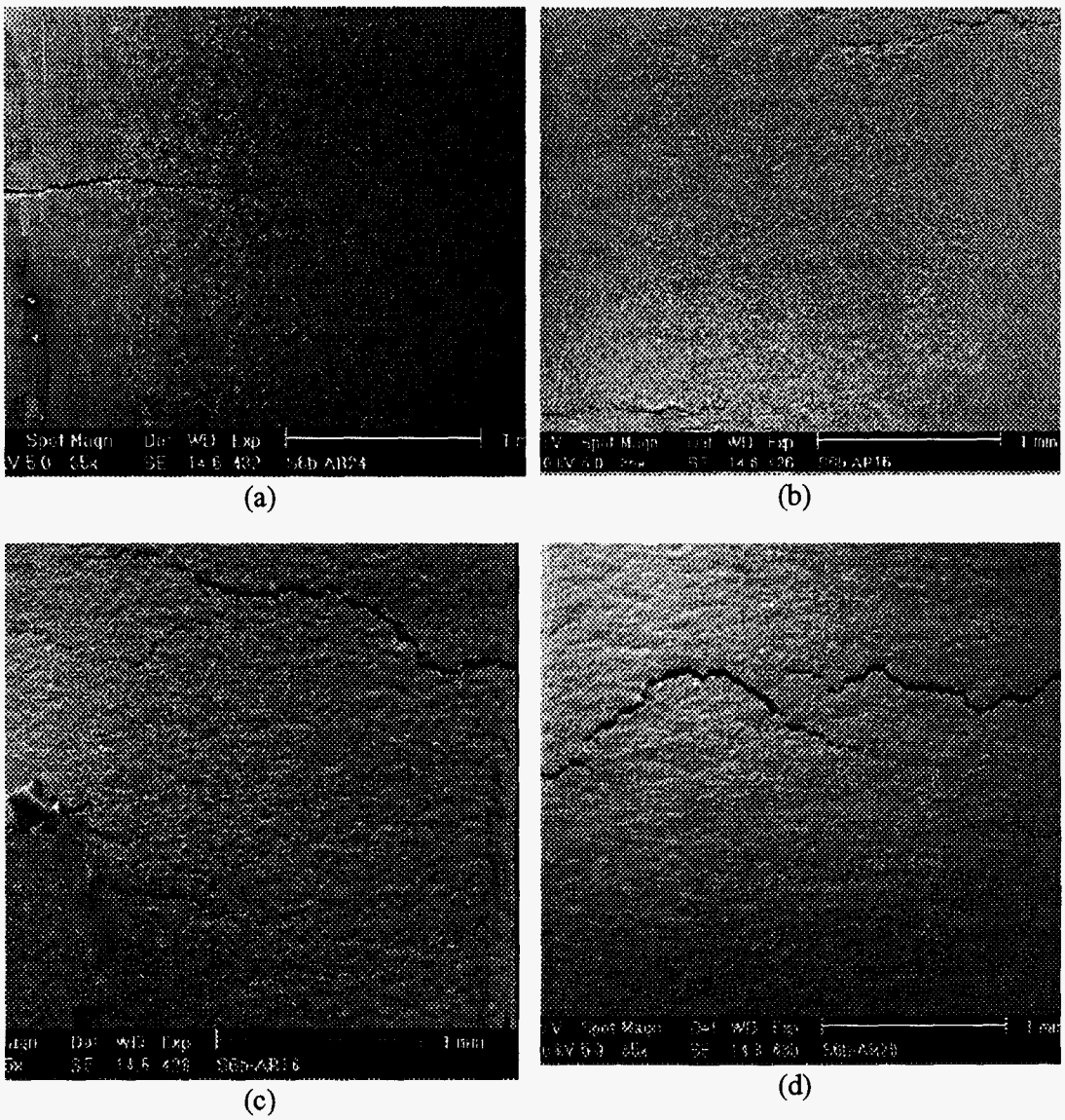

Fig. A-22. Fatigue cracking along specimen surface – as-rolled condition – for applied strain amplitudes of (a) 0.15%, (b) 0.2%, (c) 0.3 %, and (d) 0.4%. The number and lengths of fatigue cracks at the surface are shown to increase with increasing strain amplitude.

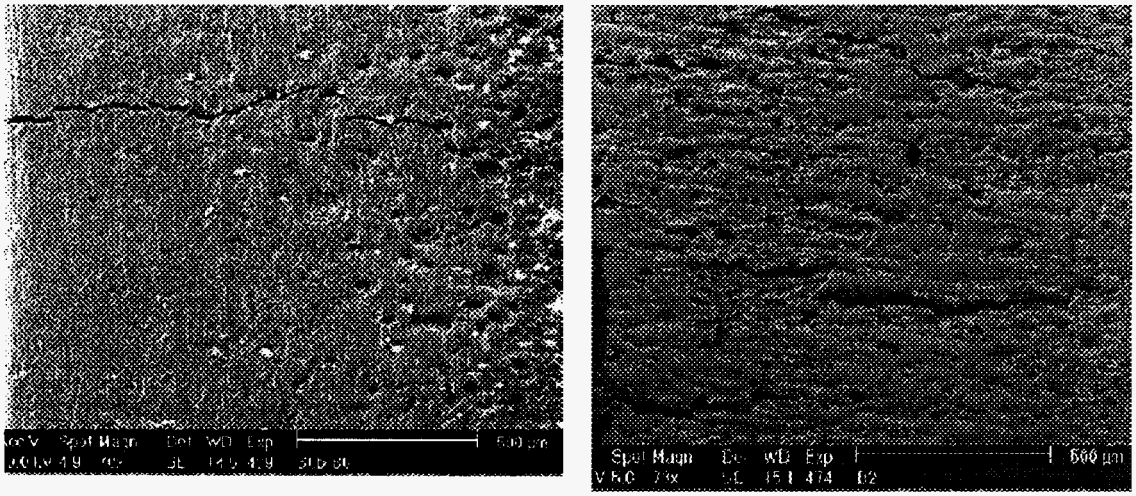

(a) (b)

Fig. A-23. Fatigue cracking along specimen surface – deep drawn condition – transverse to major strain - for applied strain amplitudes of (a) 0.2%, and (b) 0.3%.

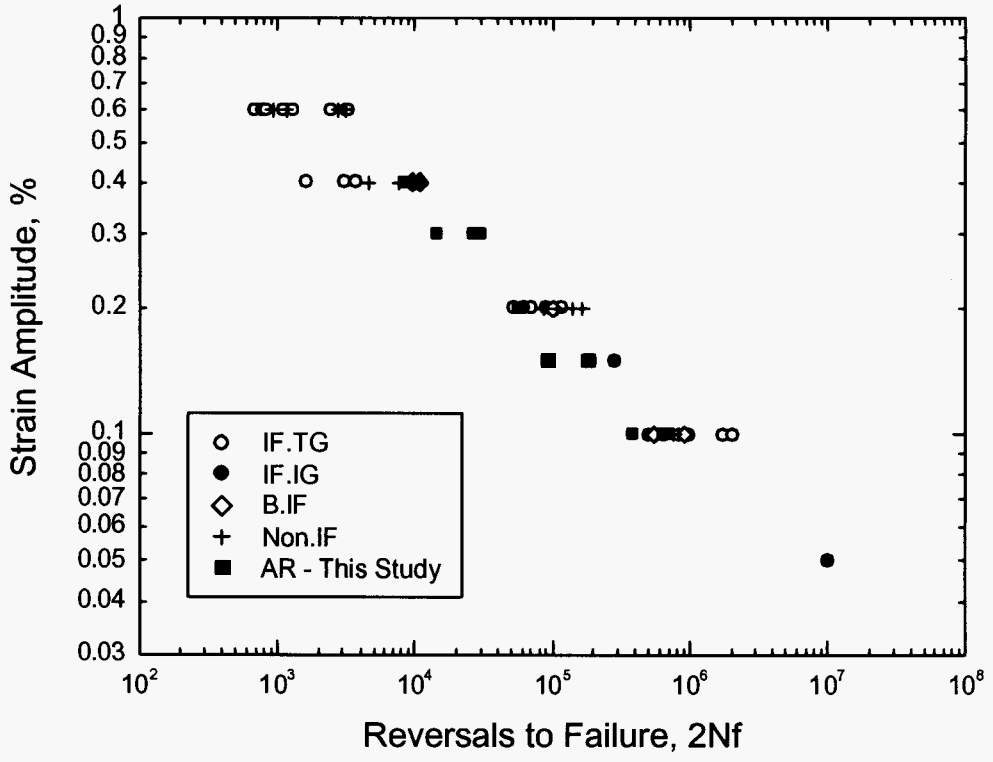

Fig. A-24. Strain amplitude vs. reversals to failure results for IF, Boron IF, and non-IF sheet steels from Yan [1] compared to the as-rolled condition results in this study.

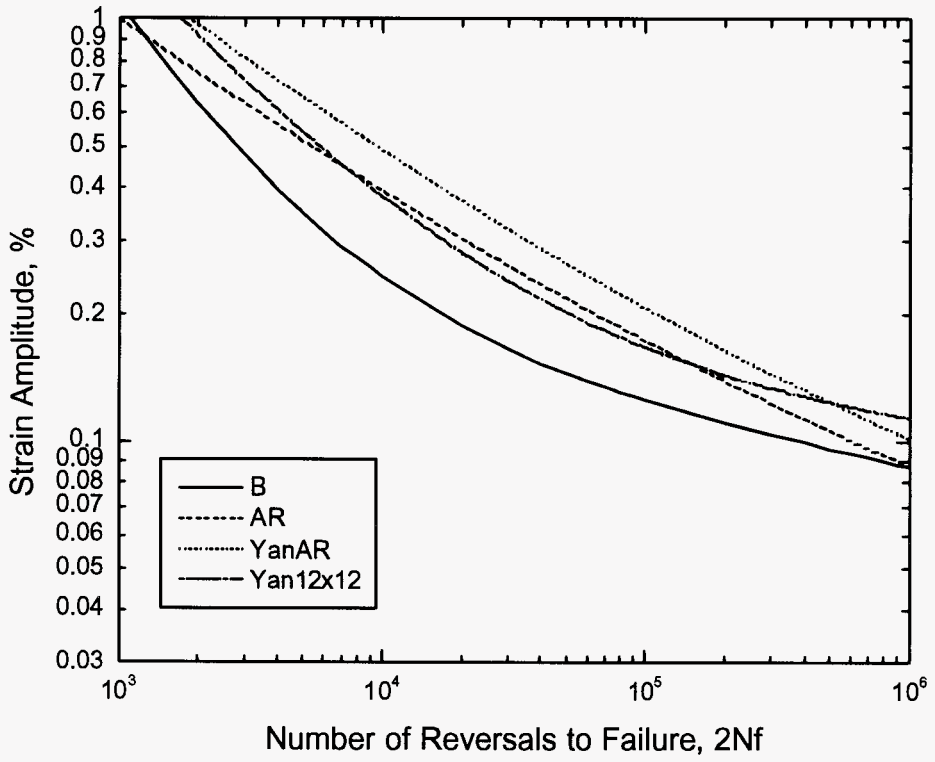

Fig. A-25. Strain – life curves for as-rolled and prestrained conditions for this study and Yan et al. [5].

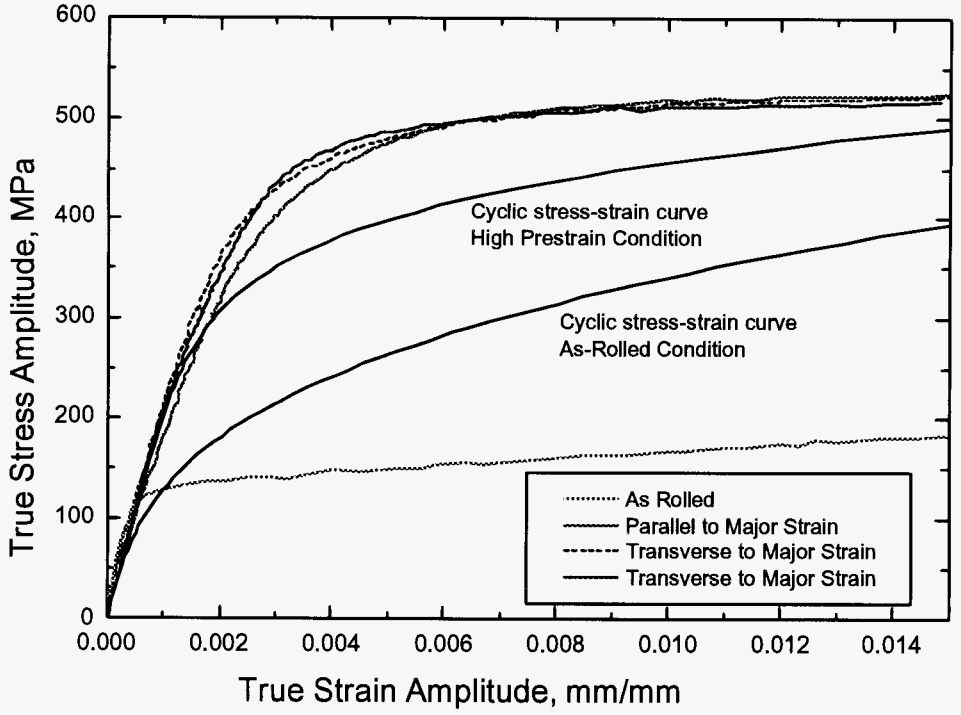

Fig. A-26. Monotonic and cyclic true stress – true strain curves for the as-rolled and deep drawn conditions.

Sponsor TBD Report No.:_____

AISI/DOE Technology Roadmap Program

Final Report

Cold Work Embrittlement of Interstitial Free Steel

by

Pierre Martin and John T. Bowker

Octobe 31, 2000

Work Performed under Cooperative Agreement
No. DE-FC07-97ID13554

Prepared for
U.S. Department of Energy

Prepared by
American Iron and Steel Institute
Technology Roadmap Program Office
Pittsburgh, PA 15220

DISCLAIMER

"Any opinions, findings, and conclusions or recommendations expressed in this material are those of the author(s) and do not necessarily reflect the views of the US Department of Energy."

Number of pages in this report: 144

TABLE OF CONTENTS

LIST OF TABLES

LIST OF FIGURES

LIST OF FIGURES (Cont.)

Page

LIST OF FIGURES (Cont.)

Page

LIST OF FIGURES (Cont.)

Page

LIST OF FIGURES (Cont.)

Page

LIST OF FIGURES (Cont.)

Page

EXECUTIVE SUMMARY

This report presents the results of the research project "Cold Work Embrittlement of Interstitial-Free Steels" initiated in February 1998. This work addresses the issues of measurement of secondary cold work embrittlement in deep-drawn parts using laboratory tests, and its correlation with real part fracture. It aimed at evaluating the influence of the steel chemistry and processing condition, microstructure, and test conditions on SCWE. The approach was based on the utilization of the cup/expansion test to evaluate the ductile-to-brittle transition temperature.

The objectives of this project defined in the research proposal dated March 13, 1997 were:

- to determine the effect of deformation of IF steel drawn parts on SCWE by measurement of a DBTT/strain map using cup expansion test;
- to develop an alternative method to the cup expansion test for measurement of SCWE in parts of any geometry;
- to establish a relationship between the two laboratory SCWE tests and SCWE in service; and
- to determine the relationship between fatigue resistance and deformation in IF steel parts.

To meet the first objective, 6-in. cups produced with various draw ratios or trimmed at different heights were tested. The DBTT as a function of strain was determined. For the second objective we conducted a parametric study to determine the effect the parameters that affect the DBTT obtained by

the cup expansion test. The 2-in. cup/expansion test, bend test and fracture of notched specimens were also used to generate information complementary to that provided by the 6-inch cup/expansion test. The relationship between laboratory tests and fracture in real parts was established by testing large-scale parts. For the last objective, prestrained specimens taken from the wall of a formed part were tested in fatigue.

From the work presented in this report we can draw the conclusions below. However, in some cases the conclusions are based on a limited number of experiments, so additional work will be needed for further confirmation.

- A good relationship was found between the cup test and the bend test. However the bend test DBTT was significantly higher than cup test DBTT. This effect was attributed to the higher strain in the ID region of the bend specimen. The major problems with the bend test appears to be the control of strain during 0t bending and the high temperature of this test when evaluating high SCWE sensitive material. The test could also be sensitive to sheet thickness.

- In general fracture of high-sensitive steel near DBTT showed a high percentage of intergranular fracture. A linear relationship was found between DBTT and fraction of IG fracture in unstrained IF steel. However, straining affects the relationship between DBTT and fraction of IG fracture. One steel, S7, showed a surprisingly high fraction of IG fracture (DBTT of -30°C). The reason for this anomaly was not explained. The SCWE tests showed the beneficial effect of free-carbon, boron and the detrimental effect of P, as well has the difference in SCWE sensitivity between batch and continuous anneal products.

- This work showed the detrimental effect of primary strain on SCWE for strain levels between 45% and 65%. For higher strain DBTT decreased. It was found that a same level of primary strain can produce two different DBTT depending on the draw ratio and cup height. This effect coincided with a decrease in residual stresses. But the possible relationship between residual stress and DBTT is unclear.

- In general straining increases the fraction of IG and DBTT. This effect was confirmed for crack propagation parallel to the direction of grain elongation. For crack propagation in the direction normal to grain elongation, straining did not increase the fraction of intergranular fracture, the resulting effect on DBTT in unknown. It was shown that fracture in the transverse orientation (propagation perpendicular to direction of grain orientation) occurred at lower DBTT than fracture parallel to the direction of grain elongation.

- No significant effect of sheet thickness was found when testing reduced-wall thickness cups. However, test made on sheet steels produced with varying gauge thickness gave erratic results, which were attributed to the processing conditions.

- Sheet planar anisotropy generates earing and wall thickness variation at the edge of cups. In trimmed cups, SCWE were found to formed in the thinner region of the wall (earing area). This effect has been associated with the higher stress generated in the thinner edge regions during the cup/expansion test. The resulting effect on DBTT is unknown.

- An increase of impact speed from 4.34 to 7.41 m/s increased DBTT by 5°C.

- No significant difference in DBTT was observed for flanged cups with draw ratio of 2.0 and 2.3 compared to full drawn trimmed cups. This is in contradiction with observations reported previously in the literature. For the test conditions used it was shown that whether initiation occurs at the edge or in the wall DBTT can be the same.

- The presence of pre-machined or pre-cracks at the edge of cups did not significantly influence DBTT.

- SCWE fracture was observed during forming 6-inch cups and large oil pans. In both cases fracture occurred at temperature higher than predicted by the 2.0-draw ratio cup test. It is possible that in both cases local deformation would have been higher than in the cup test, which would explain the brittle fracture, but in the two cases fracture occurred in quasi static forming conditions.

- Significant difference in DBTT was observed between the 2-inch and 6-inch bend test when comparing DBTT in trimmed cup, flanged cup and cups with different draw ratios or cup heights. Those results show the limitation of laboratory small-scale tests to simulate specific test conditions.

- Surface embrittlement associated with Zn diffusion at the surface during galvannealing was observed. The phenomenon lead brittle cracking in the ferrite grains beneath the surface during cup drawing. This phenomenon also led to an higher fraction of IG fracture near the surface. FIB observation made on two rephosphorized IF steels reported in Annex A did not show any evidence that this phenomenon contributed to the initiation of SCWE cracks.

- The data generated using laboratory cup tests to predict the behaviour of the large scale parts used in this study show that the cup tests were conservative. Localized testing of high strained regions produced DBTT values slightly below those obtained from the cup tests. A significantly lower test temperature than the 2-inch DBTT was needed to produce brittle fracture in a region of high strain remote from the location of impact. For large scale parts with regions of lower strain (<50%) no brittle fracture was observed down to test temperatures of -95°C.

- The fatigue strain – life behaviour of the as-rolled condition is consistent with other IF and non-IF sheet steels.

- Fatigue cracking initiated at the as-rolled or deep drawn surface.

- Fatigue cracking at strain amplitudes of 0.3% and lower was by a mixed intergranular/transgranular

mode consistent with previous work by other researchers for IF steels.

- The major strain of the deep drawn condition specimens was estimated to be 89% compared to 12% and 30% by other researchers. This resulted in highly elongated grains oriented in the drawing direction.

- Over the strain amplitude range studied, the fatigue strain – life behaviour of the deep drawn condition showed a significant orientation effect. The life for the transverse orientation was lower than the as-rolled condition by a factor ranging from 2 at 0.1% strain amplitude to 4 at 0.3% strain amplitude. The life for the longitudinal orientation was the same as the as-rolled condition at 0.2% strain amplitude and significantly increased (run-out) at 0.1% strain amplitude.

- The stress – strain behaviour showed cyclic hardening for the as-rolled condition and cyclic softening for the deep drawn condition. However, the cyclic stress-strain behaviour of the deep drawn material is significantly above that of the as-rolled material. This is attributed to the differences in high starting prestrain levels and grain elongation in the deep-drawn condition compared to the as-rolled condition that would result in different cyclically stabilized conditions.

- The observed results indicate that there is no real difference in the monotonic or cyclic stress – strain behaviour for the transverse and longitudinal orientations for the deep-drawn condition.

- The significant decrease in fatigue life for the deep drawn condition in the transverse orientation is thought to be an effect of the orientation of the highly elongated grains. This orients the elongated grain boundaries and their associated surface features transverse to the loading direction thus increasing the number of favourable initiation sites. Cyclic stress-strain results show minor orientation effects at low prestrain levels while at high prestrain levels, the current data suggests that there are no orientation effects due to cyclic stress-strain behaviour.

- It is not clear that SCWE has an effect on fatigue performance in deep drawn IF sheet steels. The results for the as-rolled condition support earlier work in that fatigue life is not affected but the mode of cracking is affected. In the deep drawn condition, the results of this study suggest that the effect on cracking mode persists but there is no effect on cyclic stress strain behaviour. However, an orientation effect was observed related the highly elongated grain structure developed during the deep drawing process. Further tests are required in the deep drawn condition in non-SCWE sensitive IF and non-IF steel grades before a definitive statement can be made.

COLD WORK EMBRITTLEMENT OF INTERSTITIAL FREE STEEL*[1]

by

P. Martin, J. Bowker, O. Dremailova, M. Braid, R. Bouchard, B. Voyzelle, D. Linkletter, X. Su, S. Dionne, J. Brown, R. Canaj and E. Essadiqi

1. INTRODUCTION

The absence of solute interstitial elements in interstitial-free (IF) ultra-low carbon (ULC) steel leads to sensitivity to secondary cold work embrittlement (SCWE). For this phenomenon to occur, cold work deformation (primary strain) is requiredso that material strengthening creates conditions by which the flow stress will exceed grain boundary strength or resistance to cleavage. The brittle fracture will normally occur at low temperature during secondary deformation such as during impact loading. It can also occur during progressive forming and trimming operation of drawn parts. To avoid occurrence of brittle fracture in formed parts it is important to better understand the factors that affect SCWE and establish the relationship between laboratory tests that are used on a routine basis with brittle fracture in deep-drawn components.

Because SCWE is mainly observed in deep-drawn parts, the most common method to evaluate sensitivity to SCWE is by cup expansion of the end of a cup. This test can be executed under various experimental conditions, permitting an investigation of the the parameters that affect SCWE. However, it is still unclear how the ductile-to-brittle transition temperature (DBTT) obtained by cup/expansion test can be used to determine the occurrence of fracture in real parts. Since primary strain is a key parameter during SCWE, it was proposed to use strain as a control parameter to establish the relationship between the cup/expansion DBTT and fracture in formed parts for which the strain distribution has been established.

This report presents the results of the research project "Cold Work Embrittlement of Interstitial-Free Steels" initiated in February 1998. This work addresses the issues of measurement of secondary cold work embrittlement in deep-drawn parts using laboratory tests, and its correlation with real part fracture. It aimed at evaluating the influence of the steel chemistry and processing condition, microstructure, and test conditions on SCWE. The approach was based on the utilization of the cup/expansion test to evaluate the ductile-to-brittle transition temperature.

The objectives of this project defined in the research proposal dated March 13, 1997 were:

---

* The authors are with Materials Technology Laboratories, Canada Centre for Minerals and Energy Technology (MTL/CANMET), Ottawa, Canada

- to determine the effect of deformation of IF steel drawn parts on SCWE by measurement of a DBTT/strain map using cup expansion test;
- to develop an alternative method to the cup expansion test for measurement of SCWE in parts of any geometry;
- to establish a relationship between the two laboratory SCWE tests and SCWE in service; and
- to determine the relationship between fatigue resistance and deformation in IF steel parts.

To meet the first objective, 6-in. cups produced with various draw ratios or trimmed at different heights were tested. The DBTT as a function of strain was determined. For the second objective we conducted a parametric study to determine the effect the parameters that affect the DBTT obtained by the cup expansion test. The 2-in. cup/expansion test, bend test and fracture of notched specimens were also used to generate information complementary to that provided by the 6-inch cup/expansion test. The relationship between laboratory tests and fracture in real parts was established by testing large-scale parts. For the last objective, prestrained specimens taken from the wall of a formed part were tested in fatigue. The results of this work is presented in Appendix A.

2. EXPERIMENTAL PROCEDURE

Table 1 provides a summary list of all the steels and various tests, both laboratory and full-scale, to which they were exposed. The steel chemistry, mechanical properties and test techniques employed, as well as the experimental procedure for the parametric study and full scale tests are given below.

2.1. MATERIALS AND MECHANICAL PROPERTIES

Twelve commercial steels were selected for the study. Several participating companies provided the steels. The base chemistries are given in Table 2. The details on chemistries and mechanical properties are given in this section.

2.1.1. Materials for the Parametric Study

Seven steels shown in Table 2 as S1, S2, S3 and S4a - 4d were secured by MTL/ CANMET for a parametric study to examine the effect of steel chemistry, thickness, edge condition, impact speed and strain on secondary cold work embrittlement (SCWE). These steels were expected to show various degree of resistance to SCWE because of their chemistry or their steel processing conditions and belonged to one of the four categories given below:

- Bake-hardenable (BH) batch annealed ELC grade (low SCWE sensitivity)
- Rephosphorized ULC fully stabilized containing B (low/moderate SCWE sensitivity)

- Rephosphorized ULC fully stabilized without B (moderate/high SCWE sensitivity)
- Batch annealed ULC Ti-stabilized (moderate/high SCWE sensitivity)

A low SCWE sensitivity was expected for steel S1, the BH ELC grade because of its free carbon content. This steel had a phosphorus content slightly higher than the two rephosphorized grades, S2 and S3. The chemistries of the rephosphorized grades were similar except for the B addition in steel S2. The Nb/C ratio in steel S2 and S3 was 1.29 and 1.09 respectively, which should provide enough Nb for the stabilization of C.

The S4 series of steels were stabilized ULC grades produced by batch annealing. This steel process was expected to provide more segregation at the grain boundaries, which consequently reduces the steel SCWE resistance. S4 steels were used to study the effect of thickness on SCWE. The four steels provided were in the thickness range 0.79 to 1.45 mm and were produced from different heats with some minor differences in chemical composition, particularly C, N and to a lesser extent Ti. The coupons 24 in. x coil width were taken at 100 ft from the temper mill ID coil (samples cut in succession).

The steels were provided with various surface finishes; steel S1 was electrogalvanized (EG), steels S2 and S3 were galvannealed (GA) and series S4 were cold rolled (CR) non-coated.

2.1.2. Materials for Large-Scale Parts

Four steels, S5a, S5b, S6a, S7 were selected for the fabrication of the parts for the large-scale SCWE tests. Table 2 shows their base chemical compositions. Two real parts were fabricated, a structural part and a deep drawn part using steel grades with low and high transition temperatures for each part. Since the forming requirement and the thickness were not the same for each part it was necessary to select four different grades. The shock tower (deep drawn part) was made with steel S5b, a low transition temperature ULC steel stabilized with Ti, which contained B and a more sensitive steel, S6a, which was a batch annealed type grade stabilized with Ti. Because of the shock tower drawing severity, a rephosphorised grade could not be used. Steel S6a was electrogalvanized and steel S5b hot dip galvanized. The rear floor panel (structural part) was made with a low SCWE sensitive steel which contained Ti and Nb and is identified in Table 2 as steel S5a. The steel for this part requiring less drawability, a rephosphorized ULC grade, S7, was used for the more sensitive steel. Steels S5a and S7 were supplied with a galvannealed and hot dip galvanised coating respectively.

2.1.3. Material for the Fatigue Study

A highly SCWE sensitive steel, preferably with a high phosphorus content, produced with a thickness in a range1.5 to 1.7 mm, was sought for the project. The fatigue specimens were to be taken from the wall or flange of a commercial deep drawn part. This approach turned out to be difficult to realize because severe deep drawn large specimens made of rephosphorized IF grades were not easily

available. The only steel (steel S6b) that became available for the study was a batch annealed IF with a low P content. This steel was selected because several cases of brittle fracture had been observed during stamping or handling of the parts. This steel was used to produce large diesel engine oil pans. The steel was cold rolled (non-coated). CANMET secured five oil pans and a few blanks for the fatigue study.

As mentioned above, the commercial steels were provided with various types of surface finish: cold rolled (CR) (S4a, S4b, S4c, S4d, S6b), galvannealed (GA) (steels S2, S3, S5a), hot dip (GI) (S5b and S7) and electrogalvanized (EG) (S1, S6a). No attempt was made in the project to assess the effect of coating on SCWE. However, for the fatigue study, a CR steel was preferred because of the possible effect of the Zn coating on crack initiation in the highly formed fatigue coupons.

2.1.4. Mechanical Properties

Tensile tests were performed on S1, S2, S3 and S4a steels on specimens extracted at 0°, 90° and 45° relative to the rolling direction. Table 3 gives their yield strength, UTS, elongation, r-values and n-values. The table also presents the mechanical properties of S7 steel at 0°, 90°. The mechanical properties of this steel were provided by the steel supplier. The strength, elongation, r-value and n-value are typical of the grades and annealing conditions used.

2.2. SCWE TESTING

2.2.1. Bend Test Procedure

The bend test has been used to evaluate the susceptibility of steels S1, S2, S3 and S4a to secondary work embrittlement (SCWE). This simple method has been used to quickly compare the steels provide for the project.

The test method used was similar to that described by Henning (1992). Test specimens 13 mm wide x 100 mm long oriented with the longest dimension transverse to the rolling direction were used. The specimens were bent at room temperature to a zero degree (0τ) bend radius. The bend specimens were then opened manually by hand at various temperatures to determine the temperature at which a brittle fracture occurred. A pass rating was given to the specimens that showed metal to metal contact after they were pulled open. The failed specimens had a crack after they were pull open with no metal to metal contact at the inner radius. Five tests were performed at each temperature with the temperature varying by 10-degree increments. Close to the transition temperature the increment was reduced to 5 degrees.

The specimens were immersed in an alcohol/dry ice bath and were held for 5 min at the specified temperature. The specimens were removed and pulled within two seconds to unbend the specimen. They were then assessed for the pass/fail criteria: whether the specimen still had a metal-metal contact at the inner radius tip.

To determine the transition temperature the percentage of pass specimens was calculated at each temperature. The pass rate was then drawn for each temperature to better visualize the transition curve.

2.2.2. Cup/Expansion Test Procedure

The expansion of drawn cups is the most frequently used test for SWE evaluation. Tests were performed on both 6-in. (150 mm) and 2-in. (50 mm) diameter cups. The procedure for the 2 in. cup/expansion tests was based on a procedure specified by GM (GM 9920P Revision #6). In the case of the 2-in. cup, the draw ratio was set to 2.0, requiring a blank size of 100 mm. The circular blanks were punched from the steel sheets. In order to fabricate cups made of steel of different thickness a series of drawing dies were made to maintain a relatively constant die clearance, which resulted in cups with similar ID but variable OD. The 6-in. cups and 2-in. blanks were machined using a lathe. The size of the 6-in. blanks was determined by the draw ratio to be used which covered the range 1.8 to 2.3. A polyethylene film had to be used for 2.3-draw ratio cups because of the forming severity that produced excessive wrinkling which was eliminated by trimming the cups to a lower height. A polyethylene film was used as lubricant for the production of the 2-in. cups. A liquid lubricant was used in the production of the cups with draw ratios in the range 1.8 to 2.2. To provide information on the major and minor strain as a function of cup height and draw ratio, some of the initial blanks were marked with 2.5-mm diameter circular grids. The edges of the cups were trimmed using a lathe. For the 6-in. cups the trim height varied depending on the draw ratio and major strain. Further details on the trim height for this cup diameter are given in the next section which describes the parametric study. The trim height for the 2-in. cups made with the thinner gauge steels (S1, S2, S3 and S4) was kept at a height of 31 mm from the bottom of the cup. The cup height for the thinner gauge material was 33 mm. This translates to major strains of about +55% to +60% and minor strains of about -40%. The DBTT was determined by impacting cups at progressively lower temperatures. The samples were cooled down to test temperatures using a liquid nitrogen mist in the case of the 6-in. cups or by immersion in a liquid bath for the 2-in. cups. A total of six thermocouples, one for control and the remainder for measurement were attached to the 6-in. cups as shown in Fig. 1. This was not necessary for the 2-in. cups since they were immersed in a constant temperature liquid bath. In both instances the immersion time was 15 min, after which time the sample was impacted from a height of 1 m using a conical indentor with a 60° apex angle as shown in Fig. 2. The impact occurred within 3 s of the removal of the cup from the bath. The 6-in. and 2-in. drop weight test equipment are shown in Figs. 3 and 4, respectively. Above the DBTT, these tests produced specimens which exhibited ductile flaring. Below this temperature, a brittle fracture was initiated. The DBTT in the case of the 2-in. cups was defined in accordance with the GM specification as the lowest temperature at which at least 6 out of 8 cups did not fracture. For the 6-in. cups, however, given the additional material that was required to conduct these two tests it was decided to define the DBTT as the lowest temperature at which at least 4 out 5 cups did not fracture.

2.2.3. Fracture of Notched Specimens

Lau et al. (1998) has suggested a new method to determine the DBTT of IF steels based on the measurement of the fraction of intergranular fracture. This method is based on observations suggesting that there is a simple relationship between the transition temperature and the fracture morphology at temperatures below the transition temperature; a transition from predominantly cleavage transgranular to intergranular was observed as DBTT increased in steels with a wide range of SCWE sensitivity. Similar observations were reported by Yasuhara et al. (1994) for steels with different draw ratios. Assuming that this relation was independent of the strain condition, Lau suggested that it should be possible to evaluate the DBTT of real automotive parts by measuring the fraction of intergranular fracture. In the method proposed by Lau, the fracture surfaces were generated by cutting thin strips at the edge of the cups, machining a notch on the edge of the strips, and fracturing the notched strips at liquid nitrogen temperature.

To validate this approach and to assess the effect of strain on the fracture mode and grain morphology of steels with various degrees of SCWE sensitivity, small size notched specimens (3 mm x 20 mm x thickness), as shown in Fig. 5, were machined from unstrained and prestrained material taken from steels S1, S2, S3 and S4(a). The notch was made on one side of the coupon using a fine diamond blade to produce a stress concentration at the tip to minimize the plasticity during fracture at low temperature. The prestrained samples were taken from the wall of the 6-in. cups drawn with a draw ratio of 2.0. Since deep drawing generates elongated grains, which can significantly influence intergranular crack propagation, an investigation of the effect of the grain orientation on crack propagation was conducted by machining coupons as shown in Fig. 6. The plane of the fracture in the coupons cut in the circumferential direction will be parallel to the grain elongation (LN orientation) which is the same as for the cup expansion test. The coupons taken parallel to the height of the cup will have crack propagation normal to the grain elongation (TN orientation). All coupons were taken such that the notch location was approximately 30 mm from the cup edge. The minor and major strains were -45% and +65% respectively and the grain aspect ratio (grain length/grain width) was 2.35. The specimens were immersed in liquid nitrogen, fractured and then prepared for examination in the scanning electron microscope.

2.3. PARAMETRIC STUDY

2.3.1. Effect of Steel Chemistry and Processing on Laboratory Tests DBTT

To determine the effect of steel chemistry and processing conditions on the transition temperature obtained for steels S1,S2, S3 and S4a, which represent the four categories of steels expected to show varying degrees of SCWE sensitivity, DBTTs were measured using the bend test and both 6-in. and 2-in. cup expansion tests. These four categories as stated previously are:

- Bake-hardenable (BH) batch annealed ELC grade (low SCWE sensitive grade, steel S1)
- Rephosphorized ULC fully stabilized containing B (low/moderate SCWE sensitive grade, steel S2)

- Rephophorized ULC fully stabilized without B (moderate/high SCWE sensitive grade, steel S3)
- Batch annealed ULC Ti-stabilized (moderate/high SCWE sensitive grade, steel S4a)

All of the remaining steels were tested using the 2-in. cup expansion test. All of the cups tested in this part of the study had received a draw ratio of 2.0. The trim heights for the 6-in. and 2-in. cups were 105 mm and 31/33 mm respectively.

2.3.2. Effect of Strain

Cups 6-in. in diameter were produced from steel S3 with draw ratios of 1.8, 2.0, 2.1, 2.2 and 2.3 in order to develop a DBTT/strain map. All cups with draw ratios in the range 1.8 to 2.2 were trimmed just below the earing area. For these lower draw ratios, cups were made using a liquid lubricant. However, to obtain a draw ratio of 2.3, lubrication with teflon film was needed which resulted in wrinkling. To eliminate their presence for the impact test it was necessary to trim the cups approximately 60mm from the cup edge. Table 4 provides a summary of the various trim heights and their edge major and minor strains for the different draw ratios. As noted in the table, an additional test condition was included, namely a 2.3 draw ratio cup trimmed at a height of 70 mm from the base, producing a major strain at the cup edge of 65% which was similar to that of the full trimmed cup with a draw ratio of 2.0.

2.3.3. Effect of Thickness

A batch annealed ULC Ti-stabilized steel of varying thickness was supplied to study the effect of thickness on SCWE. Table 1 presents the thickness of the four steels identified as S4a -S4d, and Table 2 presents their base chemical compositions. Two-inch cups with a draw ratio of 2.0 were produced for each of the four steels and tested using the cup expansion procedure described previously. Although every effort was made to sample material varying only in thickness, some variability in both chemistry and processing conditions were evident. Given this variability it was decided to machine the walls of the cups produced from steel 4d which had a thickness of 1.70 mm down to a thickness of between 0.72-0.79 mm to a height of ~15 mm from the trimmed edge. In one instance a cup was machined to a thickness of 0.50 mm. Following machining the cups were tested using the expansion test procedure.

2.3.4. Effect of Impact Speed

Steel S3 was also chosen to examine the effect of impact speed on the DBTT. Tests were performed on 6-in. cups using the standard free drop height of 1 m and a maximum drop tower height of 2.92 m. These heights translate to indentor travel speeds at impact of 4.34 and 7.41 m/s.

2.3.5. Effect of Edge Condition

Steel S3, a rephosphorized ULC fully stabilized steel without boron, expected to have moderate/high SCWE sensitivity, was chosen to examine the effect of flanges and edge cracks or notches on the DBTT. To examine the effect of flanges on the DBTT, 6-in. flanged cups with draw ratios of 2.0 and 2.3 were produced. The cups were flanged at a height of 100 mm which resulted in a flange width of 15-20 mm in the case of the 2.0 draw ratio cups and 40 mm for the higher draw ratio cups. Impact tests were performed over a range of temperatures to compare the results with the full trimmed cups. Given the limited amount of steel S3 remaining following development of the DBTT/strain map and effect of flanging, it was not possible to conduct several tests to examine the effect of notches on DBTT. Six-inch cups with draw ratios of 1.8 and 2.0 were trimmed to heights of 85 and 105 mm, respectively. Notches were machined using a fine diamond blade. In two of the 1.8 draw ratio cups 4 notches were machined; 2 to a depth of 3 mm diametrically opposed to each other and 2 others 4 mm deep 90° to the 3 mm notches. One of the 1.8 draw ratio cups also received a single notch machined to a depth of 1 mm. These 3 cups were then impact tested each at a different temperature which was selected based on the DBTT measured from the unnotched cups. In addition, two of the 2.0 draw ratio cups each had two notches machined to a depth of 2 mm at positions 180° to each other. In a few cases, the 2.0 draw ratio cups exhibited delayed cracking at the cup edge after trimming. These cups were impact tested along with the machined notched cups again to temperatures which were determined from the unnotched cups at this draw ratio.

2.4. REAL PART TESTING

Following discussions with AISI project sponsors two real parts were fabricated for testing and correlation with laboratory test results. The parts were specially fabricated for this study using commercial steels provided by some of the participating companies. The parts were stamped on commercial dies, but the steel used was different than the steel employed for commercial production. No tests were conducted on real parts made of production material; however, some production parts were used to evaluate the strain. The stamping trials were coordinated by CANMET.

The first parts chosen were a deep drawn shock tower (DaimlerChrysler minivan front shock tower). Figure 7 shows a gridded stamped specimen used for strain evaluation. This part was stamped at Windsor Tool and Die in Windsor using a pre-production die. Steel S5b, a low transition temperature ULC steel stabilized with Ti, containing boron and a more sensitive steel, S6a, which was a batch annealed type grade stabilized with Ti, were selected for this component. The stamping shown in Fig. 7 comprises 4 individual parts which are stamped simultanously (2 left-side, LS, and 2 right-side, RS specimens), and each part is then laser cut from the stamping. A finished RS shock tower specimen is shown in Fig. 8 showing regions of major strain corresponding to 50-60% and 70-80%. The forming strains were similar in both parts.

The second part was a structural suspension floor panel (DaimlerChrysler LH rear suspension floor panel) which is shown in Fig. 9, with less highly strained regions compared to the shock tower. The blanking operation was performed at Massiv Tool and Die and the panels stamped at Daimler Chrysler

in Bramalea using a production die. The part was made with a low-sensitivity galvanneal Ti/Nb stabilized IF steel and a high-sensitivity hot dipped rephosphorized IF steel. The press was initially set up for forming non-rephosphorized galvanneal IF steels, and problems were encountered when forming the rephosphorized hot-dip galvanised material. Wrinkles formed in the deep drawing region. The blank holding force was increased to overcome the problem but most of the finished parts had wrinkles. The presence of those wrinkles did not affect the results of this study.

Figure 8 contains arrows indicating the regions of high major strains, which were chosen for localized impact testing. Localized impact testing was carried out using the 6-in. cup drop weight tester which was modified as shown in Fig. 10. A tup 15 mm in diameter with a rounded end was used as an indenter with a collar attached as shown. The shock tower specimen was aligned with the aid of a support pipe so that the region of interest was impacted by the tup with the collar limiting the tup extension into the sample to 5 mm. The shock tower specimen instrumented with 2 measuring and 1 control thermocouple was placed in position in the cooling box on the support pipe and cooled using a liquid nitrogen mist down to various temperatures of interest. After temperature stabilization for 15 min, the cooling box was removed and the tup released from a height of 1 m. Above the DBTT for the given region of interest the tup impact only succeeded in plastically deforming the sample; however, below the DBTT brittle fracture occurred. Sufficient test were conducted to satisfy the same DBTT criterion as the 6-in. cup test namely the transition temperature being the lowest temperature at which at least 4 out of 5 cups did not fracture. To examine the effect of general impact on the full part, the shock tower sample, oriented as shown in Fig. 11, was impacted using the CANMET drop weight tester after being cooled down to various temperatures.

Tests on the floor suspension panels were conducted at Fleet Technology using their drop weight tester. This equipment which is shown in Fig. 12 consists of a hemispherical impactor has two circular discs to provide a guide to the falling impactor inside the pipe. The total weight of the impactor with these attachments is 49.7 kg (109.5 lb). The 305 cm (10 ft) length pipe was employed to guide the impactor under gravity with a clearance between the impactor and the pipe of approximately 3 mm (0.125 in.). The pipe was rigidly fixed to the steel base by 3 legs. There was a 40 cm (16 in.) clearance space between the base plate and the pipe in order to ensure sufficient clearance for positioning of test pieces. After each drop test, the impactor was pulled up through the pipe by a cable and pulley arrangement using a winch system. The impactor was then hooked to an easy release block. Both pulley and the block were attached to the roof truss. This ensured that the impactor height was always fixed at 320 cm (10.5 ft) above the steel base plate. The parts to be tested were enclosed in Styrofoam boxes and cooling was carried out by liquid nitrogen spray. A solenoid valve, activated by the difference between the set point and the actual temperature, controlled the liquid nitrogen spray to achieve the set temperature. The solenoid valve regulates the liquid nitrogen spray to achieve temperature stability. The controlling limit of this cooling arrangement is ±2°C at the point of measurement.

In an attempt to produce a brittle fracture in the floor suspension panel various regions of higher strain indicated as 'A' and 'B' in Fig. 9 were chosen as locations for impact testing with the component positioned in various orientations and in one instance on support rollers to create 3-point bending. Figure 14 shows an example of this latter test condition. Some tests were carried out without the use of

the drop weight tester, in an attempt to produce local impact of region A which was considered to be the most susceptible region of this part. These tests include the use of a 6.8 kg (15 lb) sledge hammer and both a conical and hemispherical punch. In all tests the specimens were cooled to about 10°C below the selected test temperature. Once this temperature was reached, the specimen was removed from the cooling box and carefully placed under the pipe in the pre-selected support position so that the impact point coincided with the center of the pipe. Once the specimen warmed up to the desired test temperature, the impactor was released and dropped under gravity. After the test, photographic documentation was performed to display typical deformation and any cracking in the region of impact. Further observation of the entire part was subsequently carried out with the objective of determining any damage remote from the point of impact.

2.5. METALLOGRAPHY

A quantitative measurement of grain size was carried out on those steels which were used in the parametric study, namely S1, S2, S3 and S4a - 4d in the as-received unstrained condition. Both plane (after removal of coating and surface layer to a depth of 30 μm) and through-thickness sections were initially cleaned ultrasonically using acetone and then chemically polished. The samples were then examined in the scanning electron microscope in the back scattered electron (BSE) imaging mode which provided contrast as a result of grain misorientation. Ten images were taken for each material at an appropriately determined magnification and a standard circle intercept method applied to obtain a measure of grain size.

2.6. FRACTOGRAPHY

Notched unstrained and prestrained samples were taken from steels S1, S2, S3 and S4a as described in Section 2.2.3 on *fracture of notched specimens*. Following fracture in liquid nitrogen, the specimens were prepared for scanning electron microscopy. The purpose of fractographic observation for these specimens was to make a quantitative measurement of the percentage of intergranular fracture according to ASTM E562-95 specification at the center thickness. Quantitative measurement of intergranular fracture was conducted using a manual point counting technique. It was important to select the appropriate grid size and magnification as described in the standard to ensure a valid measurement was made. A total of ten fields of view were examined for each specimen. The fracture morphology was also examined as a function of location from edge to center.

In addition the fracture surfaces of selected 2-in. and 6-in. cups were examined after impact testing as well as selected locations of fractured samples after large scale testing. As explained previously some of the 6-in. cups exhibited edge fractures after drawing and trimming prior to impact testing. Several of these samples were also examined in the SEM.

2.7. AUGER

The segregation at grain boundaries in steels S1, S2 and S3 was investigated using Auger Microscopy. Auger spectra and secondary electron (SE) photomicrographs were collected using a Perkin- Elmer model PHI 600 scanning Auger microprobe (SAM). The specimen shown in Fig. 5 was fractured in-situ in the Auger microscope to avoid contamination with air. The Auger specimens were cooled by convection with liquid nitrogen; however, because of the temperature loss during cooling, the temperature of the specimens did not reach the liquid nitrogen temperature, as was the case for the notched specimens immersed in liquid nitrogen. The temperature of the Auger specimen was estimated to be -100°C when fracture occurred. The base pressure of the UHV chamber during fracture and subsequent data collection was $< 5 \times 10^{-10}$ mbar to minimize the rate of surface contaminant deposition onto the freshly exposed grain surfaces. A special copper holder was fabricated and a modified fracture protocol developed to permit the rectangular sheet steel coupons to be fractured using this hardware originally designed to accommodate only rod-shaped specimens.

Immediately upon fracture a steel coupon was transferred to the analytical stage for SE imaging and Auger spot and/or mapping analysis; a step requiring about 5 min. Typically 8-10 Auger spectra were generated in approximately the first hour following a fracture. Separate tests using ion-beam cleaned metal coupons showed no detectable growth (deposition) of any volatile contaminant species (C, O, etc.) for times exceeding 1 h when this UHV chamber was maintained at $< 8 \times 10^{-10}$ mbar pressure.

2.8. SECONDARY ION MASS SPECTROMETRY

Secondary ion mass spectrometry (SIMS) studies were performed on polished specimens using a Cameca IMS4f magnetic sector SIMS instrument. For the detection of C, N and P, a Cs^+ primary ion beam was used and negative secondary ions were detected. For B, however, a O^{2+} primary ion beam was used, with negative secondary ion detection. Images were acquired using the multichannel plate/fluorescent screen detector on the instrument and capturing theses images with a CCD camera.

3. EXPERIMENTAL RESULTS

3.1. PARAMETRIC STUDY

3.1.1. Evaluation of SCWE Using Laboratory Simulation Tests

The transition temperature of the steels investigated was evaluated with the bend test and both the 2-in. and 6-in. cup expansion tests. The three methods were used to study how the DBTT varied for each test when evaluating steels with a wide range of sensitivity to SCWE.

Bend Test

The bend test was used to evaluate the sensitivity of steels S1, S2, S3 and S4a to secondary work embrittlement (SCWE). This method was employed to quickly evaluate SCWE sensitivity and establish a comparison with the cup/expansion test.

Figure 15 shows the bend test results for steels S1, S2, S3 and S4a. The pass rate curve was drawn for each steel based on a minimum of five tests at each temperature. The large difference in the susceptibility of the four steels to SCWE required tests to be performed from a temperature of -40°C to +90°C, which is significantly higher than for the cup test as will be shown in the next section. As the test temperature increased in the transition region for steels S1, S2 and S4a, the pass rate changed from 0% to 100% over a relatively narrow temperature range. The transition region in steel S3 was much smoother. As a matter of fact, a pass rating of 100% could not be obtained up to a temperature of 90°C. If the transition curve is extrapolated to 100% for this steel, the 100% pass rating will be at about 105°C.

In order to determine the DBTT for each steel a criterion must be adopted. In this study two criteria were considered. The DBTT was defined as the temperature at which 50% (50%-pass rate criterion) and 80% (80%-pass rate criterion) of the coupons did not fracture during the bend test. The DBTT was determined using the pass/fail rate curve. Figure 16 shows the DBTTs for the two criteria. The steels with a similar abrupt transition region (steels S1, S2, and S4b) exhibited a relatively small shift of the DBTT when the 50% pass rating was increased to 80%; the increase in the pass rate raised the DBTT by 3°C to 6°C. Due to the smoother transition curve for steel S3, the 80% pass rate criterion shifted the DBTT more significantly (DBTT with the 80% pass rate criterion is 16°C higher than with the 50% pass rate criterion). The two methods do not affect the steel ranking but they significantly affect the apparent DBTT, especially when the transition is more gradual. This emphasizes the importance in standardizing the criteria for this test.

2-in. Cup/Expansion Test

For this test, the criterion defined in the GM9920P procedure was used to determine the DBTT. According to the procedure, the DBTT is defined as the highest temperature at which at least two cups out of eight fracture. This criterion is equivalent to the lowest temperature at which at least 6 out of eight cups does not break (75% pass rate), and its severity would be between the 50% and 80% pass rate criteria defined for the bend test.

The GM procedure specifies that the cup height after trimming should be 2/3 the diameter of the cups ±1 mm. In the present study, if the cups were cut at 2/3 of the cup diameter (2/3·50 mm), the cup height would be 33 mm. Since the strain profile is relatively flat near the peak strain, the trimming position is not critical. Trimming at a position equivalent to 2/3 of the cup diameter (33 mm for 50-mm cups) translates to strain at the edge close to the peak strain in the wall (see strain distribution in Fig. 17 for three sheet thickness). In this study, the thinner gauge S1, S2, S3 and S4a cups were cut at 31 mm

and the remaining cups were cut at 33 mm, providing a major strain at the edge of the cups in a range 55% to 60%.

The steels used in this study had various degrees of anisotropy that led to cup earing. Trimming of the cup edge aims at the elimination of the ears, however the phenomenon is associated with strain and wall thickness variation across the circumference. The effect of planar anisotropy on major and minor strain at three angular positions in steel S3 is shown in Fig. 18. The wall thickness variation in cups made with S3 and S4b steels is depicted in Fig.19 and 20. The planar anisotropy had generated a thickness variation of about 2 and 8% in S3 and S4b steel cups respectively at the position where each cup was trimmed. The planar anisotropy of steel S4b was not evaluated in this study, but the large earing suggests a strong planar anisotropy, which may affect the formation of the SCWE cracks at the cup edge through the effect on wall thickness. The effect of wall thickness on SCWE crack formation will be discussed later in this section.

The DBTTs of the twelve steels investigated in this study were evaluated. The results are presented in Table 5. The DBTT of the four steels with similar thickness (S1, S2, S3, S4a) was between -0°C to -70°C. The S4 series steels used for the study on the effect of thickness showed a DBTT between -10°C and -45°C. The DBTT of the low-sensitivity steel S5b and high-sensitivity steel S6a used for the fabrication of the shock tower was –50°C and –10°C respectively, which can be considered as appropriate for the tests on real parts. The low-sensitivity (S5a) and high-sensitivity (S7) steels employed for the suspension floor panel had a DBTT of -≤70°C and -30°C respectively. The DBTTs for the those two steels were lower than expected, especially steel S5a which did not fracture at temperatures as low as -70°C. Steel S6b used for the fatigue study had a DBTT of -20°C.

The DBTT measurements made using the 2-in. cup/expansion test have highlighted some interesting facts such as:

- the beneficial effect of boron in steels S2 (-40°C) and S5a (≤70°C);
- the beneficial effect of free carbon in steel S1 (-70°C), even in presence of P;
- the detrimental effect of batch annealing in steels S6a (-15°C) and S6b (-20°C); and
- the detrimental effect of phosphorus in steel S3 (0°C) without boron or free carbon.

The following surprising results were however observed:

- steel S7 (-30°C) had a relative low DBTT in spite of a high P content and high yield strength;
- the series S4 produced by batch annealing showed a wide spread of DBTT (-10°C to -45°C).

Those results suggest that chemistry and annealing process are not the sole indicators of SCWE.

6-in. Cup Expansion Test

This test was specially developed at CANMET for this study to scale up the 2-in. cup test in order to investigate the effect of test conditions on SCWE. The strain distribution in the wall of a 6-in., DR = 2.0, cup is shown in Fig.21. Similarly to the 2-in. cups, the peak strain is observed at a height of about 2/3 of the cup diameter (2/3·150 mm = 100 mm). The 6-in. cups made with a draw ratio of 2.0 showed a peak strain of about 65%, which is slightly higher than the 55 to 60% observed in the 2-in. cups. The 6-in. cups were trimmed at 105 mm from the base. The DBTT values for 4 steels obtained with the 2-in. and 6-in. cups are given in Table 6 and plotted in Fig. 22. The comparison of the DBTT revealed that the 6-in. cup generated a DBTT 10 to 15°C higher than the 2-in. cups. This effect can be considered significant given the resolution of the cup test estimated at ±5°C.

The fracture in both 2-in. and 6-in. cups was quite similar. At temperatures near DBTT, a brittle crack formed at the edge and propagated in the lower strain region of the wall toward the cup bottom. A transition from brittle fracture to ductile fracture was clearly observed in each cup, indicating that as the brittle crack propagated toward lower strain regions, the fracture mode changed to transgranular ductile before the crack arrested at the bottom of the cup. The transition from brittle to ductile fracture occurred at a lower strain (closer to the cup bottom) at lower test temperature. At a temperature significantly lower than the DBTT more than one crack was occasionally observed. Although fractures occurred in a brittle manner at temperatures near DBTT, a significant amount of plastic deformation took place before the initiation of a brittle fracture. Figure 23 illustrates this phenomenon for steel S3, where the amount of flaring at various temperatures below and above DBTT is depicted. The flaring values given in the Figure represents the displacement of the cup edge (refers as flaring index below in the text) from its original position after the cup/expansion test. This flaring value increases with the expansion of the circumference of the cup edge. From the expansion of the cup circumference, plastic strain at the edge of the cup can be estimated. Near the transition temperature the flaring index reached about 5.5 mm for steel S3, which translates in a hoop strain of 7.3%. As the test temperature dropped below DBTT, the amount of flaring decreased to reach a flaring index of 0.5 mm (0.7%) at a temperature 15°C below DBTT. At this temperature, two cracks formed in one specimen. In this specimen the formation of two cracks coincided with conditions during impact loading where secondary plastic strain was negligible. At the DBTT ductile flaring was also observed in 2-in. cups. A hoop strain between 7 and 8% was observed and the cups fractured near the DBTT of steel S3.

The impact energy has not been measured during the cup/expansion test, however the flaring index might be a good alternative to direct measurement of fracture energy since this parameter is related to the hoop strain, which is a direct measurement of the plastic deformation before brittle fracture. The potential of this method has not been fully investigated in this study. Its utilization however would be more difficult if the smaller 2-in. cups are used because the flaring index is proportional to the cup diameter.

Similarly to the 2-in. cups, the 6-in. cups showed earing and wall thickness variation. Figure 24 showed the thickness variation at the edge of a 6-in. cup with a 2.0 draw ratio. A thickness variation of 7% was observed. This value was higher than the 2% value reported previously for a 2-in. cup made with steel S3. Figure 25 illustrates the wall thickness variation and the position of SCWE cracks in two S3 steel

cups. The position of the SCWE cracks in the regions of smaller wall thickness indicates that the thickness variation due to sheet planar anisotropy affects SCWE crack formation.

Notched specimen test

The notched specimen test has been used in this study to generate brittle fracture in un-strained and prestrained coupons taken from the wall of cups. The specimen geometry was identical to that used for Auger microscopy. The test is appropriate to generate fracture parallel and normal to the grain elongation direction of prestrained specimens, which is not possible with other methods. Fracture observations on notched specimens fractured in liquid nitrogen are presented in Section 3.5 on this report.

The authors have also used this technique to generate DBTT in the transverse and longitudinal orientation (Martin et al., 2000). Table 7 shows a comparison between notched specimen DBTT and cup/expansion DBTT for material prestrained with a major strain in a range 40 to 67%. A significant lower DBTT was found with the notched specimen test. The low temperature needed for the tests on the low-sensitivity steels S1, S2, S4a did not permit the characterization of their DBTT with the notched specimen test. To use this method for DBTT measurement, modification of the impact method will be needed to increase the DBTT to more workable temperatures.

3.1.2. Effect of Strain

A DBTT/strain map was generated using steel S3 by testing 6-in. cups with draw ratios varying from 1.8 to 2.3 trimmed mostly at peak strain, but in some cases at lower strain. Figure 26 shows the strain distribution and trimming location for each of these draw ratios. The trimmed positions are identified in the figure with the letters C, which corresponds to the 1.8 draw ratio through to G identifying the location for a draw ratio of 2.3. Cups which had received draw ratios of 1.8, 2.0, 2.1 and 2.2 were trimmed just below the earing at heights of 82 mm, 105 mm, 120 mm and 125 mm corresponding to edge major strains of 52, 65, 69 and 100% respectively. In the case of the 2.3 draw ratio it was necessary to trim the cup at a height of 105 mm to avoid the wrinkling produced during forming using the teflon film. This still resulted in an edge major strain of 100%, higher than that observed in the lower draw ratios. As stated previously, for one of the test conditions, the 2.3 draw ratio cup was trimmed to a height of 70 mm indicated in Fig. 26 as G" and having an edge major strain of 65% which was equivalent to the fully trimmed cup with a draw ratio of 2.0. Table 8 summarizes the trim height, strain at the cup edge and presents the measured transition temperature for each of the above described conditions, together with results for the 2-in. cup. This information has been transferred to a FLD as a DBTT/strain map as shown in Fig. 27. In general the strain along the cup wall can be shown as straight lines where the ratio of minor to major strain remains constant and the slope of the line varies with draw ratio. The results are presented in the form of the letters C to G representing the edge strain condition for each of the raw ratios together with its DBTT. G" represents the trimmed 2.3 draw ratio and D" represents the 2-in. cup. It can be seen that the DBTT increases from -10°C to +10°C for the fully

trimmed cups between draw ratios of 1.8 and 2.2 which represent edge major strains of 52% and 90% respectively. This observation is consistent with results previously reported in the literature. However, at a draw ratio of 2.3 the DBTT decreases to -5°C. Another inconsistency in the results which makes the production of the DBTT/strain map more complex than previously expected is the difference in DBTT observed between the fully trimmed cup at a draw ratio of 2.0 and the 2.3 draw ratio cup trimmed at 70 mm. Both of these cups have a major strain at the edge of the cup of 65% yet the DBTT for the 2.3 draw ratio trimmed cup is 50°C below that with a draw ratio of 2.0.

To further investigate these inconsistencies it was decided to measure the residual stresses at the cup edges for the cup conditions whose results are summarized in Fig. 28. Strain gauges were attached to the edge of cups at three locations 120° apart to measure the hoop strain change occurring when the material containing the strain gauge was removed using a fine blade saw. A cup to which strain gauges were attached is shown in Fig.29 prior to their removal. Table 9 presents the strain gauge data which reveals some interesting differences. For the cup with a draw ratio of 2.3, trimmed at a height of 70 mm which had a DBTT significantly below that for the fully trimmed 2.0 draw ratio cup, the hoop residual microstrain was less than half that of the latter cup. A less significant but consistent difference was observed for the two fully trimmed cups with draw ratios of 2.0 and 2.3. The cup tests had revealed a drop in DBTT with increasing draw ratio, however a lower residual hoop strain was observed for the higher draw ratio cup as shown in Table 9. The mechanism by which these residual stress differences can affect the DBTT is unclear and further work is required to gain a better understanding of these anomalies. It is clear that strain has a significant effect on DBTT but its effect seems to be influenced by other factors. For this reason, the DBTT strain map generated by the cup test could encompass the effect of other factors.

3.1.3. Influence of Sheet Thickness on DBTT Cup/Expansion

Material thickness may play an important role in brittle fracture because it affects the stress condition during impact. To investigate how DBTT cup/expansion is influenced by sheet thickness, DBTT were measured in steels with thickness varying from 0.77 to 1.42 mm. The tests were performed on S4 series steels. Figure 30 shows the DBTT cup/expansion results obtained with 2-in. cups. The sheets with intermediate thickness, 1.02 and 1.26 mm, had the lowest DBTT, which does not support the assumption that DBTT might decrease with a reduction of thickness. Although, the chemistries of the S4 series steels were quite similar, some differences in the processing conditions were used to produce the sheets in this thickness range, namely cold reduction. Figure 31 shows the cold reduction used for each steel. The Figure shows that the thicker gauge materials, S4c and S4d were produced using a significant lower cold reduction. It is possible that DBTT results encompass the effect of cold reduction on SCWE; this effect being superimposed on a possible thickness effect.

In view of the difficulties to determine the effect of thickness with the steels supplied, an alternative method was adopted. The wall of some cups made with the thicker material was machined to determine if cups with a reduced wall thickness produce the same DBTT as the as-drawn trimmed cups with the original wall thickness. Figure 32 shows brittle fractures in as-drawn and reduced-wall trimmed cups. For this study, the outside wall was machined over a distance of about 15 mm. The results

obtained with reduce-wall cups (0.51 to 0.79 mm reduce-wall thickness) are compared to the pass/fail results obtained with as-drawn trimmed cups in Table 10. Pass/fail tests were made on a limited number of specimens, however the two pass-specimens obtained at the DBTT and 5°C lower suggest that smaller wall thickness does not shift the DBTT to a lower temperature. This result suggests that the effect of thickness in sheet in a range 0.51 to 1.42 mm does not play an important role in SCWE.

3.1.4. Effect of Impact Speed

Unless stated otherwise, the speed of the 6 in. cup/expansion tests presented in this report was 4.34 m/s (15.6 km/h). This speed was obtained with a plunger droppe from a height of 1 m. Some tests were also performed with a plunger dropped from a height of 2.92 m. The corresponding speed was 7.41 m/s (26.7 km/h). Table 11 shows the pass/fail results for the two speeds. The increase in speed raised the DBTT by 5°C, from –30°C to –25°C, in steel S2 with a 2.0 draw ratio.

The strain rate ($\dot{\varepsilon}$) during the cup expansion test can be calculated using the following equation:

$$\dot{\varepsilon} = C\text{-}C_o / C_0 \cdot t, \qquad (1)$$

where the term C - C_0 is the difference between the initial and final cup circumference after the time t during impact. In its simplified form, the strain rate can be calculated from the equation:

$$\dot{\varepsilon} = v \cdot \tan (90\text{-}\theta)/r_0, \qquad (2)$$

where θ is the cone angle, v is the punch impact velocity and r_0 is the cup initial radius.

For the same impact speed, the equation indicates that the strain rate increases with a decrease in cup diameter. In this study, the strain rate was estimated at: 32.9 s^{-1} for the 6-in. cup, 1 m-height; 56.2 s^{-1} for the 6-in. cup, 2.92-m height; 98.5 s^{-1} for the 2-in. cup, 1-m height.

3.1.5. Effect of Edge Condition

Flanges with widths of 40mm and 15-20 mm were produced on cups with draw ratios of 2.3 and 2.0 respectively. Figure 33 shows the strain distribution for these cups together with that for the full drawn cups. The diagrams indicate that the major strain at the edge of the trimmed cups is marginally above that for their corresponding flanged cups. The results of impact testing the flanged and unflanged cups are given in Table 12 which suggests, even with the limited number of tests performed for the 2.3 draw ratio flanged cups, that there was no significant difference in the transition temperature between the two edge conditions. For the 2.0 draw ratio flanged cups impact testing produced bending along the flange as shown in Fig. 34 indicated by the arrows. In all instances for this flanged cup, fracture occurred at this position . In the case of the cups with a 2.3 draw ratio and larger flange width no significant difference in transition temperature was observed compared to the full drawn trimmed cups. However

for this flanged cup, fracture initiation occurred not at the cup edge which was the case for the 2.0 draw ratio flanged cup but at the maximum cup height at the flange radius.

From the limited tests conducted on notched cups there is no significant influence of notches or pre-cracks on DBTT compared to that measured from the fully trimmed cups. The results obtained for the cups tested at a draw ratio of 1.8 show that cups with both 3 and 4 mm notches when tested at 0 and +10°C produced ductile fracture extending from the notch location rather than the plastic collapse which occurred in the fully trimmed cups. The observed DBTT for the fully trimmed cups at this draw ratio was -10°C. Tests conducted on the 2.0 draw ratio cups containing machined and pre-cracked cups produced results which are summarized in Table 13 showing that at +10 and +21°C both pre-existing cracks produced ductile fractures initiating at the pre-cracks. Two tests also conducted on the machined notched cups at 0°C, shown in Fig. 35 produced one ductile fracture which initiated at the notch location and one brittle fracture which originated remote from the notch location. Although these data are rather limited it seems to indicate that there is a negligible effect of notches on DBTT for this steel in 6-in. cups.

3.2. FORMATION OF SCWE CRACKS DURING FORMING

Brittle fracture during forming was observed in two situations. First, brittle cracks formed during forming 2.3-draw ratio 6-in. cups. Figures 36a and 36b show a crack at the edge of an as-drawn cup. The strain in the region where the crack formed is shown in Fig. 37. Clearly, the figures illustrate that the crack did not initiate in the largest strain region of the cup. In Fig. 38, the strain in the cup wall, including the region where the crack was observed, is compared to the forming limit diagram (FLD). The figure shows that the strain is well below the forming limit. Fractographic observations made on fractured cups showed intergranular fracture. Those observations indicate that the edge cracks were SCWE cracks formed during forming. The observation of the cup wall near the edge revealed some small cracks, which did not initiate at the edge but at the cup wall outside surface. Some of those cracks appeared to be associated with buckling in the flange during forming. Buckling creates surface tensile stresses normal to the direction of grain elongation similar to the condition observed during cup/expansion test. This steel (S3) had a DBTT of +10°C when tested using the 6-in. cup with a strain of 65% at the edge (0°C with 2-in. cups). The strain in the area where the cracks were found was between 60% to 80% with the lowest strain near the edge. This strain level at the cup edge is close to the strain in cups with a draw ratio of 2.0. Thus it can be assumed that DBTT in this area should be about +10°C (DBTT for steel S3). If we account for the additional surface strain in the buckling area it is possible that the DBTT was close to room temperature in the buckling area. However, the brittle fracture was observed at room temperature in quasi-static forming condition (deep-drawing) that should lower significantly the DBTT. In such condition, DBTT should have been below room temperature.

In this study it was not possible to clearly confirm that edge cracking produced after forming as a result of delay cracking. However, some edge cracks were observed in cups after edge trimming (some of those cups were tested, see Section 3.1.5). Those cracks were not noticed before machining. This phenomenon needs confirmation, but it is believed to be associated with large residual stresses. The formation of residual stresses in deep drawn cups is further discussed in Section 3.1.2.

Brittle cracks were also observed in oil pan specimens made with steel S6b. Those specimens were used to sample the fatique coupons. SCWE cracks formed in the deepest draw section of the pan during forming and during part handling (Fig. 39a). As for the cups, the brittle fracture occurred at room temperature. Some long cracks had propagated from the edge to several centimeters in the wall (Fig. 39b, crack B) but many shorter cracks (Fig. 39b, cracks A and C) were only present at the bend radius suggesting an initiation at the radius. Clearly, this observation shows that cracking did not initiate at the flange edge as a result of flange bending during secondary forming operation. The DBTT obtained on 2-in. cup with a draw ratio of 2.0 was -20°C. However, the strain in the draw corner of this part is significantly higher than in the cup test with a 2.0 draw ratio. Strain in the draw corner of such a part probably exceeds 100%. The opening of the cracks suggests the presence of large residual stresses in the oil pan draw corner, which would explain the formation of the cracks.

3.3. LARGE SCALE PART TESTING

Localized impact testing of the shock tower samples was carried out at two locations as identified in Fig. 8 for both steels 6a and 5b. Above the transition temperature the denting was present at the point of impact as shown in Fig. 40 whereas below the transition temperature in all cases brittle fracture occurred extending in the direction the sample was drawn during production. An example of this fracture is given in Fig. 41. Testing was carried out to generate a DBTT based on the same criterion applied to the 6-in. cup tests. Tables 14 and 15 present a summary of the test results for steels 6a and 5b respectively with values of the DBTT obtained from the cup tests. For shock towers manufactured from steel 6a and impact tested locally in a region of strain between 50 and 60% the DBTT was -30°C, 15°C below the DBTT obtained for the cup test. At a higher level of strain estimated to be between 70 and 80% the DBTT of the shock tower specimens increased to -20°C. For steel 5b which exhibited a DBTT of -50°C for the 2-in. cup test, localized testing of the shock towers again revealed a lower DBTT than the cup tests. In this case the lower strained (50-60%) and higher strained (70-80%) regions of the shock towers produced DBTT's of -70°C and -65°C respectively. When the full shock tower samples were impacted it was necessary to reduce the temperature well below that used in the localized tests in order to generate brittle fracture. For steel 6a tested at -30 and -40°C flattening of the shock tower occurred as shown in Fig. 42 . The geometry of the part and the orientation of the impact had created bending of the flanged area close to the region of high strain as shown in Fig. 43. At a temperature of -60°C brittle fracture did occur initiating close to the flange indicated by the arrow in Fig. 44 propagating in the same direction as observed for the localized impacting tests, with fracture continuing in a brittle manner and arresting when it reached the curved edge as indicated by arrow B. The less sensitive steel, 5b, did not fracture until a temperature of –90°C was reached, brittle fracture again occurring at the flange and following a path in the direction of grain elongation and continuing to the free edge in one direction and extending to the curved region. In this case close to the crack arrest location the fracture transformed from brittle to ductile with the ductile tearing extending 10 mm before arrest.

Tests conducted at Fleet Technology did not result in brittle fracture for any of the tests carried out on the floor panels. Table 16 presents a summary of the tests carried out on this large scale part indicating

that drop weight testing was conducted at temperatures between -33 and -75°C at various locations as identified in the table and shown in Fig. 9. In one instance, (Fig. 14) this part was supported on rollers to generate three point bending. The impact location is show in Figs. 45a and 45b immediately prior to and after impact, clearly showing that plastic collapse had occurred without any fracture.

3.4. METALLOGRAPHIC EXAMINATION

Metallographic observations were made on the steels used for the parametric study and steel S6b employed for the fatigue study to determine the grain size. Table 17 shows the average grain size for each steel. The batch annealed grades S1, S4a, S4b and S4c had larger grain sizes than the continuous annealed grades S2, S3 and S6b. Figures 46 and 47 show the typical grain microstructure of steels S1 and S2 respectively. The grain microstructure of steel S3 was similar to steel S2. The microstructure in the cross section of S4 series is shown in Figs. 48-51. The Figures show that the grain size of steel S4a, S4b and S4c was quite similar. It was however not possible to determine the grain size of steel S4d because a significant fraction of the surface was composed of grains poorly defined when observed by back scattered electrons in SEM. The typical aspect of the microstructure of steel S4b is shown in Fig. 51. Metallographic examination made at larger magnification (Fig. 52) showed that the areas with a poorly defined grain structure were composed of flat elongated grains mixed with small equiaxed grains, which is an indication that the steel was not fully recrystallized. Figure 53 reveals the grain microstructure near the surface at a lower magnification. The Figure shows that the islands of non- or partially recrystallized grains are not limited to the sheet surface; the same feature was observed throughout the entire cross section of the sheet. Such a microstructure may affect the mechanical properties of the steel as well as SCWE.

3.5. FRACTOGRAPHY

3.5.1. Notched Specimens

Small size notched specimens have been fractured by impact to assess the effect of strain on the fracture mode. This technique has also been used to determine the effect of the crack orientation on SCWE when fracture occurs parallel and normal to the orientation of grain elongation in deformed material. A summary of the percentage of intergranular fracture in strained and unstained notched specimens is given in Table 18.

Notched specimens were broken by impact near liquid nitrogen temperature in air to compare the fracture surface of samples S1, S2, S3 and S4a in the unstrained condition. Figure 54 shows the fracture surfaces for these steels with their figure captions indicating their DBTT as measured using the 6-in. cup test and % of intergranular fracture. The fracture surface of steel S1 as seen in Fig. 54a was found to be mostly cleavage while steel S2, which contained boron, fractured with a mixed cleavage/intergranular mode and contained a zone approximately 50 μm deep below the surface which was primarily intergranular. The fracture surface of the rephosphorized B-free steel, S3, revealed

mostly intergranular facets. In the case of steel 4a it was interesting to note that the fracture surface consisted of large cleavage facets with smaller intergranular facets as shown in Fig. 54c.

Prestrained notched specimens were also fractured by impact in liquid nitrogen to compare the fracture surface of strained specimens with that of unstrained specimens. The prestrained specimens were taken from the wall of the 6-in. cups in a region where major strain was between 55 and 60%. The specimen/notch was oriented to produce a fracture parallel and transverse to the direction of grain elongation. Figure 6 shows the location of the test specimen in the cup wall. It was found that crack orientation had a significant effect on the fracture mode. Figures 55 and 56 present micrographs of the fracture surfaces for the LN and TN orientations respectively. Cleavage fracture remained dominant for the steels S1, S2 and S4a fractured with the notch normal to the grain elongation direction (TN orientation). For samples fractured with the notch parallel to the grain elongation (LN orientation) the % of intergranular fracture increased with the steel's sensitivity to SCWE. Steels S1, S2 and S4a revealed a higher fraction of intergranular fracture in the LN orientation compared to the unstrained material. The effect of strain on the % of intergranular fracture was, however, negligible on steel S3, although it was found that strain does affect the transition temperature in the cup test. As in the case of the unstrained condition, steel S2 in the strained condition for both orientations showed a higher fraction of intergranular at its surface. Observations made at the surface of steel S3 also revealed more intergranular fracture than in the centre of the specimen, however the effect was more difficult to quantify since this steel showed a high fraction of intergranular fracture over its entire surface.

3.5.2. Bend Test/Cup Test Specimens

Fractographic analysis was carried out on bend test samples fractured near their transition temperature near the surface at the inner radius. Since the bend specimens had only partially fractured during the bend test, they were fully broken by hand at ambient temperature to produce full fracture. Steels S2 and S3 exhibited mainly intergranular fracture with some cleavage. The low-transition temperature steel, S1, was characterized by mixed cleavage with some ductile fracture. Figure 57 presents micrographs showing the fracture morphologies for the bend test samples. Compared to the cup test (results below) the bend test fracture surfaces showed more ductile tearing which is probably due to the higher test temperature used for the bend test.

A fractographic examination was also performed on 6-in. cups with a draw ratio of 2.0 after fracture just below their DBTT for steels S1, S2, S3 and S4a. This region corresponded to a major strain of 65%. The typically observed fracture morphologies for these steels were very similar to the fracture notched specimens in the LN orientation. Steel S1 as in the case of the notched specimen consisted mostly of cleavage fracture with the % of intergranular fracture estimated between 15 and 20. Steel S2 was found to be mostly intergranular (80%) with a layer approximately three grain widths deep adjacent to the surface which was fully intergranular. Steel 4a again showed a similar fracture appearance to the fractured notched specimen with a mixed fracture containing large cleavage facets with finer regions of intergranular fracture estimated to occupy 70% of the surface. Steel S3, the most sensitive to SCWE, was found to be between 90 and 95% intergranular. In one instance the fracture surface of an S3 cup

with a draw ratio of 2.3 trimmed at a height of 70mm to give an edge major strain of 65% was examined for comparison with the fully trimmed 2.0 draw ratio cup from the same steel. The fracture surface was found to be approximately 90% intergranular which was very similar to that observed for the 2.0 draw ratio. The fracture surfaces were also examined along the length of the crack for the two most sensitive steels, S3 and S4a. This revealed a decrease in the fraction of intergranular fracture as a function of distance from the edge which was associated with a decrease in the major strain. Figure 58 shows micrographs for these two steels at the point of transition from primarily cleavage to regions where ductile fracture is first observed. In the case of steel S3 this occurs at a major strain of 25% whereas for the less sensitive steel the transition is at 42%.

In several instances some of the cups for S3 had cracked after forming and edge machining. An examination of the fracture surface revealed almost a fully intergranular mode of fracture. This is an interesting observation since this fracture had occurred at ambient temperature which was above the DBTT measured from the cup test.

Fractographic observations were also made at the edge of the 2-in. cups for the steels used in the large scale testing. The fracture surfaces of S6a and S5b which were used to produce the shock towers and had transition temperatures of -15°C and -50°C respectively are shown in Fig. 59. Both steels exhibited significant fraction of intergranular fracture estimated to be 80% for steel S6a and 70% for S5b. Steels S5a and S7 which were used for the production of suspension panels had DBTT's of <-70°C and -30°C respectively. The lower temperature steel contained approximately 40% intergranular fracture and steel S7 surprisingly was found to be almost fully intergranular as shown in Fig. 60.

3.5.3. Large Scale Testing

Fractrogaphic examination was confined to the shock tower specimens since no brittle fractures were observed for the suspension panels. As mentioned previously two points of impact were selected on the shock tower specimens corresponding to regions of lower (50-60%) and higher (70-80%) strain identified as L and H respectively. Samples were taken at these locations from selected shock tower samples that had fractured in a brittle manner. The fracture surfaces of steel S6a at the L and H locations are shown in Fig. 61. Both locations exhibit a significant fraction of intergranular fracture with the higher strained, H region exhibiting ~80% compared to 70% for the L region. These observations are representative of what was observed for the 2-in. cup tests in which ~80% intergranular fracture was noted. In the case of steel S5b, the steel with a lower transition temperature a lower fraction of intergranular fracture was observed for both locations compared to steel S6a. Figure 62 shows the fracture surfaces for the L and H regions of S5b revealing estimated intergranular percentages of 30% and 50% respectively. These values are somewhat lower than the 70% intergranular fracture seen in the 2-in. cup test.

3.6. AUGER ANALYSIS

3.6.1. In-situ Fracture of Auger Specimens

Auger analyses were performed on S2, S3 and S4a steel specimens fractured in-situ under vacuum. Due to the higher temperature of the Auger specimens, brittle fracture was more difficult to obtain than in the case of notched specimens immersed in liquid nitrogen. A brittle fracture was obtained in S3 and S4a specimens. Figure 63 shows a typical brittle fracture in steel S3. Near the surface the fracture revealed clearly the Zn coating and the intergranular ferrite grains underneath. Brittle fracture in steel S2 could not be obtained. All specimens fractured in a ductile manner except for a layer underneath the coating one or two grains deep, which was mostly intergranular brittle. Figure 64 shows the surface of a S2 steel specimen with cracks in the coating and, in areas where the coating was detached from the substrate, intergranular fracture in the ferrite grains. The brittle fracture underneath the coating is better illustrated in Fig. 65. No attempt was made to fracture steel S1 because of its low DBTT. Unstrained specimens only were used for the Auger observations. Although no attempt were made to fracture prestrained notched coupons in Auger, work hardening should reduce the DBTT to a temperature sufficient to obtain brittle fracture.

3.6.2 Auger Observations

Figure 66 shows a typical spectrum of a cleavage facet in steel S2. On cleavage facets, only Fe was detected at the surface, which can be expected since the P content in rephosphorised IF steel is too low to be detected by this method unless surface segregation occurs. In all grain boundary facets of steel S3, phosphorus was detected (Figure 67). The intensity of the signal varied from grain to grain and within grains. Table 19 presents typical Auger analyses obtained on 10 grains in steel S3. The phosphorus signal varied from 1.1 to 7.8 at. %. The carbon and oxygen signal was mainly due to surface contamination. Even in optimal vacuum condition surface contamination occured rapidly after specimen fracture. To illustrate this effect the time after specimen fracture is indicated in Table 19. To minimize the effect of contamination, analyses were normally performed within the hour following fracture. In general a lower phosphorus segregation was detected in steel S4a (between 1 and 2 %) probably due to its lower phosphorus content (Fig. 68). The detrimental enrichment of P at grain boundaries of this low P content IF grade produced by batch annealing appears to be the cause for its high SCWE sensitivity.

Auger analyses were performed in the region near the surface where more pronounced intergranular fracture was observed in steel S3. A Zn signal was detected in the first one or two grains beneath the galvanneal coating, which confirms grain boundary Zn diffusion in this steel. The Zn peak is clearly shown in the spectrum in Figure 67 taken at the grain boundary of a ferrite grain beneath the coating.

It was found that all Auger analyses performed near the surface revealed the presence of carbon. The cause for the high carbon signal near the surface has not been determined. In the present study, the Auger analyses were undertaken before significant surface contamination in the grains in the centre of

the specimens occurred. This was verified by measuring the intensity of the carbon peak in each analysis. It is not believed that the carbon detected near the surface is due to deposition in the microscope. Since surface carbonizing is not expected during steel processing, it is believed that oil residue in the coating could have generated the high carbon signal observed along the interface. This hypothesis is supported by the fact that no carbon enrichment was detected in the non-coated CR S4a steel. Further investigation would be needed to clarify the source of carbon in the ferrite grains near the surface.

3.7. SECONDARY ION MASS SPECTOMETRY ANALYSIS

Secondary Ion Mass Spectrometry (SIMS) is a microbeam analytical technique providing good spatial resolution capabilities (~1 μm spatial resolution) coupled with very good detection limits, which makes the technique useful to detect segregation of elements in many materials. In this study, SIMS analyses were performed on polished S1, S2 and S3 steel specimens to evaluate grain boundary segregation of C, N, P and B.

SIMS images obtained from the bake hardenable extra-low carbon steel S1 are shown in Figure 69. The O image (image mode used to reveal the grain microstructure) in Figure 69a shows the grains in an area 100 μm in diameter. The same area analyzed for P segregation (Figure 69b) did not reveal the presence of P at grain boundaries. C and N were detected at grain boundaries as shown on the image in Figure 69c obtained by combining C and N signals. Figure 69d presents a SIMS image obtained in the same area using the C signal only. The presence of free C and N in this extra-low carbon steel can explain the C and N signals detected at grain boundaries; however, the technique was unable to show P grain boundary segregation. Analyses made on steel S3 slao did not reveal P segregation at grain boundaries (Figure 70b). In this steel, the Auger analyses clearly showed significant P segregation to grain boundaries. Thus, it can be concluded that SIMS is unable to image P segregation in steel with a low P level (<~600 ppm) when the segregation occurs as a monolayer coverage due to its limited spatial resolution. The SIMS analyses made on steel S3 did not show C or N at grain boundaries (Figures 70c and 70d). This result is expected since this steel was fully stabilized. Boron was analyzed in each steel. Typical B SIMS analyses for steels S2 and S3 are shown in Figures 71a and 71c, respectively, and the corresponding O images shown in Figures 71b and 71d. Although some B was detected in steel S3, this element appeared to be present in higher quantity in steel S2. According to the steel suppliers, small amount of B should be present in steel S2 and no B in steels S1 and S3. It should be pointed out that Figure 71a does not show a continuous distribution of B at grain boundaries, but it rather suggests precipitation at grain boundaries and within grains. The fact that B could be detected and that DBTT is significantly lower in steel S2 compared to steel S3 (without B) are indications that significant B grain boundary segregation occurred. The extremely low level of B probably makes its detection difficult even if significant segregation occurred to affect SCWE.

4. DISCUSSION

4.1. DBTT MEASUREMENT WITH LABORATORY SCWE TESTS

The parametric study has shown that test conditions have a strong effect on DBTT. The DBTT can vary significantly depending on the type of laboratory test used and the conditions of those tests, because they determine many controlling factors such as the prestrain and the stress condition during the secondary deformation. In this study, the bend test and both the 2-in. and 6-in. tests were employed. An analysis of the results of each test method is presented below.

4.1.1. Relationship Between bend test and cup test

It should be pointed out that in the present study the cup draw test exhibited a DBTT much lower than the bend test. The relationship between the two tests is shown in Figure 72. The two methods showed a good relationship, especially when the cup test is compared to the bend test using the 50%-pass rate criterion. The good correlation between the two tests has also been reported elsewhere (Henning 1992, Yan and Gupta, 1997). However, inYan and Gupta's study the two methods showed similar DBTT values, whereas in Henning's work as well as in this study the DBTT-bend test values were at least 70°C higher than the DBTT-cup/expansion values. The similarities between the bend test and the cup test have been discussed by Yan and Gupta (1997) who showed that the type of deformation produced during the primary deformation and the orientation of the crack during the secondary deformation were quite similar, at least during the crack initiation stage. Both tests generate tensile stresses normal to the grain elongation direction during the secondary deformation. However, a number of differences exist between the two tests such as the amount of prestrain, strain rate and edge condition at the initiation. There is no clear explanation for the difference in bend test DBTT obtained in this study and in Yan and Gupta's work, but the difficulties in controlling the primary strain might be a key factor that could differ from one laboratory to another. For instance, Yan and Gupta (1999) reported that the bend test results are more operator dependent because of the difficulties in making consistent zero-thickness (0-t) radius bending. In a study by Lewis et al. (1998) on two rephosphorised IF steels with a thickness of 0.8 and 2.3 mm, the authors reported that they were unable to determine the bend test DBTT. Cracking was observed from –50°C to ambient temperature. The authors concluded that the bend test was too severe for SCWE sensitive steels such as high phosphorus IF grades. The present study tends to confirm this conclusion since the bend test with high rephosphorus content IF grades such as steel S3, needed temperatures in the range +50°C to +90°C in order to obtain pass-specimens.

It is difficult to identify all the factors that could explain the difference of about 70°C between the bend and cup expansion test, but strain is probably the most important contributing factor. Yan and Gupta (1997) have determined by a metallographic measurement method that the minor and major strain in 0.8 mm sheet was –80% and 233% respectively. Clearly, this indicates that DBTT could be much higher than that indicated by the 2.0-draw ratio cup/expansion test if primary strain is larger than the strain corresponding to that for 2.0-draw ratio cups. But as mentioned in Yan and Gupta's paper the

unbending stress in small radius bending part regions, such as hem flanging areas, is minimal in real service condition. Consequently, SCWE in severely bend part should not be a major concern.

The DBTT values obtained by each test depends on the criteria adopted. The severity of the criteria, whether it uses 50%, 75% or 80%-pass rating, will simply shift the DBTT values without affecting the steel ranking as far as the profile of the transition curves for each steel is similar. In order to compare the ductile-to-brittle transition region measured by cup/expansion test and bend test, the pass rate curves were drawn for both tests using steel S3. The results are shown in Figure 73. The cup/expansion test showed a significantly more abrupt curvewith a transition region extending over a temperature range of 15 to 20°C. If the 50% pass and 80% pass rate criteria be used for the 6-in. cup/expansion test, the difference in DBTT would have been about 6°C, which is similar to the difference observed for the less sensitive steels S1, S2 and S4a during the bend test. It should be noted that for a rigorous comparison the same number of tests should have been made for each method. Nevertheless, the observations suggest that the smooth ductile-to-brittle transition observed in the bend test might be specific to the bend test and to steel S3 (possibly because of its high bend test DBTT). Significantly more data scatter was observed in the bend test than in the cup test when testing steel S3. In spite of the large difference in temperature between the two tests, the fractographic examination of the bend test and cup expansion specimens showed quite similar features near DBTT. The fracture surface is primarily intergranular in the more sensitive steels and becomes mostly transgranular in the less sensitive steels. More tearing is generally observed in the bend test specimen, probably due to the higher temperature used. In the cup expansion test, the fracture near crack initiation remains mostly brittle with very limited tearing.

The bend test results reported in this study were obtained on similar gauge materials. A limited amount of information is available in the literature on the effect of thickness on DBTT. Henning (1992) showed that specimens with a reduced surface thickness (surface machined to reduce sheet thickness) had a higher DBTT than standard specimens. In a different study Yan and Gupta (1997) showed that an increase in bending radius increased DBTT. Since thicker material may lead to less strain at the inner radius if the bend radius during 0T bending is increased, thickness may affect the bend test DBTT. This phenomenon has not been investigated in the present study.

In summary, a good relationship was found between the two tests, which confirms the findings of other studies. However the control of the primary strain for the production of 0T bend appears to be a critical factor, which makes a comparison between labs difficult. Furthermore, sheet thickness is expected to affect the apparent DBTT obtained by the bend test. If this test is to be adopted, round robin tests should be undertaken to better identify the causes of the variability between labs, and possibly establish a more reliable method to control the deformation during bending. In view of the problems expected with the effect of thickness, it might be difficult to find test conditions that will eliminate this effect. In this study, the bend test was found to be reliable as a bench mark method to rank steels, although it showed significant scatter for steel S3. This problem could have been related to the high temperatures used for the most sensitive steel. A possible solution to this problem is to reduce the amount of prestrain so that the bend test DBTT will be closer to the cup test DBTT. Also from a practical point of view the 0t- bend should be replaced by a 0.5t-bend which would represent more

closely the bending condition during hem flanging. According to Yan and Gupta (1997) 0.5t bend radius decreased the DBTT by 30°C. In spite of the large difference in temperature, the bend test and cup test showed similar fracture morphology, which is an indication that the two methods are sensitive to similar grain boundary embrittlement mechanisms. The tests reported in this study were limited to similar gauge materials. In view of the work on effect of thickness reported in this study, the effect of thickness observed by Henning (1992) appears to be specific to the bend test as stated above. Comparison between bend test and cup/expansion test should be made using materials with different thickness to confirm the assumption presented in this report on the effect of thickness.

4.1.2 Effect of Cup Test Parameters on DBTT

Planar anisotropy:

The planar anisotropy affects the strain distribution at the edge of the cup as well as the thickness. In this study, the maximum major strain and thickness variation observed at the edge of DR = 2.0 cups was about 7 to 8%. It is well know that this effect varies with the sheet texture. The minor strain variation was less significant. Since the higher major strain regions in the cup wall are also areas where the thickness is lower, SCWE cracks are more likely to initiate in these areas. This phenomenon has been reported by Lau et al. (1998) and confirmed in this study. Although the thinner region of the wall may favor SCWE crack formation, this factor is not likely to affect the DBTT value. This assumption is based on the study on effect of thickness reported in this report, which indicated that in reduced-wall cups the DBTT is not decreased. However, based only on mechanical considerations local thinning will increase the stress during impact, which will favor crack initiation. An important factor in SCWE is material strengthening due to cold work deformation. The workhardening is a function of the degree of deformation. Although Figure 18 showed that cup earing is associated with variation in major strain, it is not necessarily associated with higher workhardening, since this effect is the result of a lower thickness strain combined with a higher major strain when compressive stresses are applied during cup drawing. The resulting effect on DBTT remains debatable. On one hand, if workhardening is relatively constant at the cup edge, flow stress variation will be negligable, which leads to a negligable effect on DBTT. On the other hand, it is well know that grain shape plays an important role in SCWE. The effect of this phenomenon on intergranular fracture has been shown by Boyle et al. (2000) using a fracture mechanics approach. If we consider the grain morphology variation associated with earing at the cup edge, higher major strain would promote SCWE. However, when combined with lower thickness strain, the resulting effect on DBTT is more difficult to predict. Experimentally such a question could only be answered by testing prestrained material with various ratios of thickness strain to major strain.

Sheet thickness:

The absence of stress triaxiality in thin sheet reduces the tendency for brittle fracture, which translates into an apparently lower DBTT. It is however unclear whether or not for the range of sheet thickness employed in this study, initial sheet thickness played a role in SCWE. Based on the concept of stress

triaxiality, one can expect that a reduction in thickness may reduce DBTT. In this study, sheets with thickness in a range 0.74 to 1.45 mm were tested. However, the results obtained with the S4 series steels did not permit any conclusion to be drawn about the effect of thickness on DBTT. The metallographic examination of the 4 steels showed that the most SCWE sensitive steel, S4d, exhibited a microstructure composed of regions with non- or partly recrystallised grains and regions of equiaxed recrystallised grains. Although this steel was produced with the lowest cold reduction, this phenomenon was rather unexpected in a batch annealled steel. This phenomenon can affect DBTT by influencing SCWE crack propagation and increasing yield strength. The mechanical properties of the S4 series steels have not been measured (except steel S4a), but clearly indications are that processing conditions affected DBTT. Since the details of the processing conditions are not know it is not possible to determine the exact cause.

The alternative method used in this study to investigate the effect of thickness did not show any evidence that initial sheet thickness played a role in SCWE during the cup test. This conclusion was based on a limited number of tests made on reduced-wall thickness cups with wall thickness in a range 0.51 to 1.45 mm. To our knowledge no data have been published in the literature on the effect of thickness on cup test DBTT. Additional tests would be necessary to confirm the test results obtained with the reduced-wall thickness cups if appropriate material with a range of thickness can not be obtained.

Cup size:

To understand the relationship between laboratory tests and fracture in large part it is important to determine the influence of the cup size on DBTT. This study has highlighted three situations where specimen size has significantly affected DBTT. First, it has been shown in Fig. 22 that the DBTT with the 6-in. trimmed cup was 10 to 15°C higher than the 2-in. cup. On one hand, the higher strain in the 6-in. cup (65% vs 55 to 60%) could have contributed to the effect observed. However, the strain rate is higher in smaller cups, which would tend to increase DBTT. Those two factors produce an opposite effect on DBTT, thus there is probably no resulting significant effect on DBTT, so it can be concluded that the difference observed is due to an effect of cup size. Secondly, the comparison of the effect of flange in 2-in. and 6-in. cups showed completely different results. In the present study, it was found that the trimmed and flanged 6-in. cups had similar DBTT. In smaller flanged 50-mm cups, Bhat et al. (1994) found a DBTT decrease of 35°C. Lewis et al. (1998) reported a decreased of 90°C in cups with 2.08 draw ratio and 10°C in 1.7 draw ratio cups. Those results indicated that strain, specimen size and geometry have a strong effect on DBTT. Furthermore, it is clear that the assumption that flanged parts should have lower DBTT is not valid for any part geometry. Thirdly, the effect of strain in 2 and 6 in. cups does not show the same trend. The results of round-robin tests reported by Yan and Gupta (2000) indicated that the DBTT increases with strain for small cups with draw ratio in a range 1.8 to 2.41; this translates in a major strain in a range 58% to 99%. In the present study, the decrease in DBTT observed for the higher draw ratio, clearly indicated an important difference with the effect reported in smaller cups.

Those results show the limitation of laboratory small-scale tests to simulate specific test conditions. Number of factors can play a role when changing specimen size, such as elastic compliance, strain rate, loading mode, etc.

Cup edge condition:

In this study no significant difference in DBTT was observed for flanged cups with draw ratios of 2.0 and 2.3 compared to the fully trimmed cups for a rephosphorized ULC fully stabilized steel without boron. This is in contradiction to the observations made by Lewis et al. (1998) and Bhat et al (1994) who showed that the presence of flanges on 2-in. cups produced a decrease in DBTT. Bhat showed that the DBTT for flanged cups with a draw ratio of 2.03 produced from a batch annealed titanium stabilized ULC steel was -25°C compared to +10°C for the standard as-drawn cups with no flanges from this steel. This difference is explained in terms of the difficulty in initiating a crack during secondary working in the presence of a flange due to a lowering of the local stress concentration because of the radius associated with the flanges. An additional observation made on their flanged cups showed that the cracks initiated close to the top radius at a strain lower than that which existed at the edge of the as-drawn cups. In our case cracks initiated at either the cup edge for the smaller flanged 2.0 draw ratio cups or at the inner flange radius for the larger flanged 2.3 draw ratio cups at a position with a strain of 90% which is almost equivalent to the 100% major strain measured at the edge of the untrimmed cups. Following testing of cups with both flange widths, it was evident that bending had occurred along the flange, particularly in the case of the 2.0 draw ratio cups as shown in Fig. 34. The severity of bending was much greater for the smaller flange, and the crack initiation location always coincided with the position at which the flange was kinked. The observation of crack initiation occurring at the flange radius of the 2.3 draw ratio cups resembles the corner cracking that occurred in the oil pans as described in Section 3.2 and shown in Fig. 39b. To further investigate this observation it is necessary to perform more comprehensive testing to establish the effect of such parameters as cup size and flange width on DBTT.

An investigation of the effect of pre-machined notches or pre-cracks on DBTT of 6-in. cups revealed no significant influence on the DBTT as compared to unnotched cups. This observation is based on limited tests conducted on notched 1.8 draw ratio cups and pre-cracked and notched 2.0 draw ratio cups. The 2.0 draw ratio cups which had a DBTT of +10°C displayed ductile fracture propagation from the notch in tests conducted at +10 and +21°C rather than the plastic collapse which occurred in the unnotched cups indicating that the notches had created a stress concentration that had promoted ductile fracture. Below the DBTT however there was no indication that stress concentration from machined or pre-existing cracks contributed to a change in DBTT. Indeed when brittle fracture did occur in a notched cup, the initiation site was remote from the notch. Certainly in previous studies such as that conducted by Bhat et al. (1994) on trimmed and untrimmed cups the presence of irregularities such as ears, small cracks and overlaps have shown that these defects have resulted in an increase in DBTT compared to trimmed cups by as much as 35°C. This is another observation which requires further study to gain a better understanding of the factors contributing to this result.

Effect of speed:

This study showed that an increase in speed from 4.34 m/s (15.6 km/h, 32.9 s^{-1}) to 7.41 m/s (26.7 km/h) increased the DBTT by 5°C. This result is consistent with the DBTT obtained by Bhat et al. (1994) in static and dynamic cup/expansion tests. The study showed that the static test ($\varepsilon = 0.01$ s^{-}

^{1}) had a DBTT 30°C lower than the dynamic test (11.4 km/h, $\varepsilon = 43\ s^{-1}$). The effect reported in the present study is however smaller than the effect found by Lewis et al. (1998) who reported an increase of 20K for an increase in speed from 3.13 m/s ($54\ s^{-1}$) to 4.43 m/s ($77\ s^{-1}$). In this last study, the same impact energy was used by changing the load. According to Lewis the effect of speed is more important than that of energy since very little energy is absorbed during impact. Lewis also reported that the speed effect was a function of the draw ratio and cup edge condition. The explanation for this effect is unclear and the present study does permit us to clarify this effect.

The speeds used in the present study are within the range of speeds proposed in the GM specification. However, much higher strain rates may occur in some impact situations. SCWE data at higher test strain rate would be useful. However it is difficult to cover higher speed rate regimes with the standard drop weight system.

Effect of strain and DBTT strain Map:

An increase in draw ratio from 1.8 to 2.0 produced an increase in DBTT from -10 to +10°C for steel S3, between 2.0 and 2.2 no increase in DBTT was observed and on increasing the draw ratio to 2.3 a decrease in DBTT to -5°C occurred. An increase in DBTT with draw ratio has been reported by Teshima and Suzuki (1964), Lewis et al. (1998), Yasuhara et al. (1997), Bhat et al. (1994), Takahashi et al. (1982) and Yan and Gupta (1999). There is a lack of a standardized test procedure to test for SCWE susceptibility in terms of specimen geometry, the method by which the secondary strain is introduced and the evaluation criteria. In order to compare the effect of strain on DBTT observed in this study with other workers it was necessary to ensure that their results were generated using a similar cup testing procedure. Round robin testing was conducted at five North American steel research laboratories in which steel blanks were cut from the same coil. Each participating company carried out drop weight testing on trimmed cups using existing testing at their facility. These results from Yan and Gupta (1999) are plotted in Fig. 74 together with data from Lewis et al (1998) in which trimmed cups with draw ratios of 1.70 and 2.08 were impact tested using a drop weight technique. The results obtained from the MTL/CANMET study are also shown. It is difficult to make direct comparisons because of the different steels that were tested but it is worthwhile commenting on the general trends observed between the various studies. Between a draw ratio of 1.8 and 2.0 corresponding to edge major strains of 50 and 65% respectively the CANMET study revealed an increase in DBTT of 20°C whereas in Yan and Gupta's study for the same difference in draw ratio produced a 10°C difference in DBTT. It should also be noted that the major strains corresponding to the 1.8 and 2.0 draw ratios were 58% and 78% respectively, higher than those measured in this work. Lewis et al. observed an increase in DBTT of 32°C between draw ratios of 1.7 and 2.08 but provided no data on the edge major strains for these draw ratios. Tests conducted in a separate study by the authors (Martin et al., 2000) on prestrained notch specimens taken from the cup wall with strains in the range 40 to 67% revealed a similar shift in DBTT in proportion to that observed for the cup tests in this work. The absolute values of DBTT, however were much lower than those measured in the cup tests because of the difference in the stress conditions between the two methods. The results of Yan and Gupta show a change in DBTT from -20°C to +10°C on increasing the draw ratio from 2.0 to 2.4, these draw ratios corresponding to edge major strains of 78 and 98% respectively. In this study the drop in DBTT from

+10°C to -5°C on increasing the draw ratio from 2.2 to 2.3 which represent edge major strains of 69 and 100% respectively, is not consistent with the above observation. Bhat et al. (1994) has stated that a higher draw ratio led to a greater elongation of the grains and hence more alignment of the boundaries along the cup wall. During secondary working a tensile hoop stress is generated which is concentrated along the grain boundaries and can thus produce intergranular fracture. Since SCWE is characterized by grain boundary fracture, the more aligned the boundaries are the greater the likelihood of grain boundary fracture. An increase in draw ratio also produces a higher yield strength associated with work hardening which raises the DBTT. The observations made at the high edge strains associated with these draw ratios in this study cannot be explained in this manner. Most of the previous observation of the effect of strain on DBTT have been carried out on smaller 2-in. cups. The fact that a drop in DBTT occurs on increasing draw ratio from 2.2 to 2.3 and that a significant decrease in DBTT is evident for the 2.3 draw ratio cup trimmed at a height to produce an edge strain equivalent to the 2.0 draw ratio cup suggests that additional factors are affecting the cup fractures for the 6-in. cups. A lower residual stress was noted at the edge for those cups which exhibited an unexpected decrease in DBTT. The presence of residual stresses will reduce the applied stress to produce brittle fracture but are not expected to affect the transition temperature because the increased plasticity at the transition temperature will exceed the less than yield residual stresses that are present.

Cup expansion tests using a draw ratio of 2.0 provide an estimate of the DBTT up to a strain level of 55 to 65%. It is not clear whether this estimate is conservative or not for larger strain. This anomalous behaviour at higher strain and in strained material where residual stresses are high or low needs to be clarified.

4.2. RELATIONSHIP BETWEEN FRACTURE MORPHOLOGY AND DBTT

Strain is a critical factor in SCWE since it affects the flow stress. Brittle fracture occurs when material flow stress exceeds the stress for intergranular (IG) fracture or cleavage fracture. Material strengthening during SCWE testing occurs during primary cold working, also additional strengthening arises when increasing strain rate during the secondary deformation. However in most cold work embrittlement situations, fracture occurs during secondary forming operations where the strain path is changed, unless fracture occurs during metal forming such as reported in the Section 3.2 of this report. Even during metal forming, SCWE fracture can form as a result of a change in strain path such as the fracture associated with wrinkling and fracture during flange hemming. The flow stress during secondary forming can be sensitive to the strain path which can affect SCWE (Boyle et al., 2000). The resulting effect on DBTT is still unclear and this phenomenon is beyond the scope of this study. However, it is clear that primary strain generates grain morphological texture that affects DBTT. For the purpose of the discussion we will limit our discussion to the effect of grain morphology.

The fractographic observations reported in this study have shown interesting results concerning the effect of grain orientation on SCWE. The notched specimen tests revealed that fracture in the transverse orientation is characterised by a higher percentage of cleavage facets and consequently a lower percentage of IG fracture (see Fig. 56) compared to the longitudinal orientation (see Fig. 55).

The magnitude of this phenomenon depends on the fracture mode; the effect is less pronounced in the low-sensitive steel (low fraction of IG fracture) and high-sensitive steel (high fraction of IG fracture). In the longitudinal orientation, the intergranular cracks can propagate over a longer distance before deviating and following another grain boundary. Such an orientation will favor IG fracture. It is worthwhile noting that the relationship between fraction of IG fracture and DBTT is similar in un-strained and transverse notched specimens. This result indicates that in this orientation cold working has a negligible effect on the fracture mode (the resulting effect on DBTT needs to be determined). This observation can be explained by the fact that in the transverse orientation an increase in minor strain reduces the grain boundary length in the direction of crack propagation which is not favourable to SCWE but also increases work hardening, resulting in two opposite effects. Clearly, this study showed that the two opposite effects resulted in a similar relationship for both un-strained and transverse notched specimens. It is however unclear why in steel S3 the fracture mode was quite similar in the three types of notched specimens, probably the high fraction of IG makes the phenomenon less noticeable.

If the fracture mode is an indication of the DBTT, lower DBTT should be expected for fracture in the transverse orientation. The present study did not permit to answer directly this question because of the difficulties to generate DBTT results in directions other than parallel to the grain elongation direction when using laboratory SCWE tests. However it was clearly demonstrated during the impact test on shock tower specimens using a small punch that fracture always occurred parallel to the direction of grain elongation (see Fig. 31). Since the stress condition in this test during impact loading was equibiaxial, fracture occurred in the weakest direction dictated by the cold worked microstructure. This infers that fracture parallel to the direction of grain elongation should occur at a lower DBTT than in the longitudinal orientation. This hypothesis has been confirmed elsewhere (Martin et al., 2000), where the authors have shown that the notched test DBTT in the transverse direction was more than 45°C (in 67% major strain region) lower than the DBTT in the longitudinal direction. This has an important practical impact on fracture in real parts since it indicates that stress condition with respect to the grain morphology in formed parts is a factor probably as important as strain during SCWE. This study also showed that fraction of IG fracture can be misleading when comparing crack propagation in longitudinal and transverse orientation. For instance, steel S3 showed in both orientations a similar high fraction of IG fracture; however, as mentioned above a significant difference in DBTT was observed. Similarly the fracture morphology was quite similar in the longitudinal and transverse notched specimen for steel S1. This can be explained by the fact that brittle fracture in this steel is primarily controlled by cleavage, which appears to be less sensitive to grain orientation.

As a consequence of the observation discussed above it is seems that the effect of grain morphology is affected by the controlling mechanism of brittle fracture whether it is IG, cleavage or intergranular/cleavage. This should affect material SCWE sensitivity to the orientation of crack propagation, and consequently to the loading mode during SCWE fracture in real part testing.

4.3. CORRELATION BETWEEN CUP TEST RESULTS AND FRACTURE IN LARGE SCALE PARTS

Attempts to correlate the results obtained in laboratory cup tests to those conducted on large scale parts need to take into consideration not only the difference in the forming strains that are present between the two types of test pieces but also the nature and location of the stress applied in the testing procedure. In this study 2-in. cup tests have been conducted to generate data on the DBTT of steels used to form two types of large scale parts. The major strain measured at the edge of these cups was ~55% and the load was applied with a conical impactor dropped from a height of 1m which generated a high hoop stress and a strain rate of ~100 s^{-1}.

The shock tower samples it has been shown contained regions of high strain which were tested locally using a drop weight machine with an indentor. Two regions were selected for testing, the first with a major stain of 50-60% equivalent to that measured at the edge of the cups. Localized testing using this technique generated DBTT values of -30 and -70°C for steels S6a and S5b respectively, a 20° difference in both cases compared to the DBTT's obtained from the cup tests. Upon locally testing the regions of higher strain (70-80%) a small increase in the DBTT (5-10°C) was observed for both steels. The orientation of fracture on the shock towers was in the direction of grain elongation as shown in Fig. 41 and a comparison of the fracture morphology at the lower strained (50-60%) with the fractured edge of the cup test specimen revealed very similar results. The difference in the DBTT between the cup tests and the localized shock tower tests can be explained in terms of the difference in the stress state at crack initiation, the cup test being more severe. Upon testing the full shock tower parts the geometrical configuration of the test piece and the orientation of impact at temperatures down to 50°C below the DBTT measured from the cup tests produced a plastic collapse with some kinking of the flange close to the region of higher stress as shown in Fig. 43. Once the temperature was low enough, in this case 60°C below the 2-in. cup DBTT's for the two steels the stress condition at the flanged region was severe enough to initiate brittle fracture as shown in Fig. 44 with a more detailed view of the region of crack initiation given in Fig.75.

For the other large scale part, the suspension panel, which contained very local regions of major strains as high as 60% it was not possible, given the various test methods and specimen orientations, to achieve the desired stress concentration at the required strain rate to initiate fracture.

The cup test results have shown they are conservative with respect to predicting the temperature at which fracture is likely to occur in the large scale parts selected for this study and the margin by which this conservatism exists is dependent on the nature of the testing procedure adopted for the large scale parts.

4.4. EFFECT OF GALVANNEALING

The effect of galvannealing has been studied by Lau et al. (1998). The authors showed beneath the coating evidence of a predominant intergranular fracture in galvanneal steel fractured below DBTT.

Similar observations were made in this study for steel S2 and to lesser degree in steel S3. No such evidence was found in non-coated CR steel. Lau et al. explained this phenomenon by the formation of outbursts at the clean boundaries of IF steel. Zinc can more easily diffuse into clean boundaries of IF steel, which will promote formation of outbursts. As a result, expansion of the outburst structure will promote nucleation and propagation of cracks into the substrate, and also will make it easier for coating cracks to propagate into the ferrite grains. The authors reported that non-coated rephosphorised IF steels had a DBTT as much as 30°C lower than galvannealed IF steels. Although the effect reported appeared to be obtained on a commercial galvanneal steel, the authors concluded that commercial galvannealed coatings have no detrimental effect on SCWE performance. This conclusion was supported by a study undertaken by the authors on the effect of the degree of alloying on SCWE. It was observed that fully alloyed galvannealed coating showed the lowest DBTT. This phenomenon was explained by the mechanism in which the intermetallic phases of the coating affect the propagation of coating cracks: in more ductile coating surface cracks propagate throughout the coating interface and subsequently into the substrate; however, in brittle coating bifurcation at the same interface occurs resulting in an arrest of the cracks. The authors suggested that in commercial galvanneal steel, coating cracks tend to bifurcate at the coating/substrate interface, which reduces cracking at the boundaries of ferrite grains. It is worthwhile noting that this study was made on a non-rephosphorized IF whereas the effect reported on commercial steels were obtained on rephosphorized grades. Since on one hand rephosphorised IF grades are less susceptible to outburst formation (Hisamatsu, 1989) and, on the other hand, are more susceptible to SCWE, it appears here that phosphorus plays a contradicting role on SCWE.

This phenomenon was not thoroughly investigated in this study. However, it was clearly shown that at least one rephosphorised IF steel used in the study exhibited significant intergranular fracture near the surface. This phenomenon was more apparent in steel S2 because of the clear contrast between the grain interior where mixed intergranular/cleavage fracture was observed. In this steel, weakening of the grains near the surface was apparent since in the notched tests conducted in Auger microscope, only the surface grains fractured in a brittle manner, the interior showed ductile transgranular rupture. This is an indication that this phenomenon reduced the DBTT of the grains beneath the surface, but in this specific case it did not lead to complete intergranular fracture. It should be pointed out that the brittle fracture observed in this experiment was the result of fracture during impact. On the other hand, it is well known that forming cracks in galvanneal steel can also promote ferrite intergranular fracture due to zinc penetration at the grain boundaries (Zhong et al., 1998). Those cracks are not related to SCWE by P embrittlement or lack of carbon but are due to Zn embrittlement as described above. It is still unclear if these surface phenomena have any effect on DBTT. It should also be noted that, in notched specimen S2, the brittle zone underneath the coating was larger than that expected from Zn embrittlement. This phenomenon has not been explained.

In an attempt to clarify if surface cracks in galvannealed coatings had any effect on the initiation of SCWE cracks, the authors made some observations using Focus Ion Beam (FIB) of forming cracks in deep-drawn cups before and after the cup/expansion test (Martin et al., 2000). Although ferrite cracks at the surface were observed, no clear evidences were found that forming cracks in the coating or in the ferrite grains had played a major role during SCWE. The observations were made on steel S2 and S3.

It is recommended to conduct similar observation on a non-rephosphorised IF to determine if similar observations can be made on a steel with more reactive grain boundaries. Additional observations in the region of secondary SCWE cracks in a rephosphorised IF should also be made to confirm the observations reported by Martin et al. (2000).

5. CONCLUSIONS

From the work presented in this report we can draw the conclusions below. However, in some cases the conclusions are based on a limited number of experiments, so additional work will be needed for further confirmation.

- A good relationship was found between the cup test and the bend test. However the bend test DBTT was significantly higher than cup test DBTT. This effect was attributed to the higher strain in the ID region of the bend specimen. The major problems with the bend test appears to be the control of strain during 0t bending and the high temperature of this test when evaluating high SCWE sensitive material. The test could also be sensitive to sheet thickness.

- In general fracture of high-sensitive steel near DBTT showed a high percentage of intergranular fracture. A linear relationship was found between DBTT and fraction of IG fracture in unstrained IF steel. However, straining affects the relationship between DBTT and fraction of IG fracture. One steel, S7, showed a surprisingly high fraction of IG fracture (DBTT of -30°C). The reason for this anomaly was not explained. The SCWE tests showed the beneficial effect of free-carbon, boron and the detrimental effect of P, as well has the difference in SCWE sensitivity between batch and continuous anneal products.

- This work showed the detrimental effect of primary strain on SCWE for strain levels between 45% and 65%. For higher strain DBTT decreased. It was found that a same level of primary strain can produce two different DBTT depending on the draw ratio and cup height. This effect coincided with a decrease in residual stresses. But the possible relationship between residual stress and DBTT is unclear.

- In general straining increases the fraction of IG and DBTT. This effect was confirmed for crack propagation parallel to the direction of grain elongation. For crack propagation in the direction normal to grain elongation, straining did not increase the fraction of intergranular fracture, the resulting effect on DBTT in unknown. It was shown that fracture in the transverse orientation (propagation perpendicular to direction of grain orientation) occurred at lower DBTT than fracture parallel to the direction of grain elongation (Martin et al., 2000).

- No significant effect of sheet thickness was found when testing reduced-wall thickness cups. However, test made on sheet steels produced with varying gauge thickness gave erratic results, which were attributed to the processing conditions.

- Sheet planar anisotropy generates earing and wall thickness variation at the edge of cups. In trimmed cups, SCWE were found to formed in the thinner region of the wall (earing area). This effect has been associated with the higher stress generated in the thinner edge regions during the cup/expansion test. The resulting effect on DBTT is unknown.

- An increase of impact speed from 4.34 to 7.41 m/s increased DBTT by 5°C.

- No significant difference in DBTT was observed for flanged cups with draw ratio of 2.0 and 2.3 compared to full drawn trimmed cups. This is in contradiction with observations reported previously in the literature. For the test conditions used it was shown that whether initiation occurs at the edge or in the wall DBTT can be the same.

- The presence of pre-machined or pre-cracks at the edge of cups did not significantly influence DBTT.

- SCWE fracture was observed during forming 6-inch cups and large oil pans. In both cases fracture occurred at temperature higher than predicted by the 2.0-draw ratio cup test. It is possible that in both cases local deformation would have been higher than in the cup test, which would explain the brittle fracture, but in the two cases fracture occurred in quasi static forming conditions.

- Significant difference in DBTT was observed between the 2-inch and 6-inch bend test when comparing DBTT in trimmed cup, flanged cup and cups with different draw ratios or cup heights. Those results show the limitation of laboratory small-scale tests to simulate specific test conditions.

- Surface embrittlement associated with Zn diffusion at the surface during galvannealing was observed. The phenomenon lead brittle cracking in the ferrite grains beneath the surface during cup drawing. This phenomenon also led to an higher fraction of IG fracture near the surface. FIB observation made on two rephosphorized IF steels reported in Annex A did not show any evidence that this phenomenon contributed to the initiation of SCWE cracks.

- The data generated using laboratory cup tests to predict the behaviour of the large scale parts used in this study show that the cup tests were conservative. Localized testing of high strained regions produced DBTT values slightly below those obtained from the cup tests. A significantly lower test temperature than the 2-inch DBTT was needed to produce brittle fracture in a region of high strain remote from the location of impact. For large scale parts with regions of lower strain (<50%) no brittle fracture was observed down to test temperatures of -95°C.

6. REFERENCES

Bhat, S.P., Yan, B., Chintamani, J.S. and Bloom, T.A., "Secondary Work Embrittlement (SWE) of Stabilized Steels: Test Methods and Applications", Procedings of the Symposium on High-Strength Sheet Steels for the Automotive Industry, R. Pradham ed., ISS, 1994, pp. 209-222.

Boyle, K.P., Embury, J.D., Perovic, D.D., Hood, J.E. "The Role of Grain Shape on Intergranular Fracture of Interstitial-Free Sheet Steels", Procedings of the Mathematical in Metals Processing and Manufacturing, edited by P. Martin et al, CIM 2000.

Henning, L.A., "Method to Evaluate the Susceptibility of Sheet to Secondary Work Embrittlement", 33th Metal Working and Steel Processing Conference, ISS, vol. XXIX, 1992, pp. 9-13.

Hisamatsu, "Science and Technology of Zinc and Zinc Coated Steel Sheet", Galvatech '89: Proceedings of the International Conference on Zinc and Zinc Coated Steel Sheet, The Iron and Steel Institute of Japan, 1989, pp. 3-7.

Lau, Y.H., De Cooman, B.C., Vermeulen, M., "The Secondary Work Embrittlement of Galvannealed High Strength Sheet Steel for Automotive Applications: Test Method and Material Evaluation", 39th Mechanical Working and Steel Processing Conference Proceedings, Iron and Steel Society, Warrendale, PA, 1997, pp. 139-148.

Lewis, S.G., Daniel, S.R., Parker, J.D., Llwellyn, D.T., and Sidey, M.P., "Testing Techniques for Cold Work Embrittlement in Interstitial Free Steels", Ironmaking and Steelmaking, vol.25, No.1, 1998, pp. 63–73.

Takahashi, N., Shibata, M., Furuno, Y, Hayakawa, H., Kabuta, K., and Yamamoto, K., "Boron-bearing Steels for Continuous Annealing to Produce Deep Drawing and High Strength Steel Sheets", Metallurgy of Continuous –Annealed Sheet Steel, B.L. Bramfitt and P.L. Mangonon, eds., The Metallurgical Society of AIME, 1982, pp. 133-153.

Takechi, H., "Developments in High-Strength Hot- & Cold Rolled Steels for Automotive Applications", Conference Proceedings Hot- and Cold-Rolled Sheet Steels, R. Pradhan and G. Ludkovsky, eds., The Metallurgical Society of AIME, Warrendale, PA, 1988, pp. 117-137.

Teshima, S. and Shimizu, M., "Recrystallization Behavior of Cold Rold Mild Steel", Mechanical Working of Steel II, Edited by T.G. Bradbury, Gordan and Breach Science Publ., 1964, pp. 279-320.

Yan, B. and Gupta, "Secondary Work Embrittlement of Interstitial Free Steels", Intergranular Fracture in Engineering Materials- Basic Science Aspects and Engineering Consequences, Organized by materials and Manufacturing Ontario, McMaster U., ASM and CIM, Hamilton, Ontario, April 8, 1999.

Yan, B. and Gupta, I., "Evaluation of Bend Test for Secondary Work Embrittlement", 38th Metal Working and Steel Processing Conference, ISS, vol. XXXIV, 1997, pp. 417-424.

Yasuhara, E., Sakata, ,K., Kato, T., and Hashimoto, O., "Effect of Boron on the Resistance to Secondary Work Embrittlement in Extra-low C Cold Rolled Sheet Steel", ISIJ International, vol. 34, No. 1, 1994, pp. 99-107.

Yasuhara, E., Sakata, K., Furukimi, O. and Mega, T, "Effect of Boron on the Resistance to Secondary Work Embrittlement in Extra-low C Cold Rolled Sheet Steel", 38th Metal Working and Steel Processing Conference, ISS, vol. XXXIV, 1997, pp. 409-415.

Zhong, W., Ng, H.F. and James, J.M., "Correlation between Adhesion Properties and the Interfacial Bonding Strength of Galvanneal Coating", Zinc-Based Steel Coating System: Production and Performance, F.E.Goodwin, ed., The minerals, Metal Society, 1998, pp. 185-194.

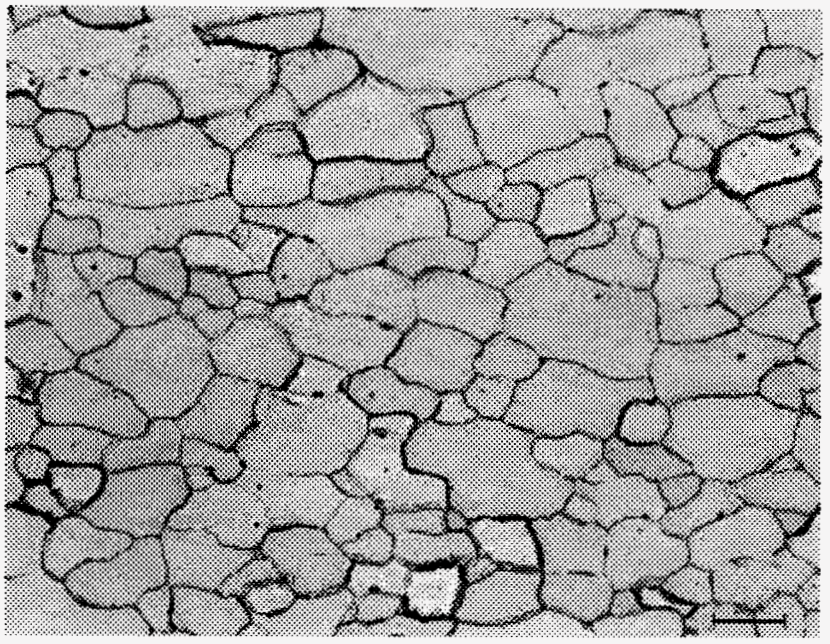

Figure 46. Microstructure of steel S1 in as-received condition obtained using optical microscopy.

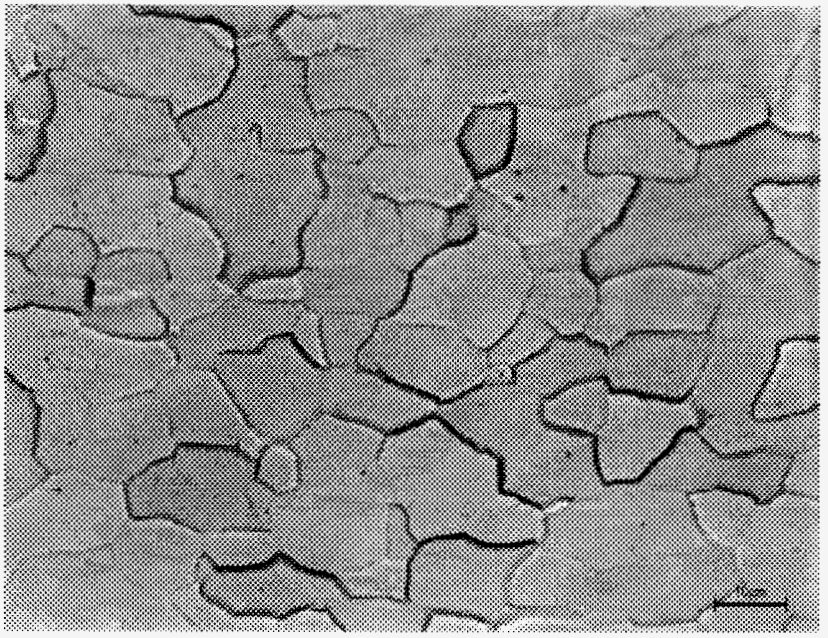

Figure 47. Microstructure of steel S2 in as-received condition obtained using optical microscopy.

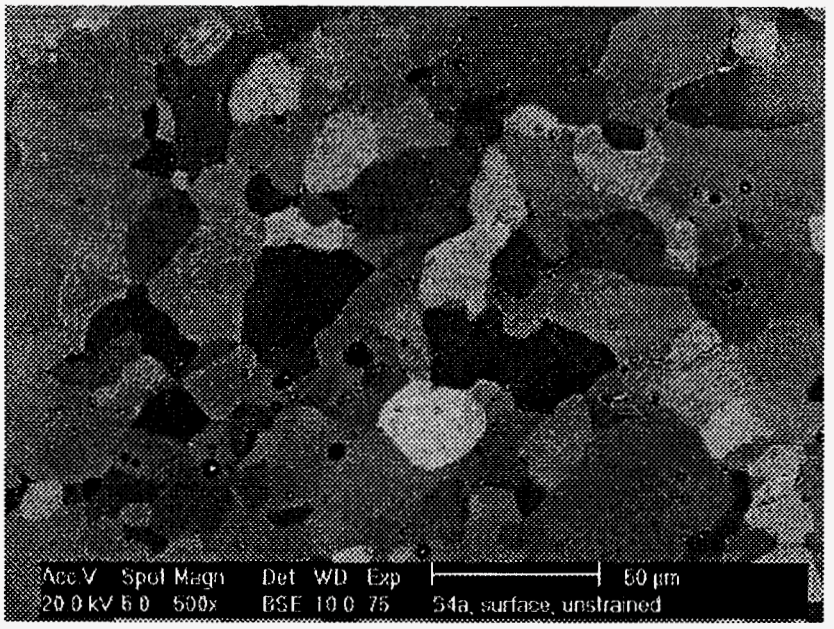

Figure 48. Microstructure of steel S4a obtained using SEM back scattered electron.

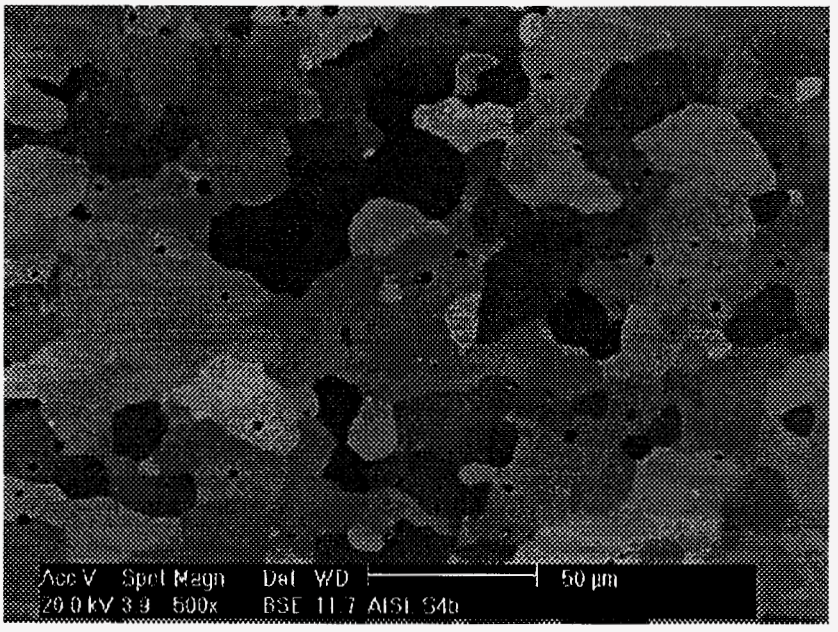

Figure 49. Microstructure of steel S4b obtained using SEM back scattered electron.

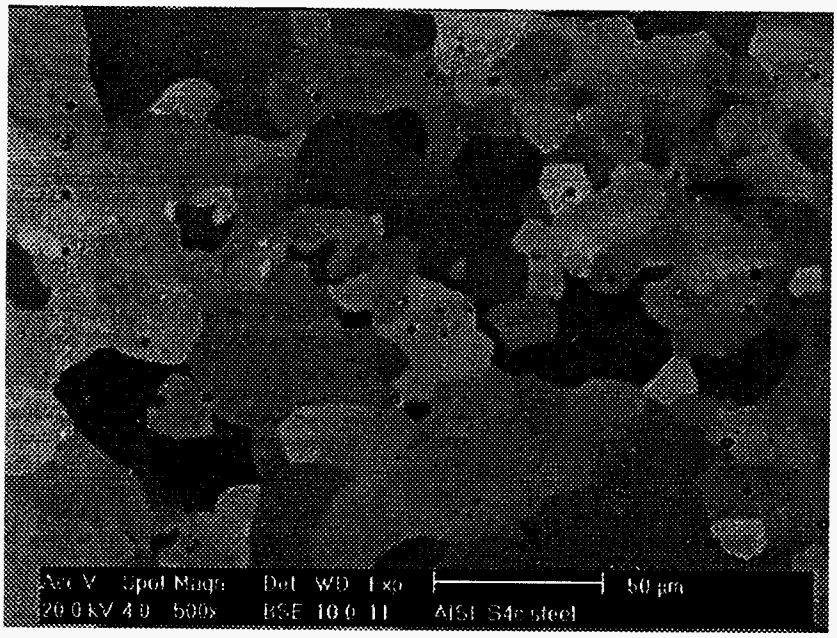

Figure 50. Microstructure of steel S4c obtained using SEM back scattered electron.

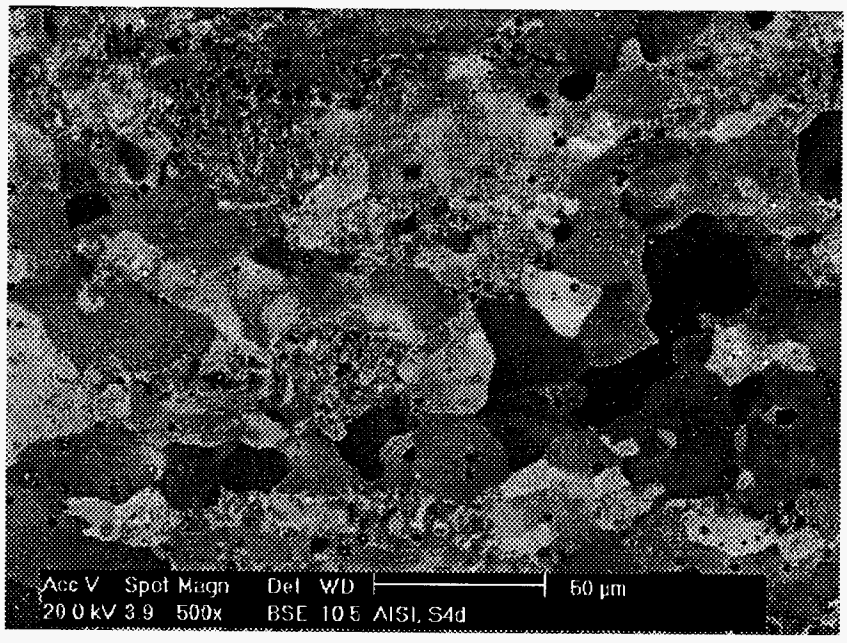

Figure 51. Microstructure of steel S4d obtained using SEM back scattered electron.

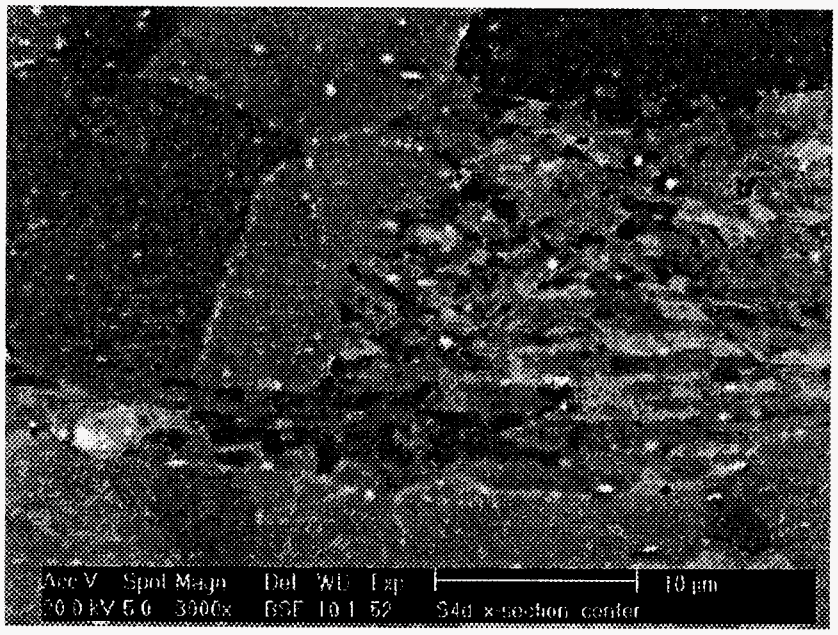

Figure 52. Larger magnification of microstructure showing an area with non- and partially recrystallized grains (steel S4d).

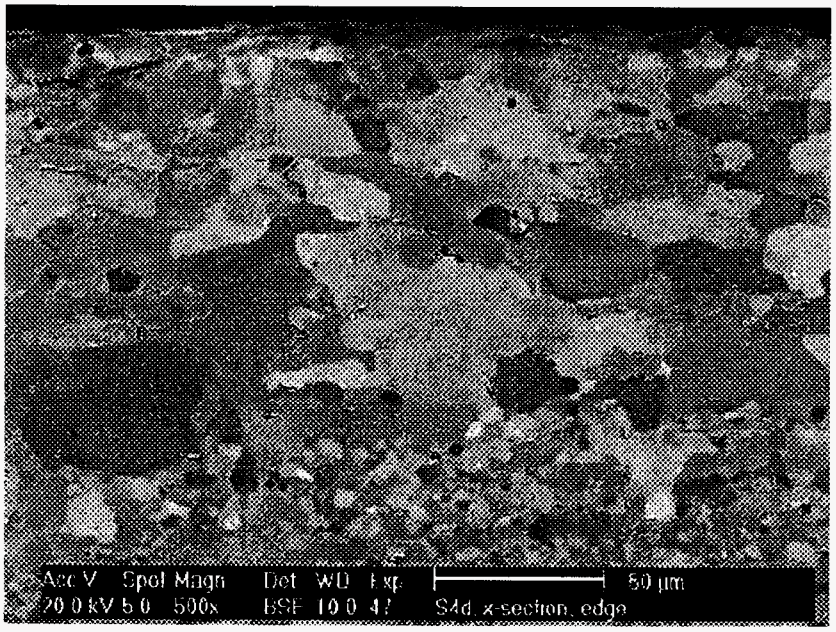

Figure 53. Microstructure of steel S4d near the surface (photo upper area).

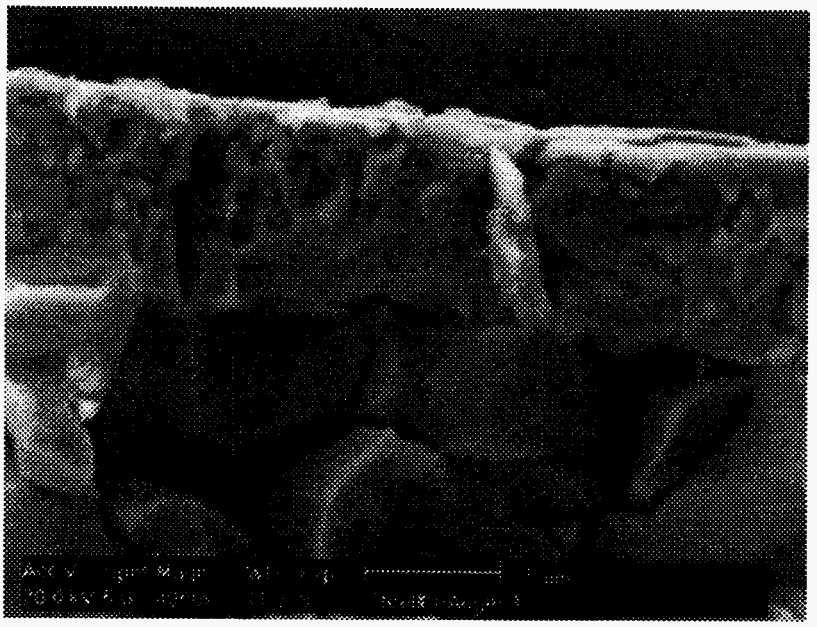

Figure 63. Intergranular fracture in S3 steel Auger specimen (upper part of image shows the galvanneal coating).

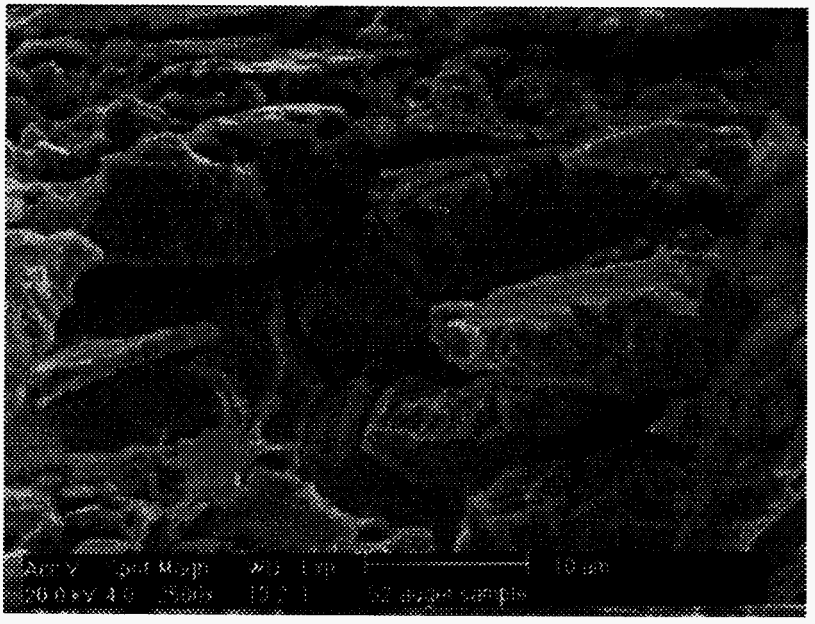

Figure 64. Surface of S2 steel Auger specimen showing brittle fracture in an area where the Zn coating was removed.

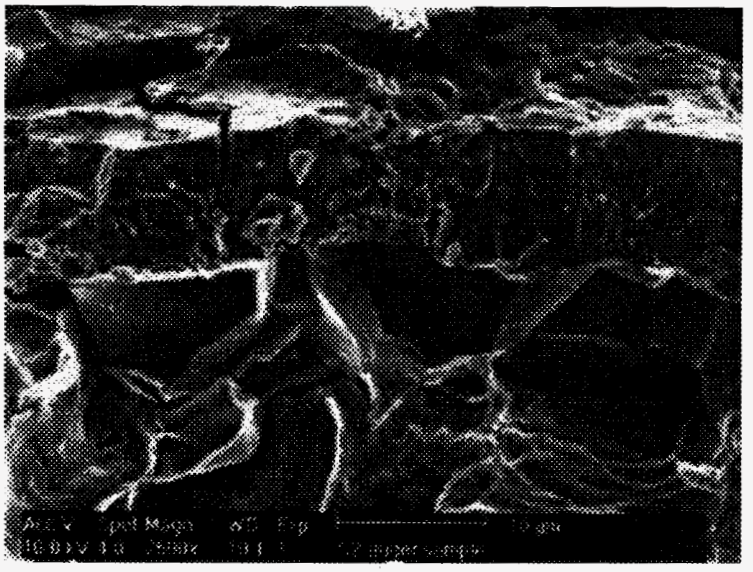

Figure 65. Intergranular fracture underneath the Zn coating in specimen S2 fracture in-situe in Auger.

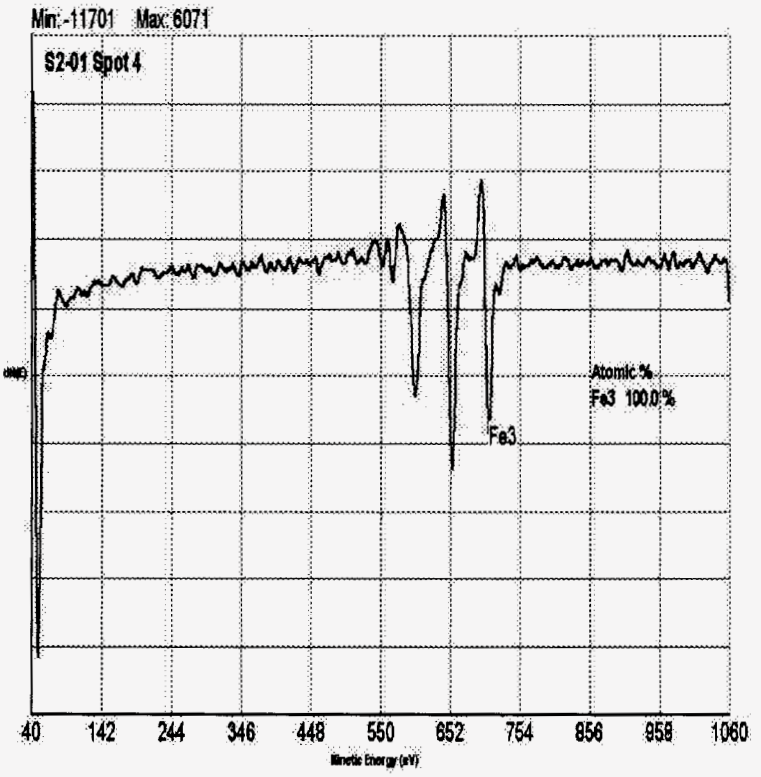

Figure 66. Auger spectrum of a cleavage facet (steel S2)

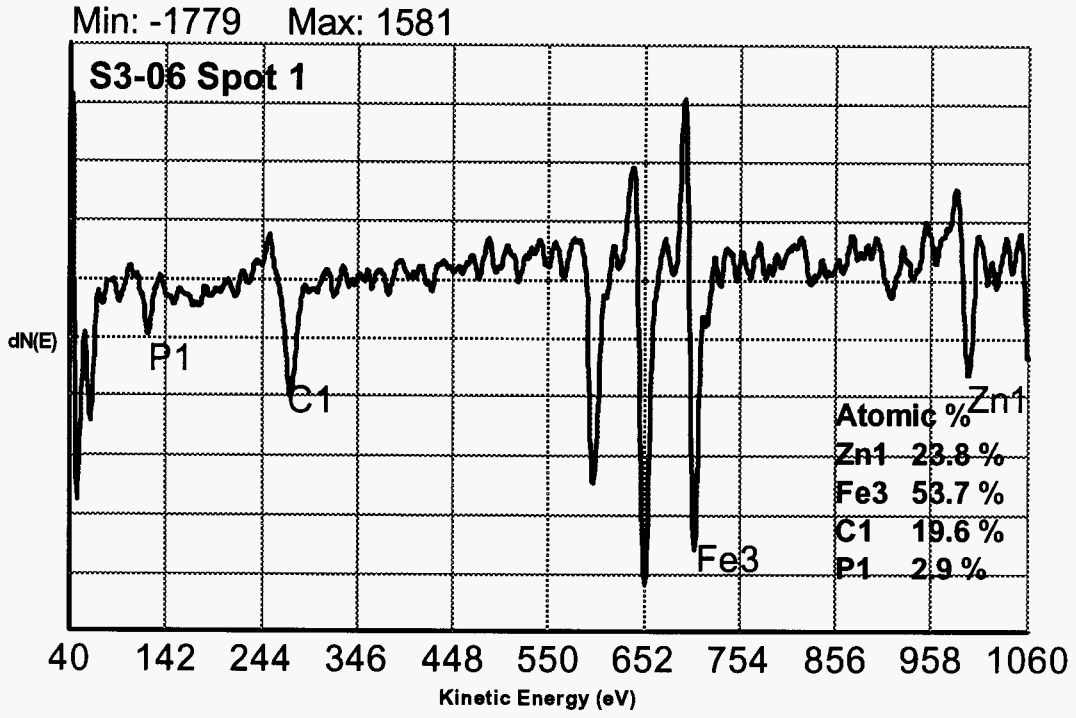

Figure 67. Auger spectrum of a grain underneath the Zn coating (steel S3).

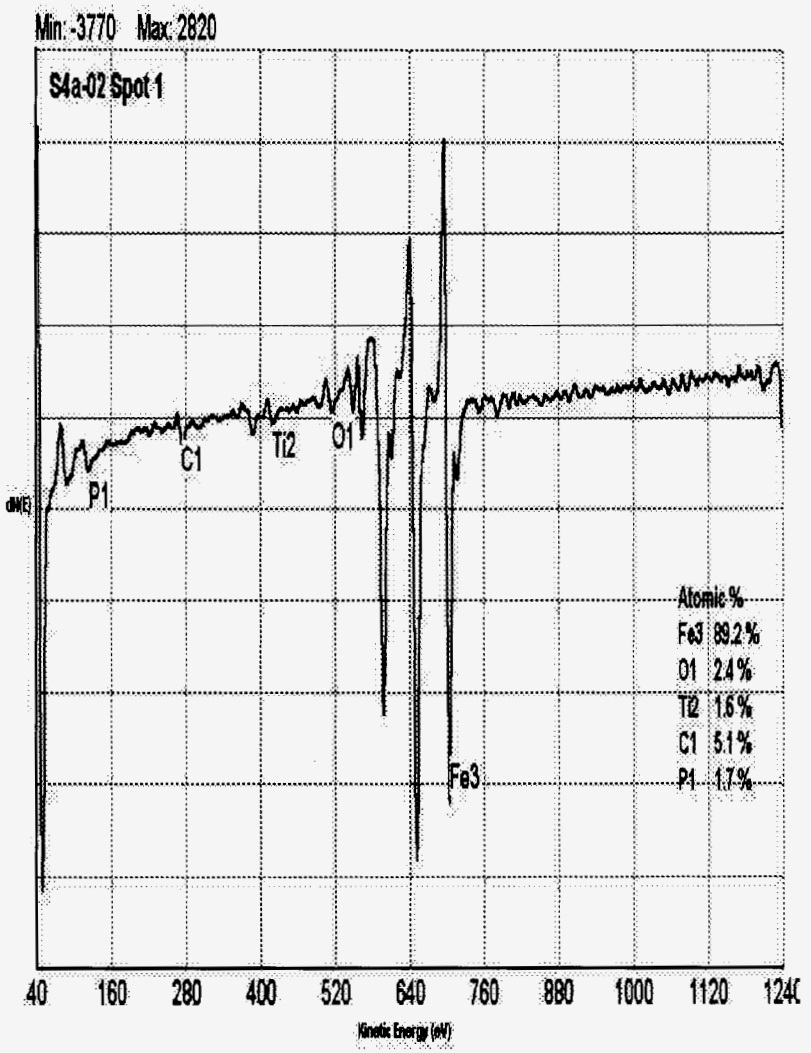

Figure 68. Auger spectrum obtained at a grain boundary in steel S4a.

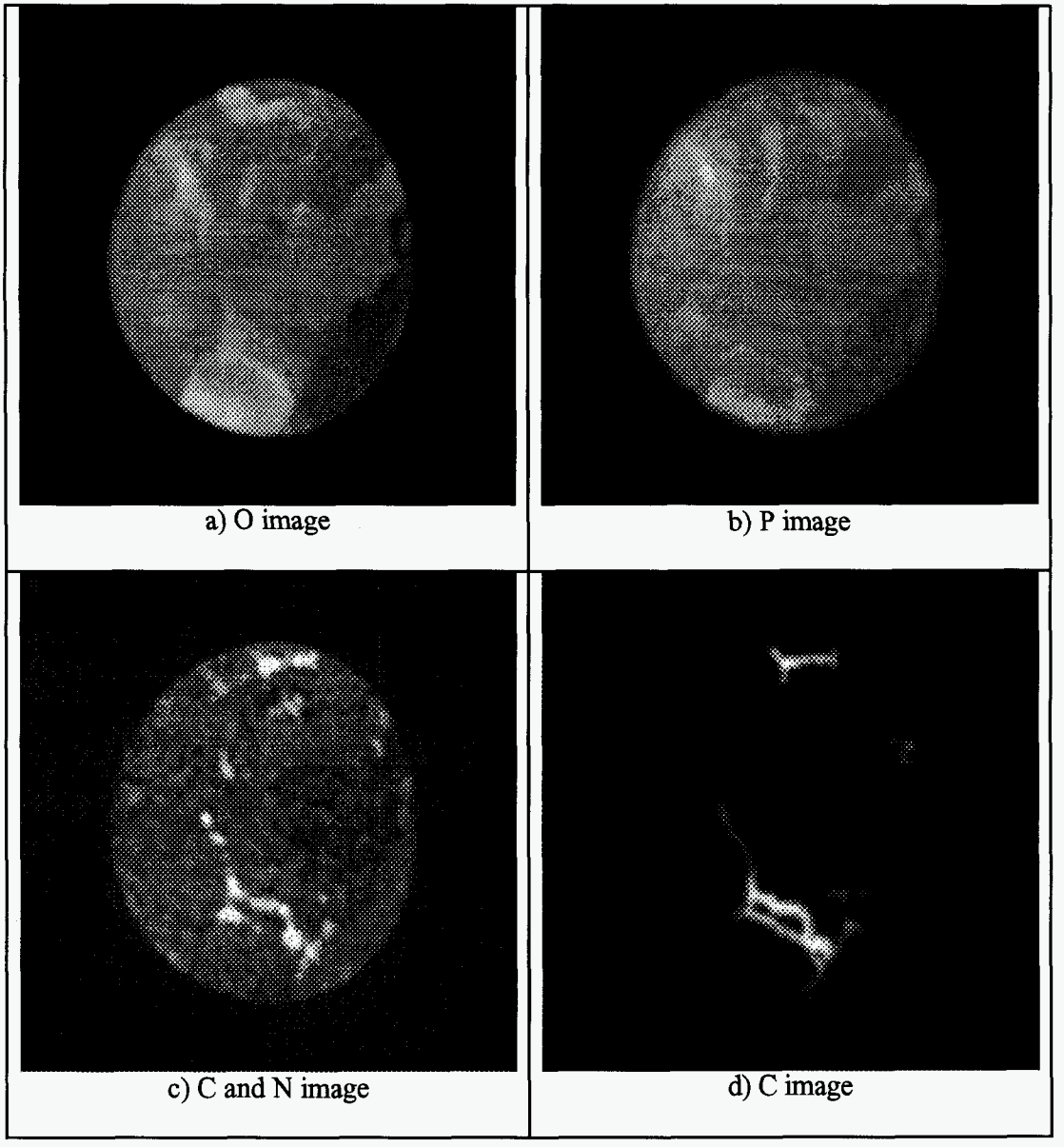

Figure 69. SIM images of steel S1 (100μm diameter)

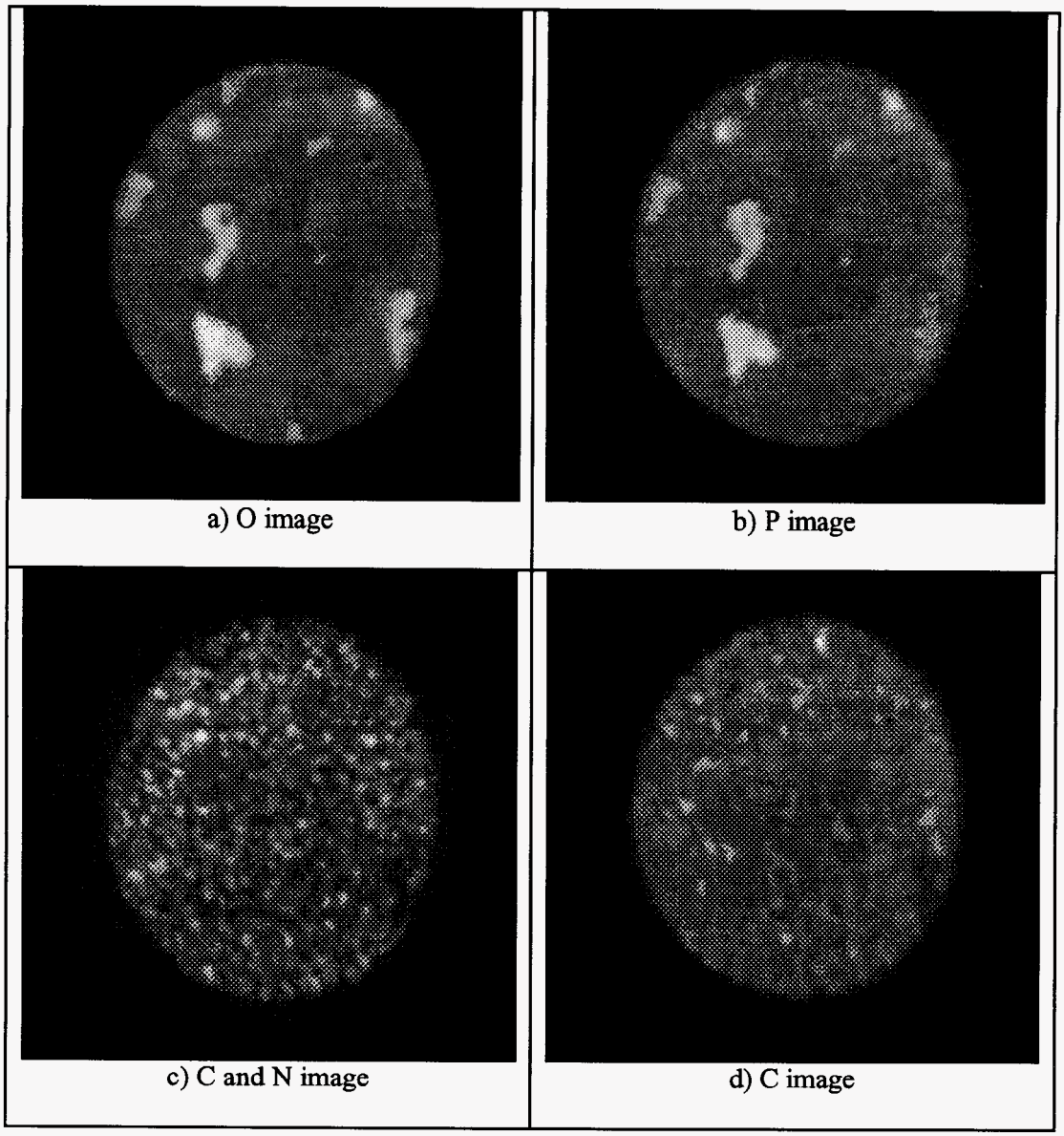

Figure 70. SIM images of steel S3 (100μm diameter)

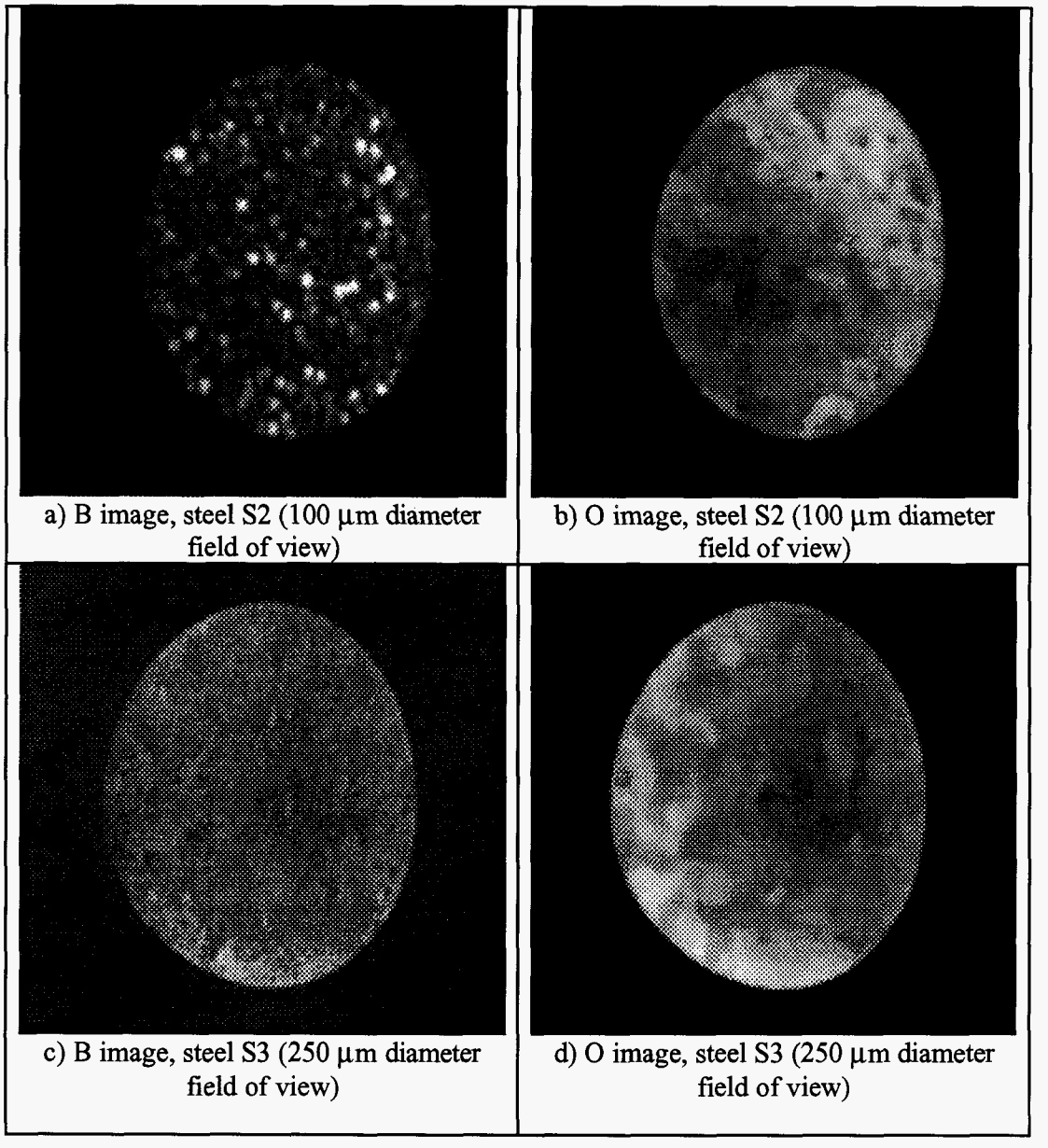

a) B image, steel S2 (100 μm diameter field of view)

b) O image, steel S2 (100 μm diameter field of view)

c) B image, steel S3 (250 μm diameter field of view)

d) O image, steel S3 (250 μm diameter field of view)

Figure 71. SIM images of B in steels S2 and S3.

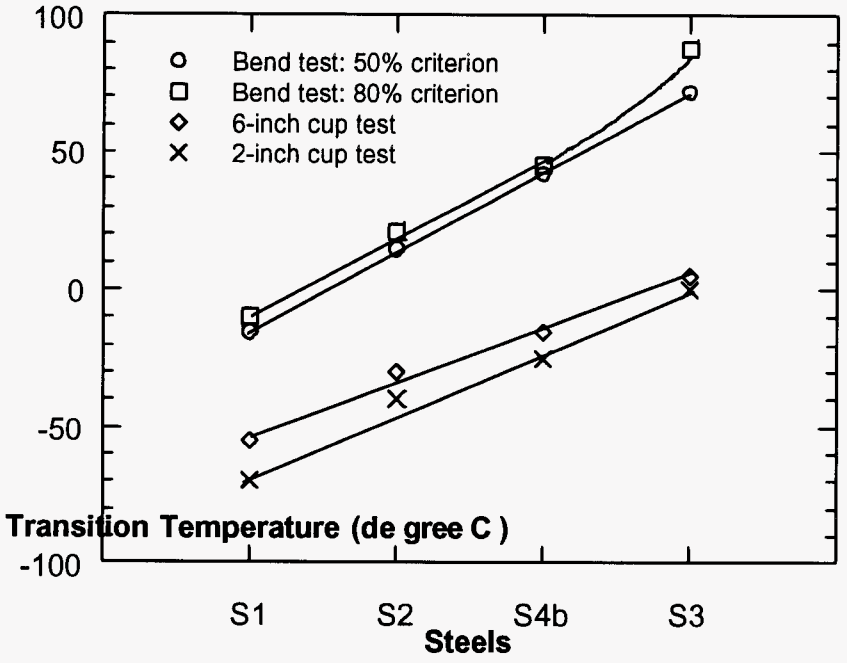

Figure 72. Comparison DBTT values obtained by bend test and 2-inch cup/expansion test (steel S3). **(Legend: o – Bend test: 50% criterion; - Bend test: 80% criterion; ◊ - 6-inch cup test; X - 2-inch cup test)**

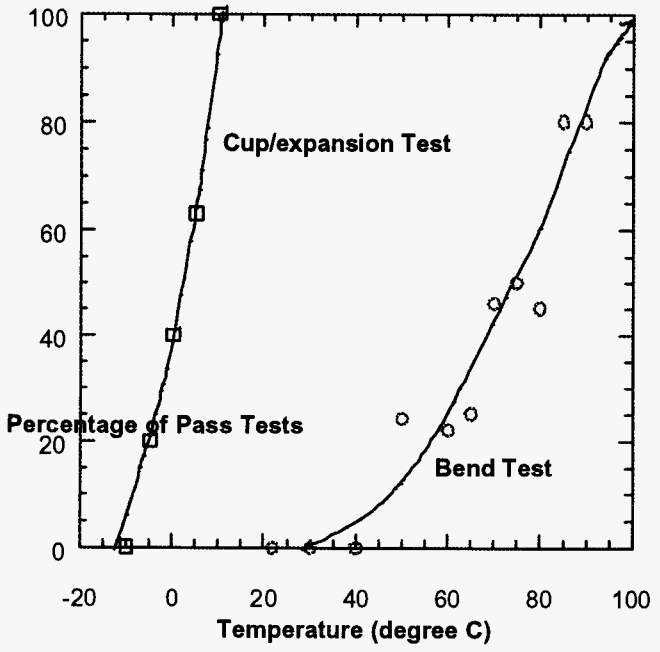

Figure 73. Comparison of the transition curves measured by the bend test and the 6-inch cup expansion test (Steel S3).

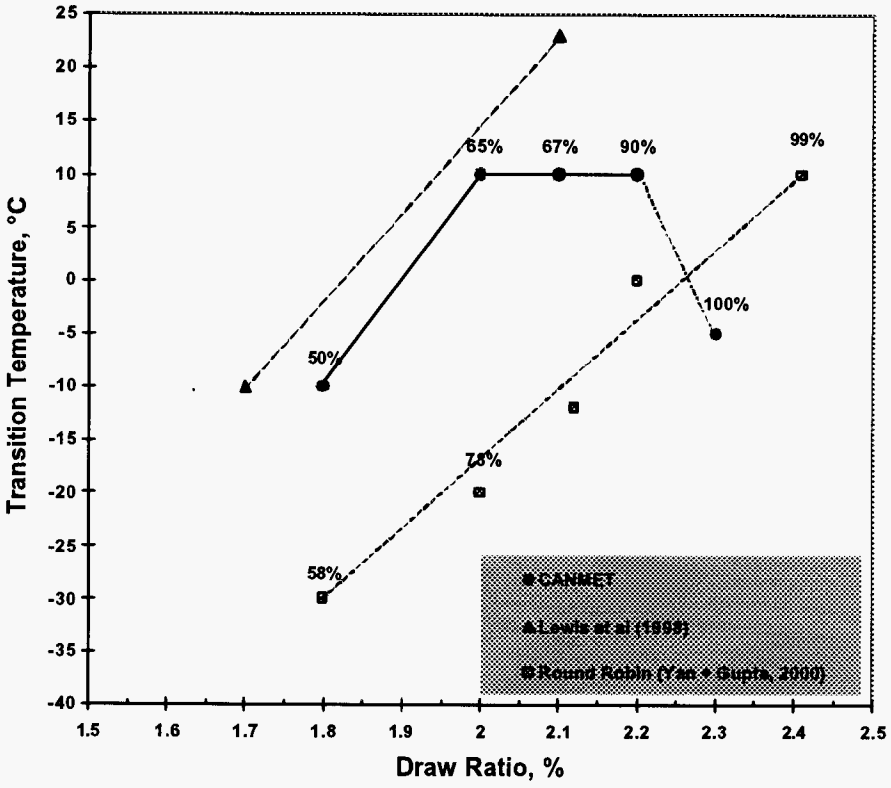

Figure 74. Transition temperature as a function of draw ratio

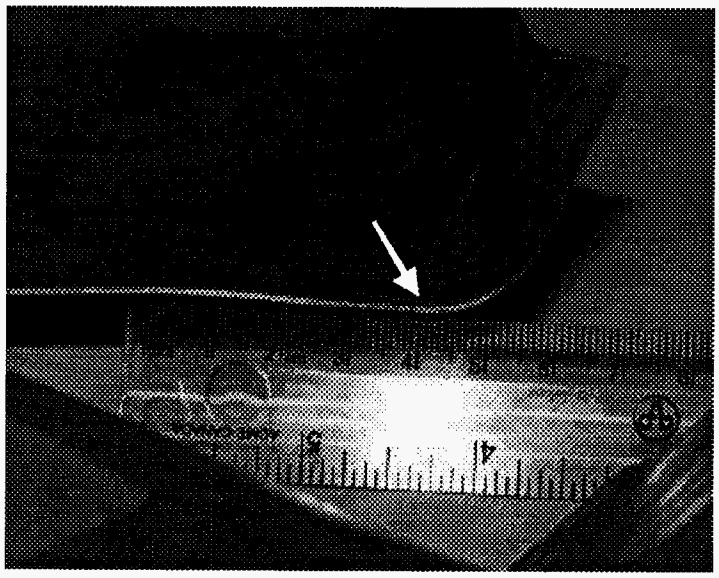

Figure 75. Crack initiation location in flange area of shock tower

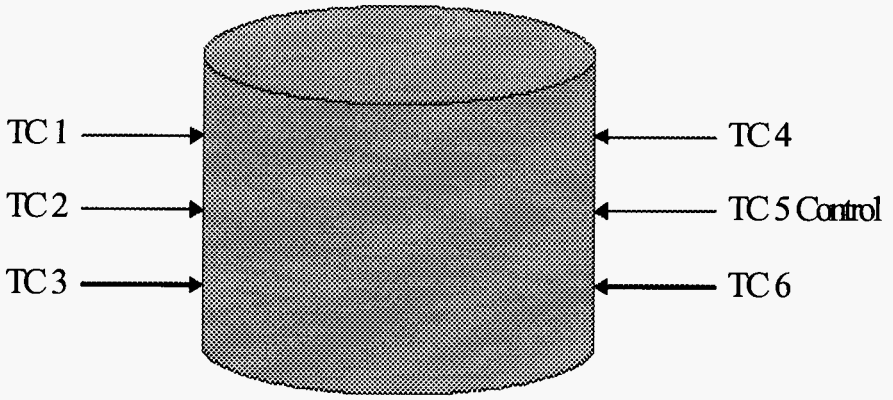

Figure 1. Location of thermocouples in 6-inch cups

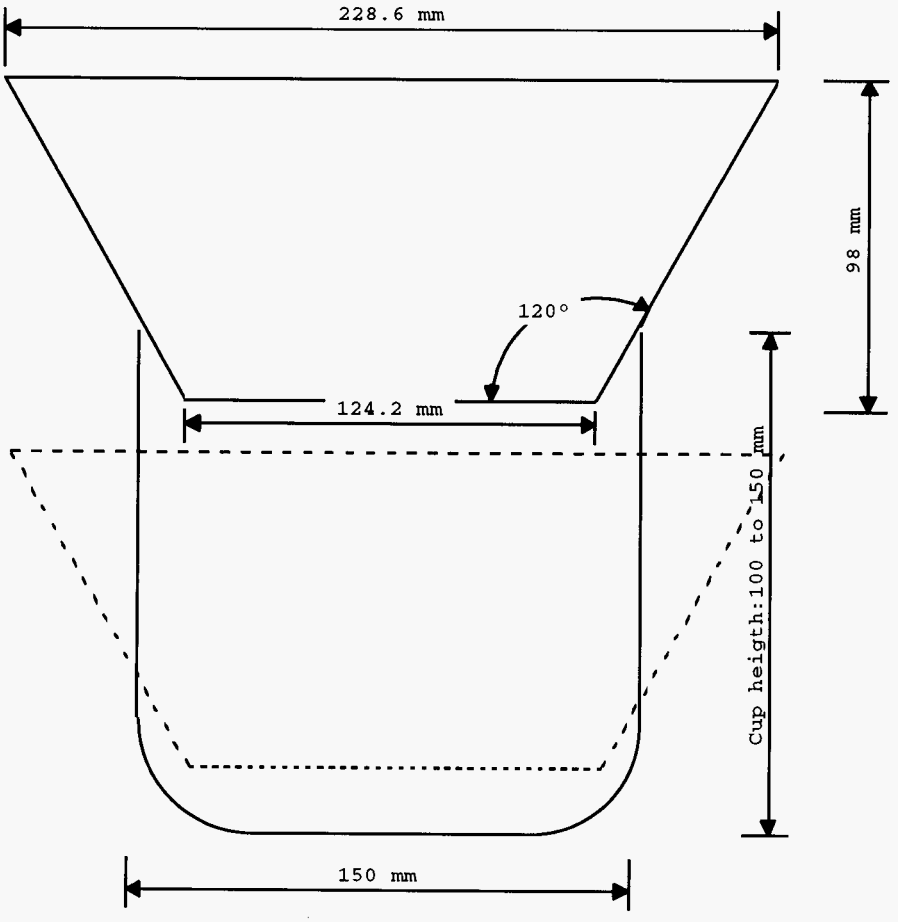

Figure 2. Dimensions of indentor used in drop weight testing of 6-inch cups

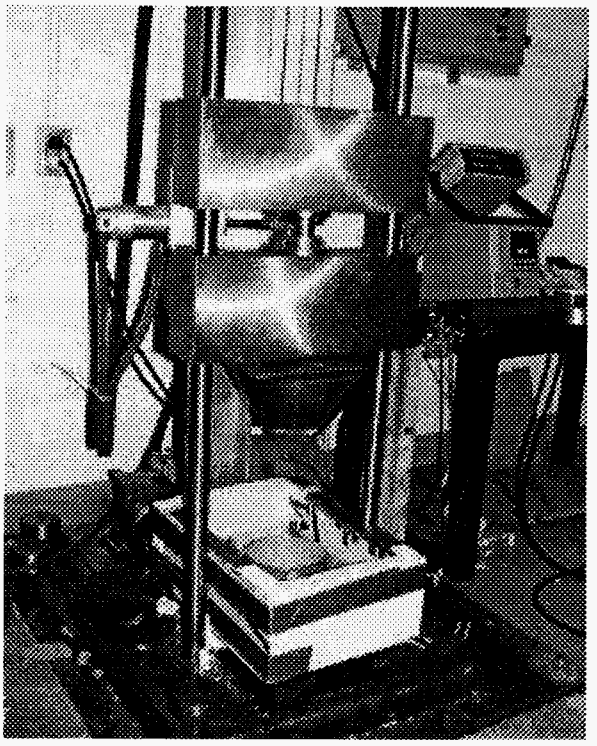

Figure 3. Drop weight tester for 6-inch cups

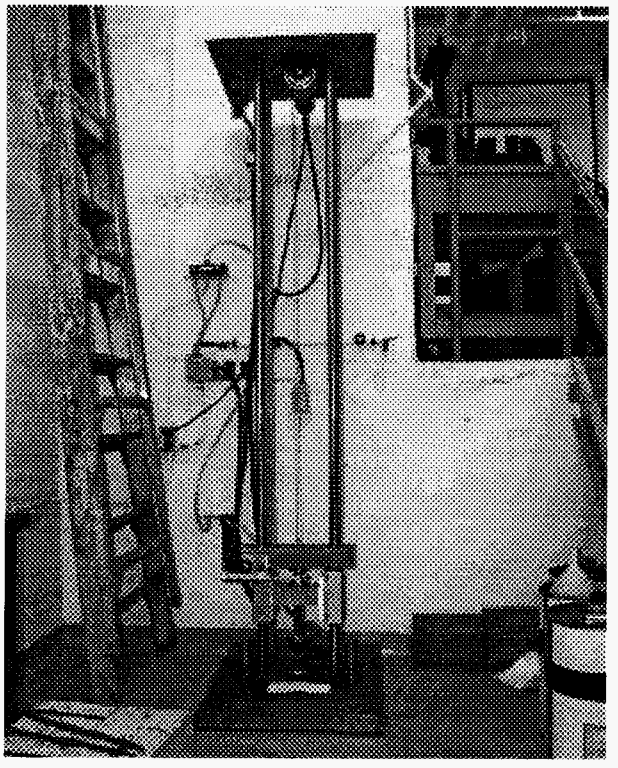

Figure 4. Drop weight tester for 2-inch cups

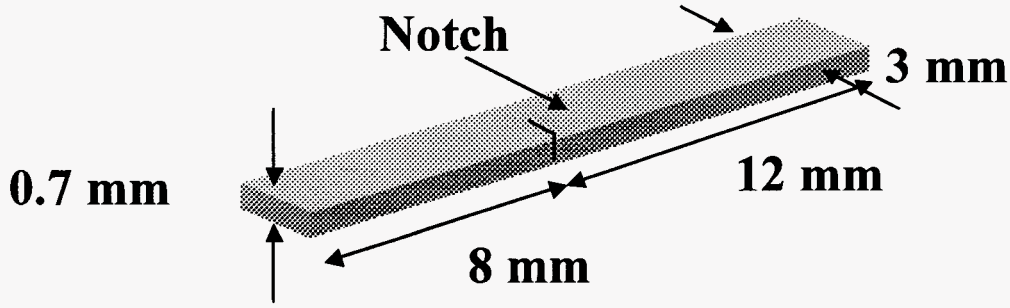

Figure 5. Sample used for notch impact testing and Auger microscopy

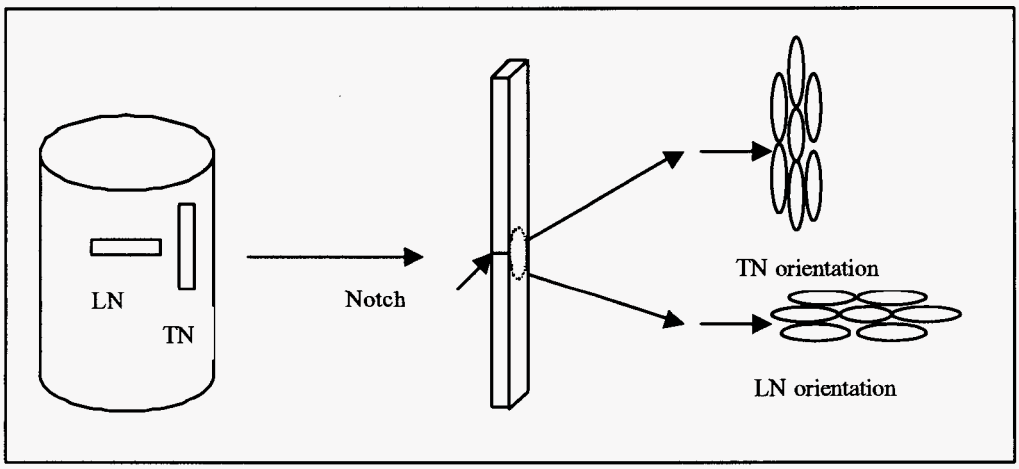

Figure 6. Schematic showing the orientation of the notched samples

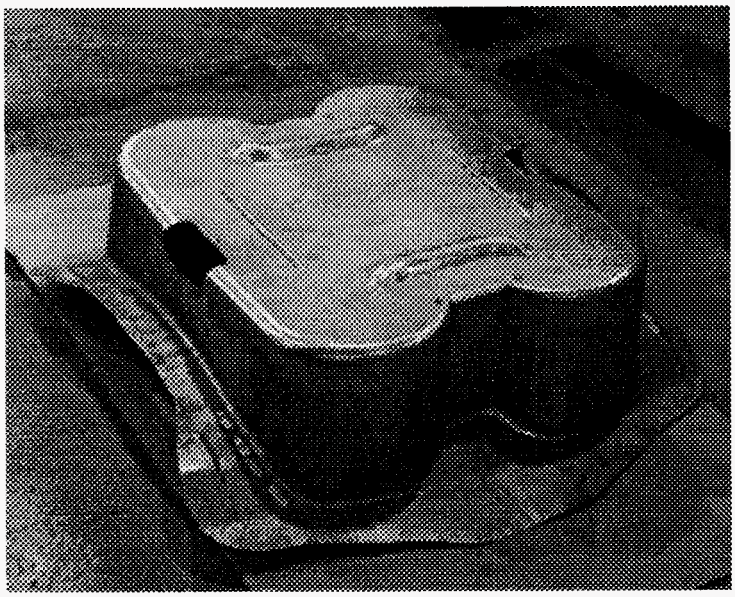

Figure 7. Shock towers after stamping

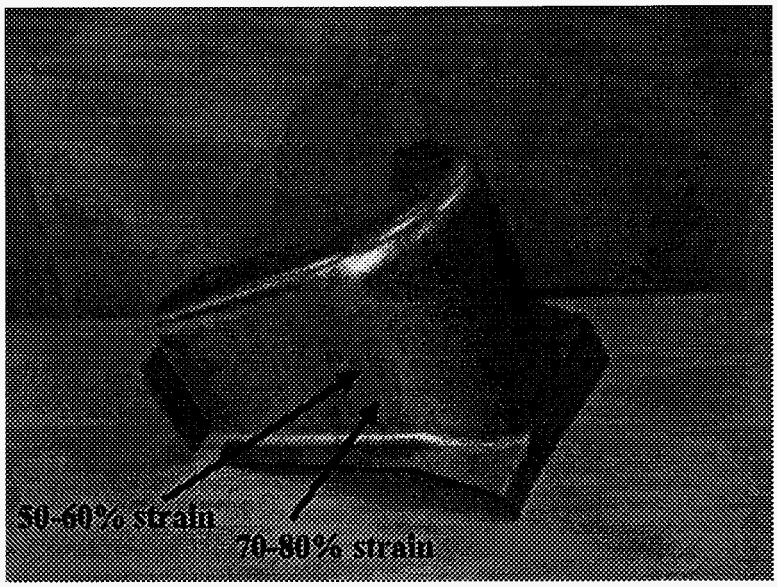

Figure 8. Shock tower part showing regions with major strains of 50-60% and 70-80%

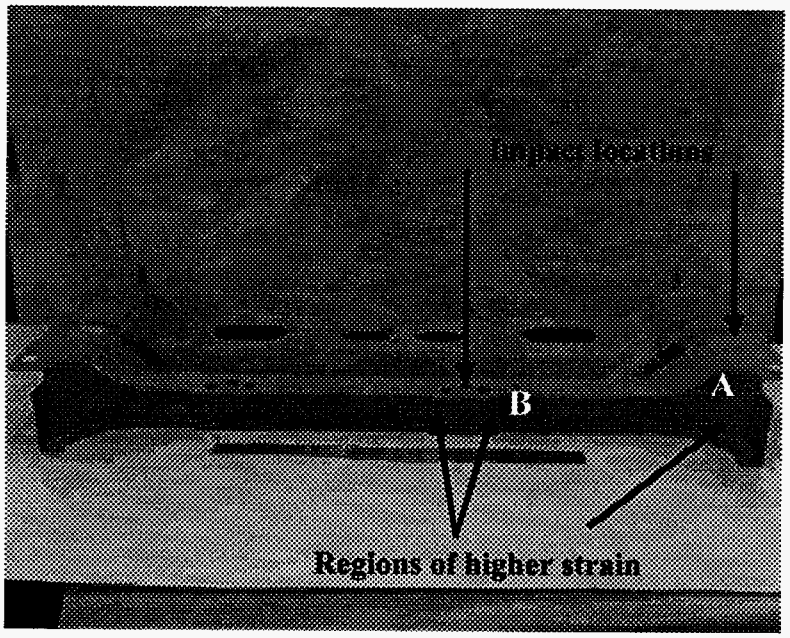

Figure 9. Floor suspension panel showing regions of high strain selected for impact testing

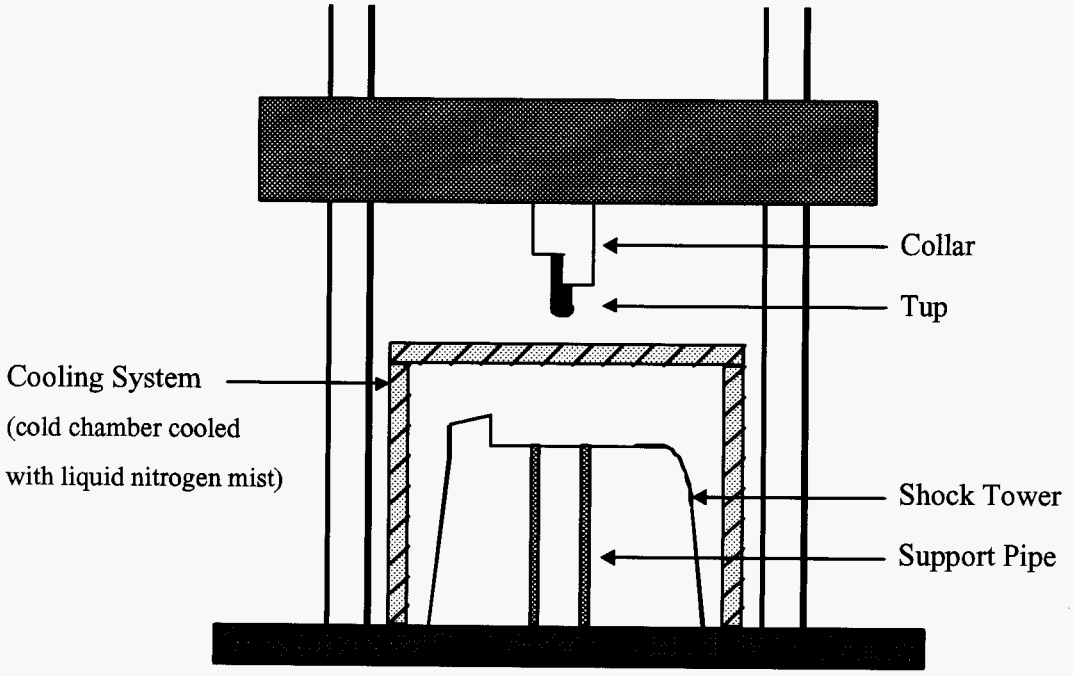

Figure 10. Schematic of localized drop weight testing of shock tower parts

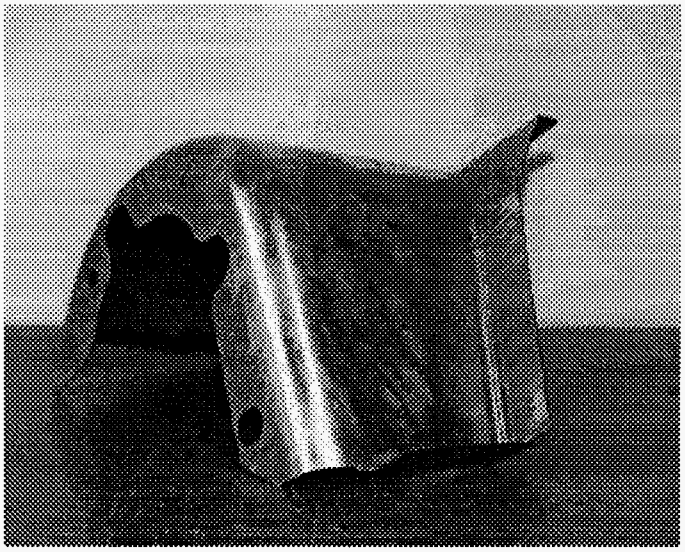

Figure 11. Shock tower part showing orientation used for general impact testing

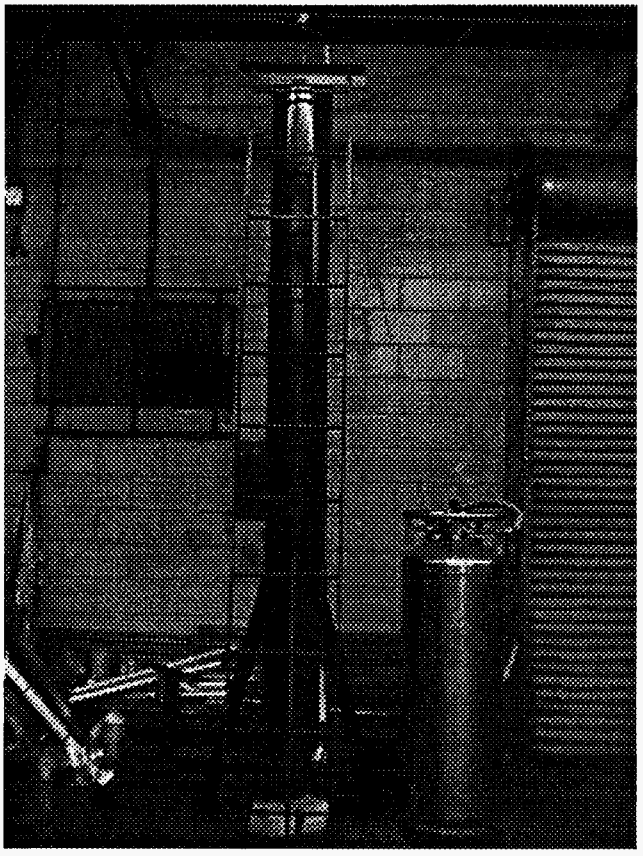

Figure 12. Drop weight tester at Fleet Technology

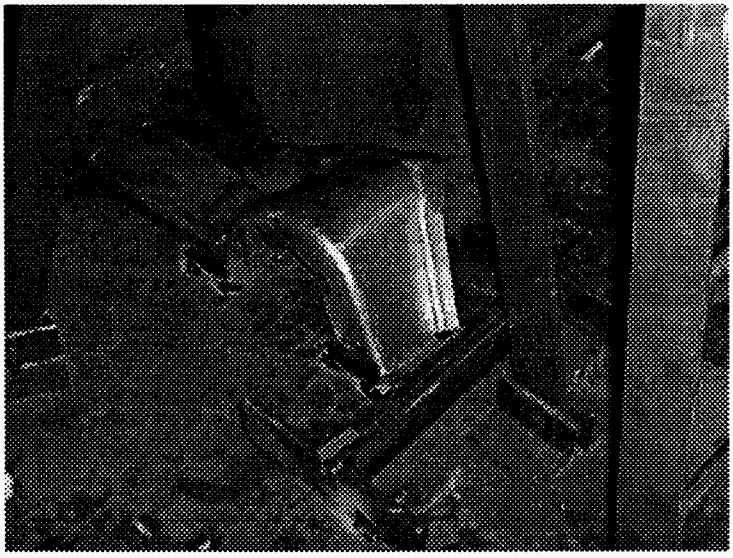

Figure 13. Orientation of shock tower beneath Fleet Technology drop weight tester

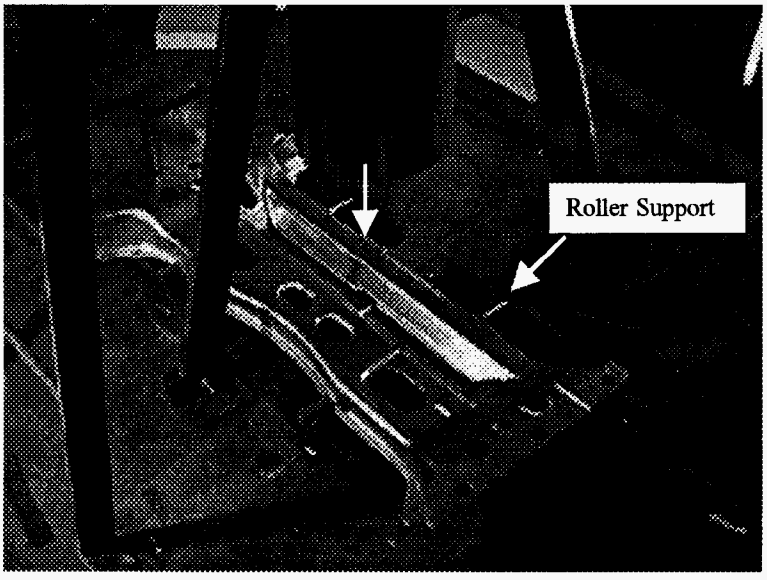

Figure 14. Floor suspension panel showing roller supports to produce 3-point bending at impact location indicated by the arrow

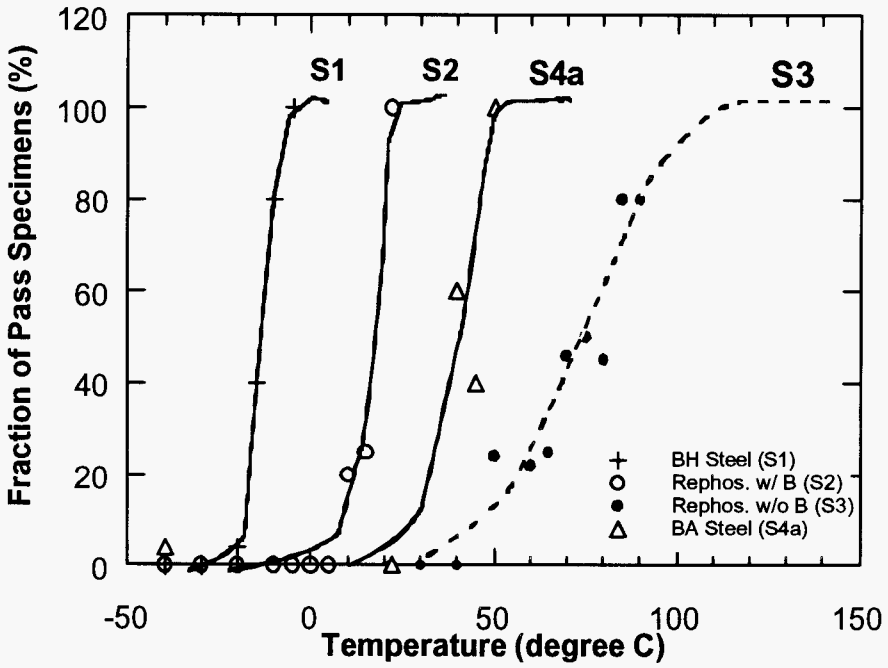

Figure 15. Bend test ductile-to-brittle transition curves.

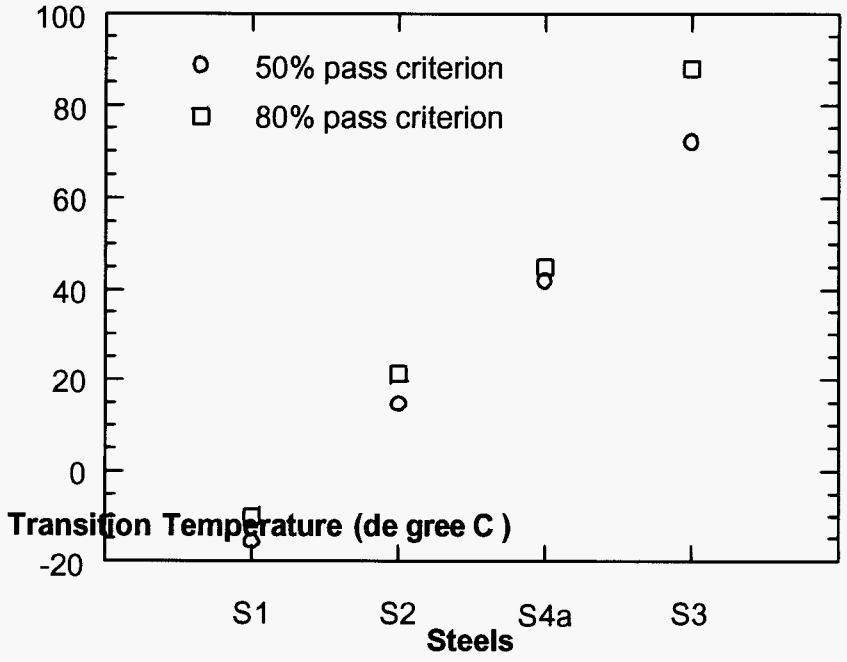

Figure 16. Bend test transition temperature for two DBTT criteria.
(Legend: O – 50% pass criteria; - 80% pass criteria)

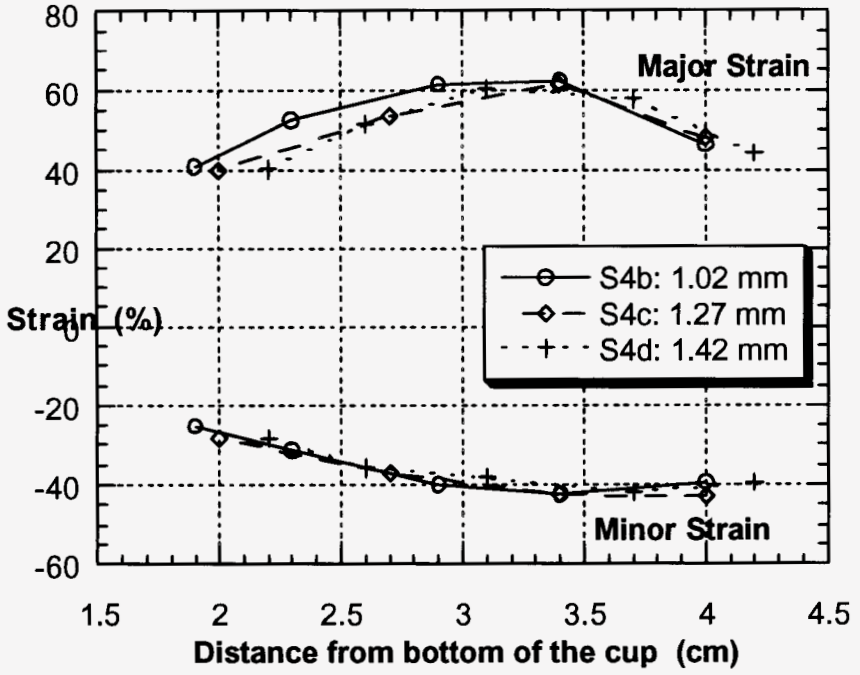

Figure 17. Strain in 2-inch cup wall with DR of 2.0 for steels of three different thickness.

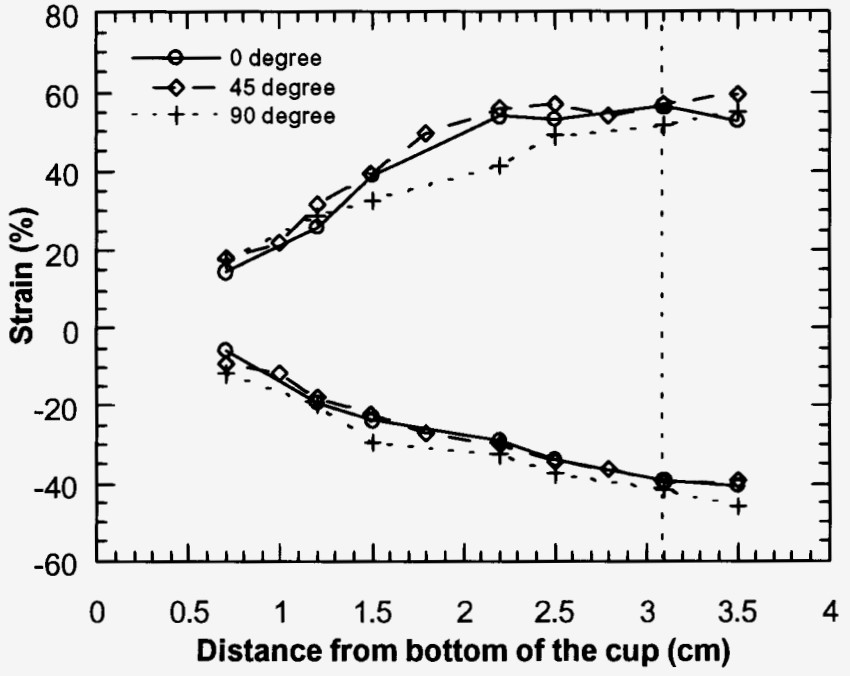

Figure 18. Strain in 2-inch cup wall with DR of 2.0 (steel S3, 0.74 mm thick).

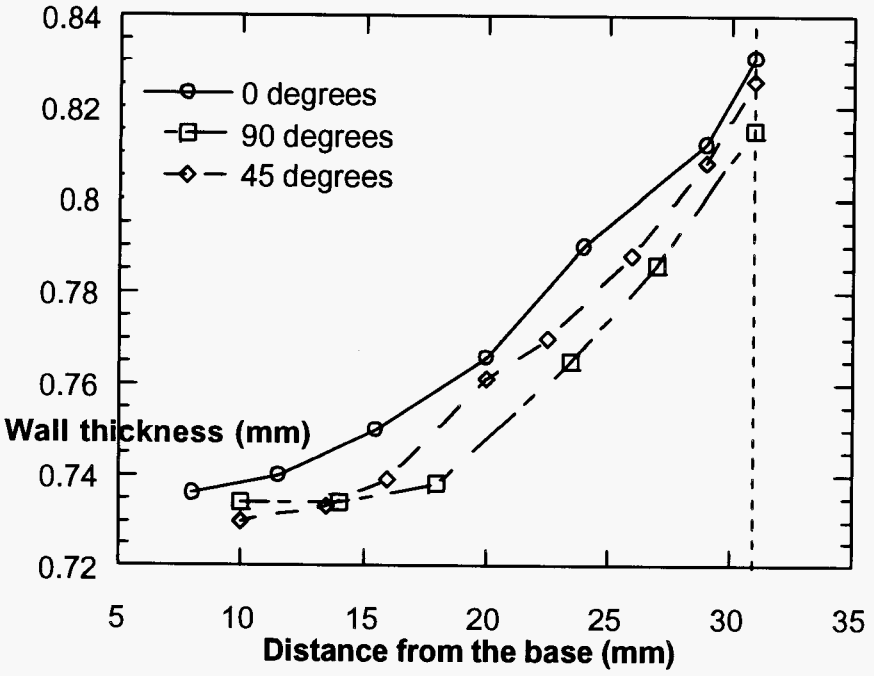

Figure 19. Wall thickness distribution at three angular positions in a 2-inch cup trimmed at 31 mm (steel S3) (Legend: o – O degrees; - 90 degrees; ◊- 45 degrees)

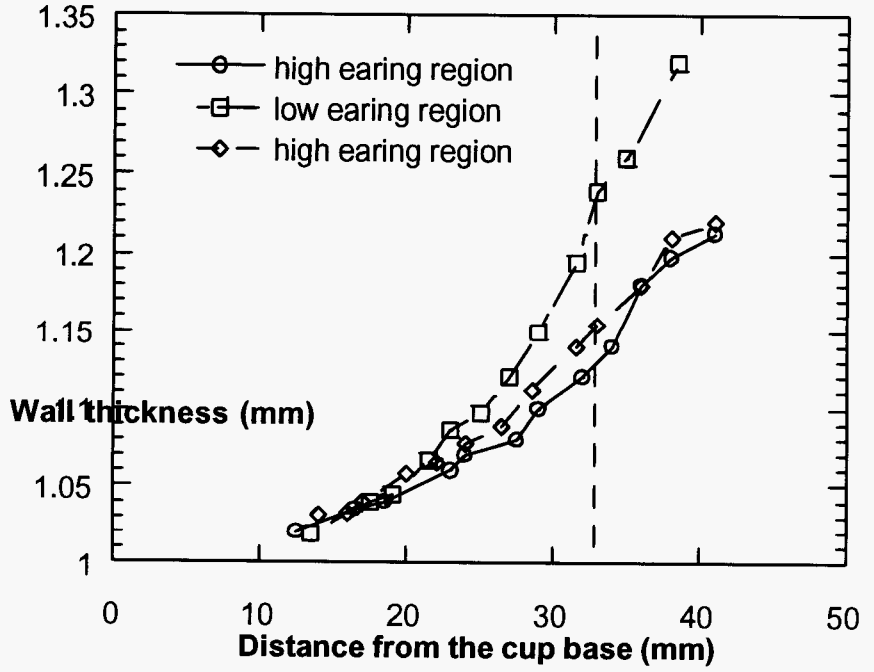

Figure 20. Wall thickness distribution at three angular positions in a as-drawn 2-inch cup (steel S4b). (Legend: o – high earing region; - low earing region; ◊- high earing region)

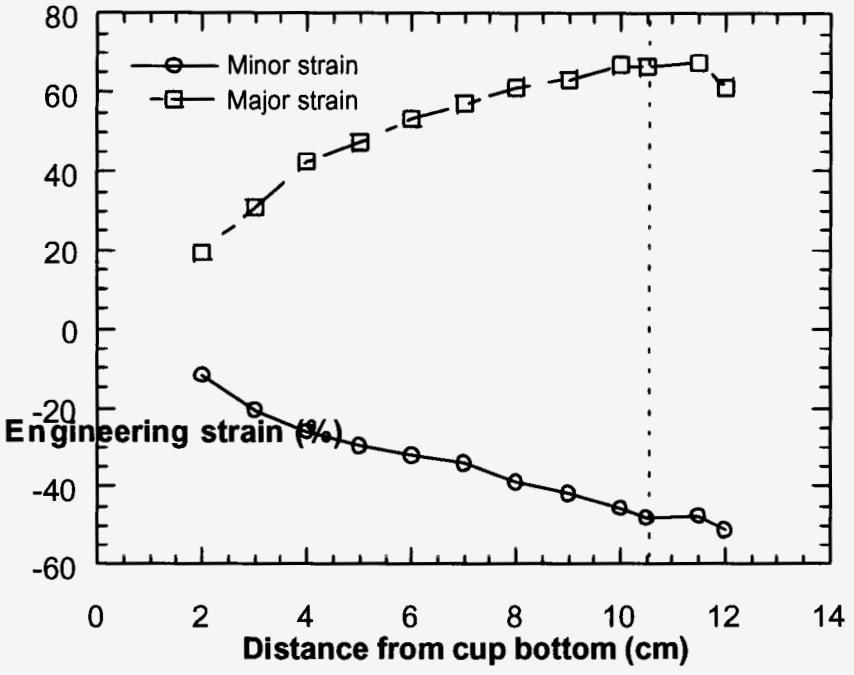

Figure 21. Strain distribution in the cup wall of a 6-inch as-drawn cup. (Legend: 0 – Minor strain; - Major strain)

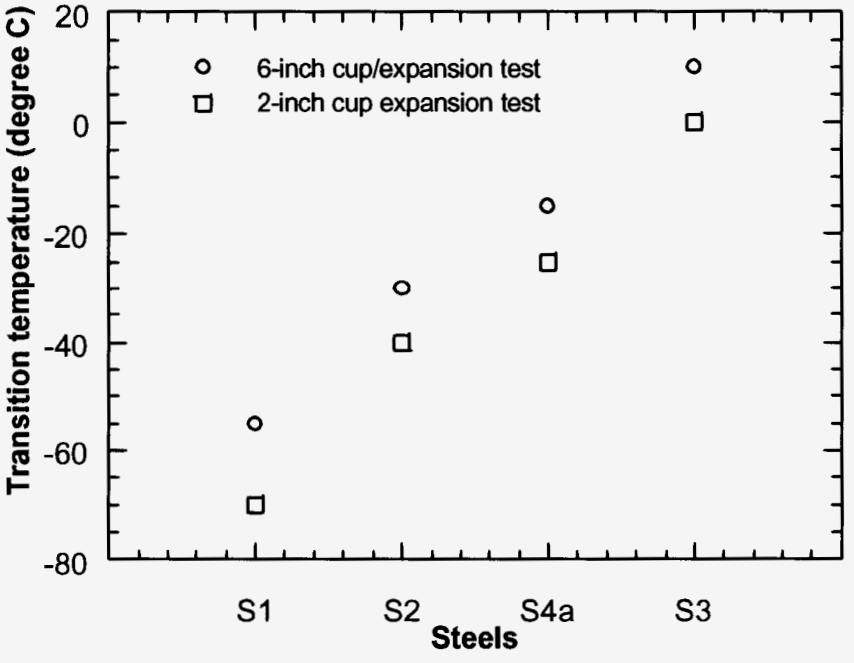

Figure 22. Comparison between DBTT obtained by 2-inch and 6-inch cup/expansion test.

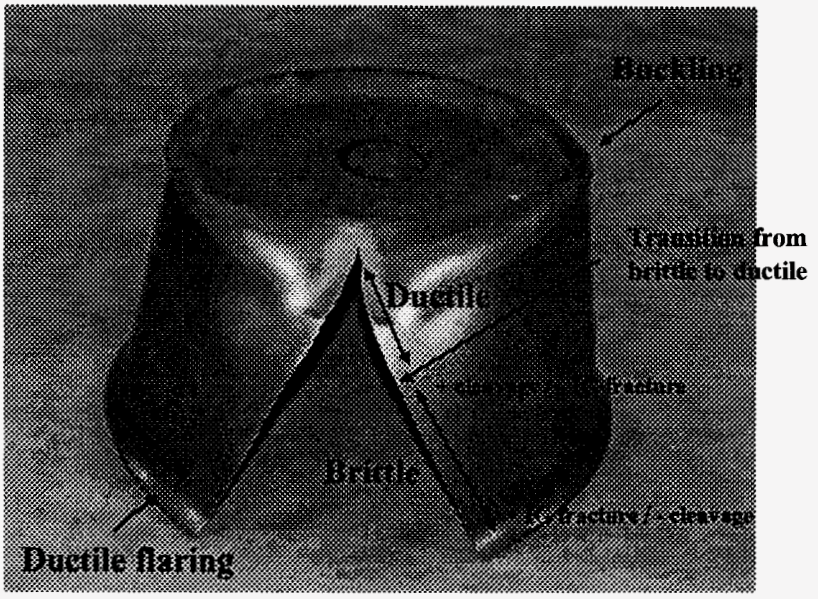

Figure 23 (a). Aspect of a crack in a 6-inch cup.

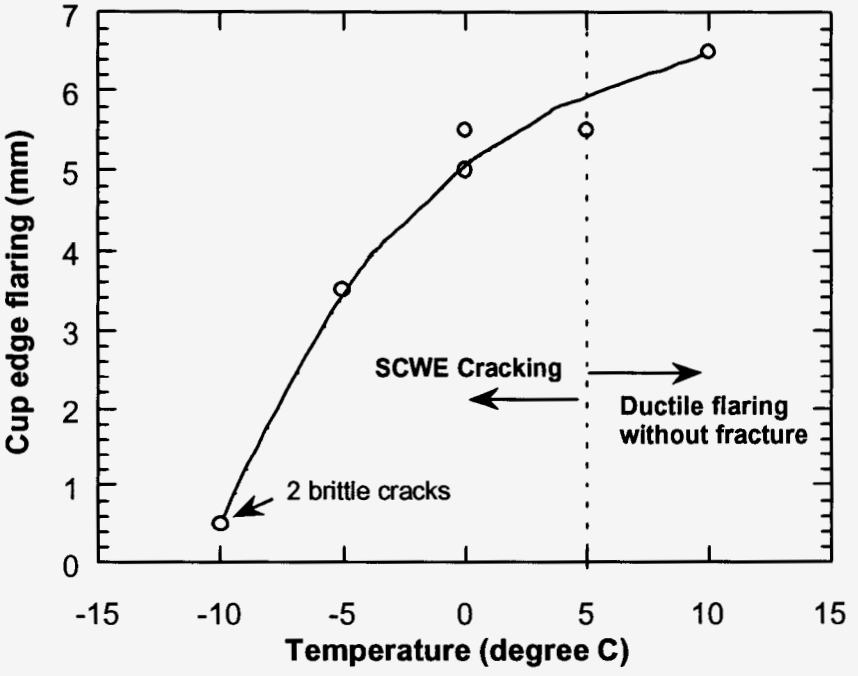

Figure 23 (b). Ductile flaring at the cup edge of S3 steel cups.

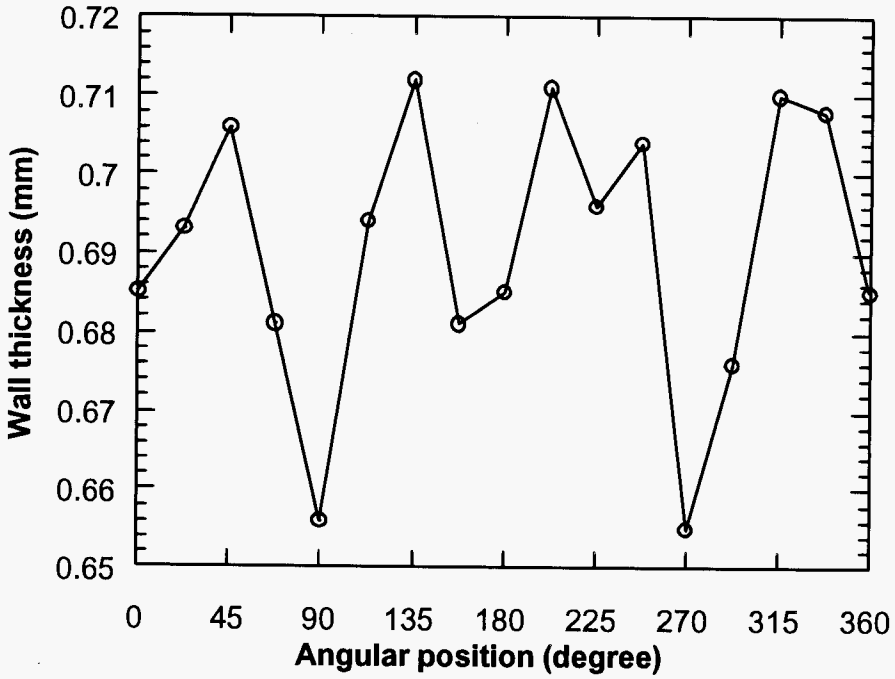

Figure 24. Wall thickness variation at the edge of a 6-inch cup with DR=2.0 (steel S3).

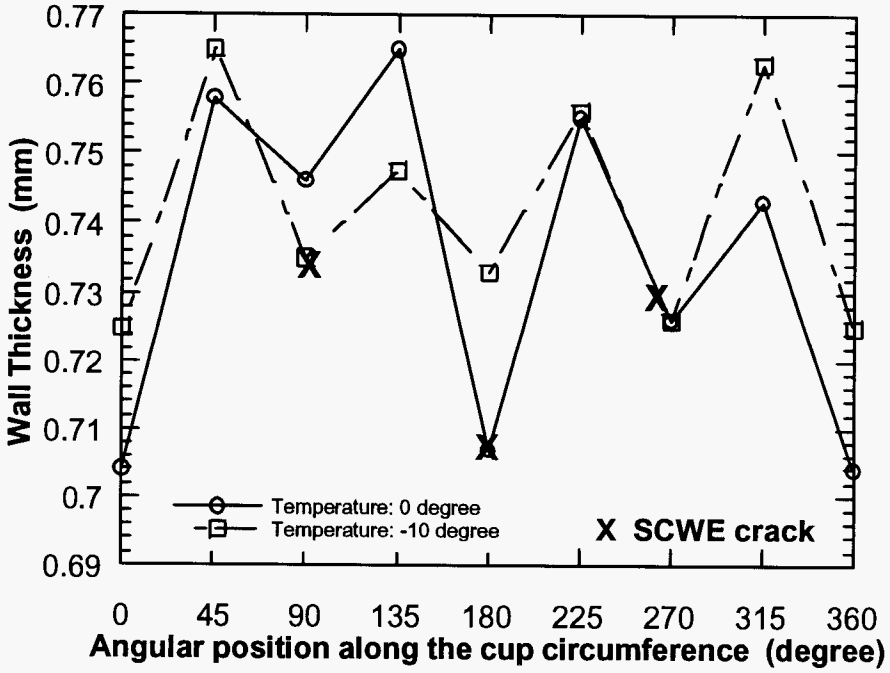

Figure 25. Wall thickness variation at the edge of 2 trimmed 6-inch cups and position of SCWE cracks.

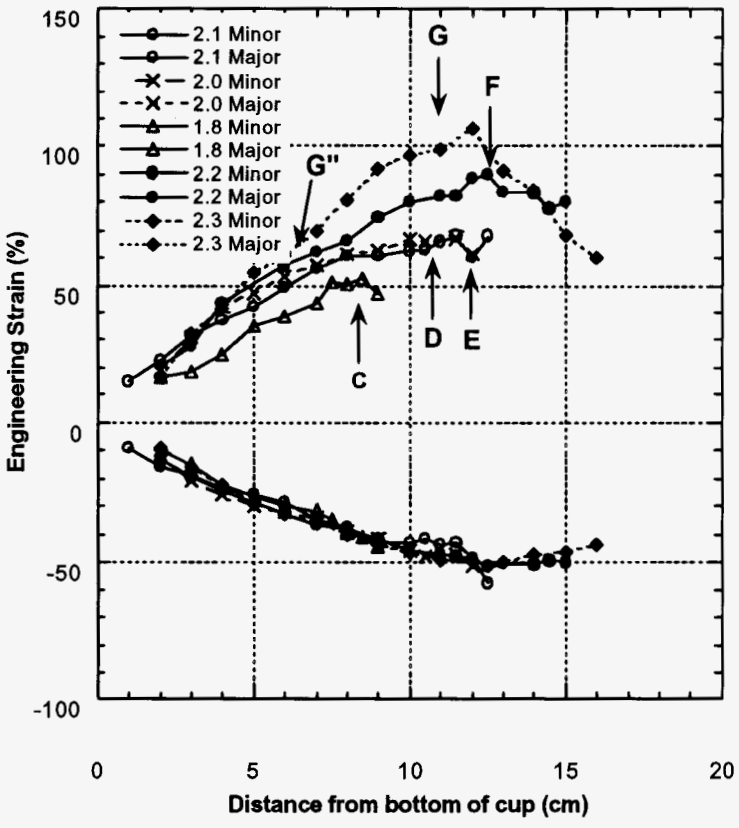

Figure 26. Strain distribution and trimming location in 6-inch cups

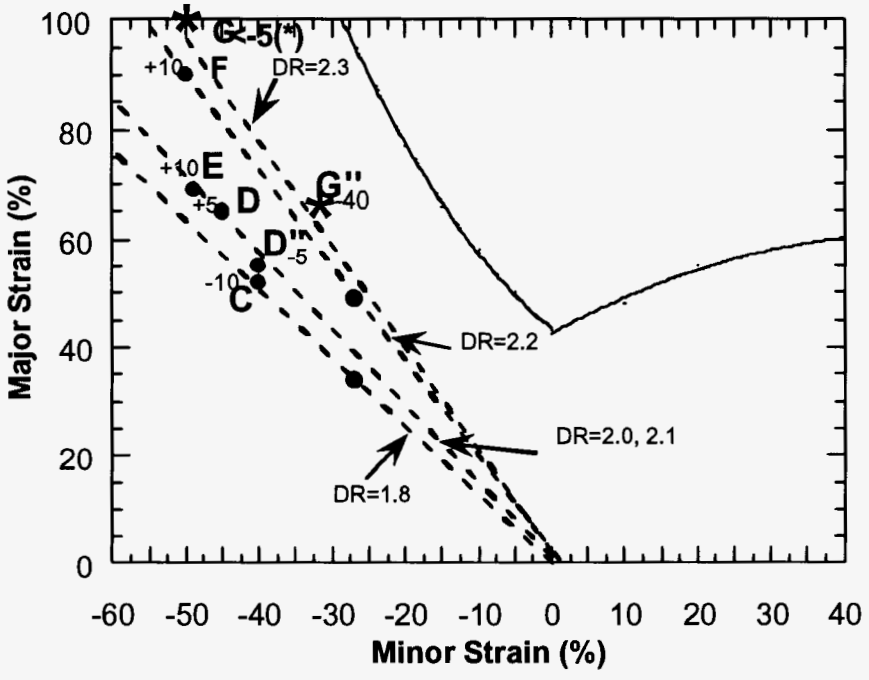

Figure 27. DBTT/strain map for 6-inch cups

Draw Ratio	Trimmed height (mm)	Strain at edge	DBTT (°C)
2.0	105	~65	+10°C
2.3	105	100	-5°C
2.3	70	~65	-40°C

Figure 28. Effect of strain and trimming location on DBTT (anomalous behaviour)

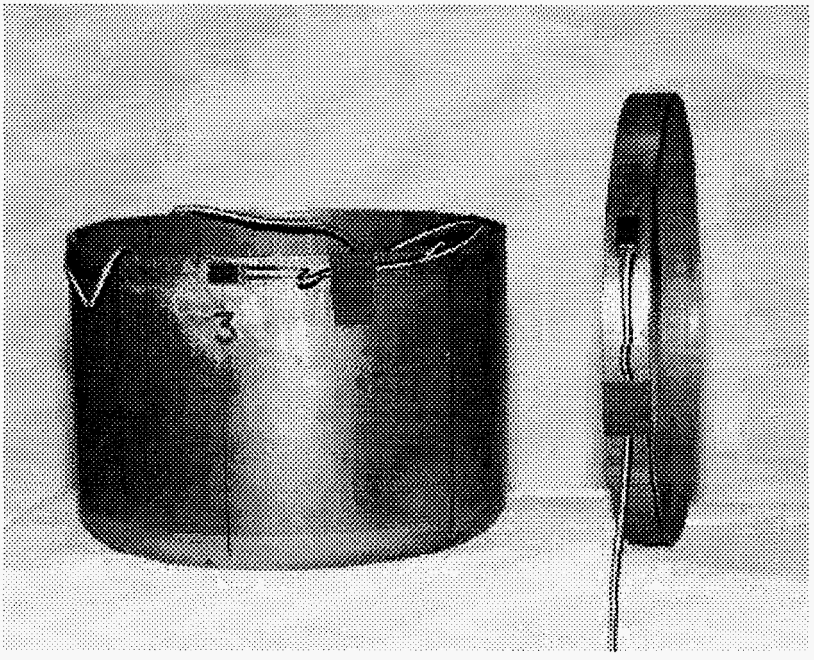

Figure 29. 6-inch cup with strain gauges attached

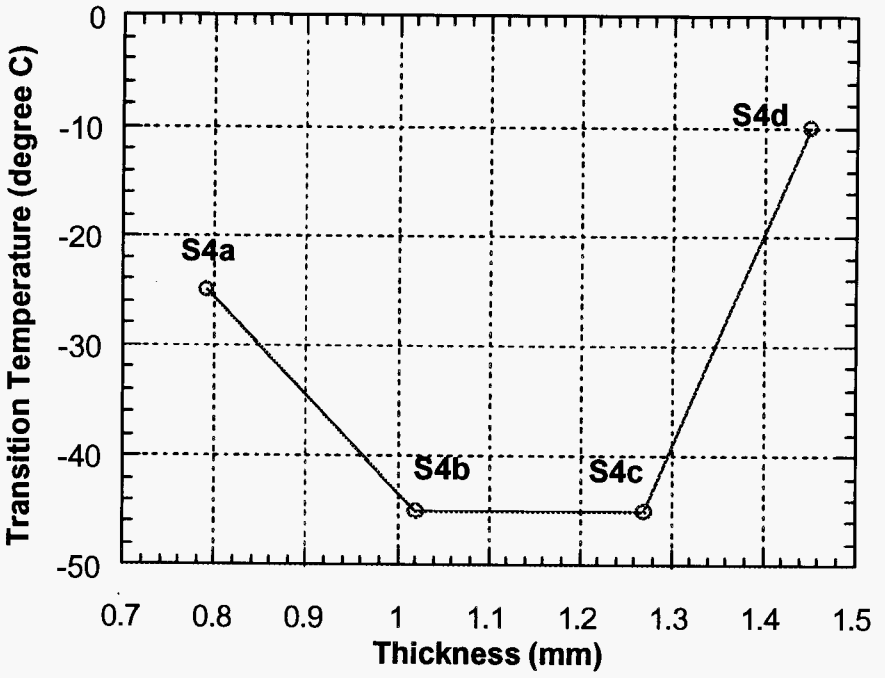

Figure 30. DBTT cup/expansion results obtained in 4 steels with different thickness.

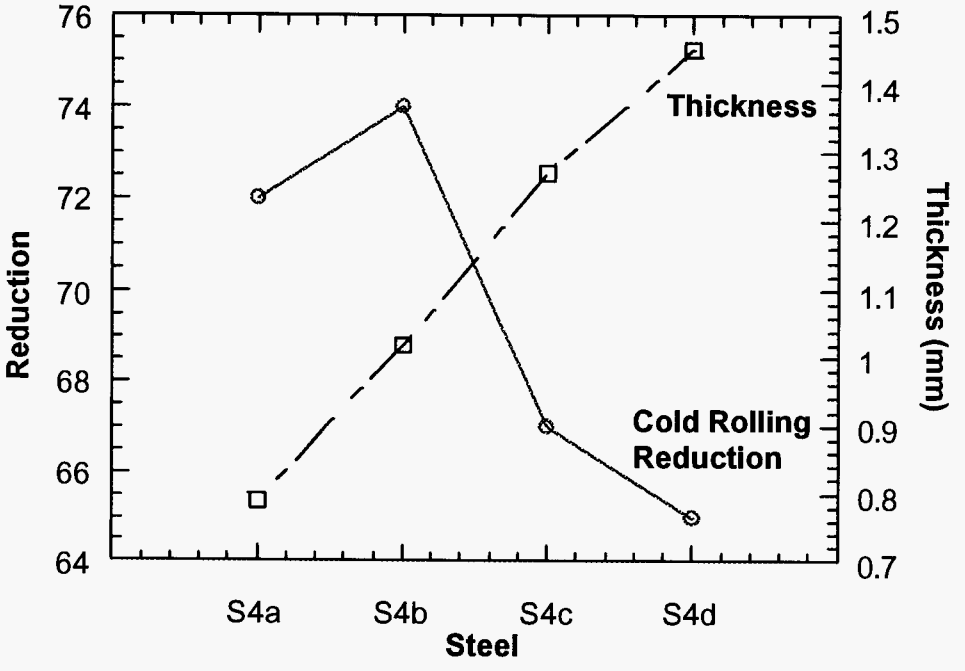

Figure 31. Cold reduction (%) and sheet thickness of series S4 steels

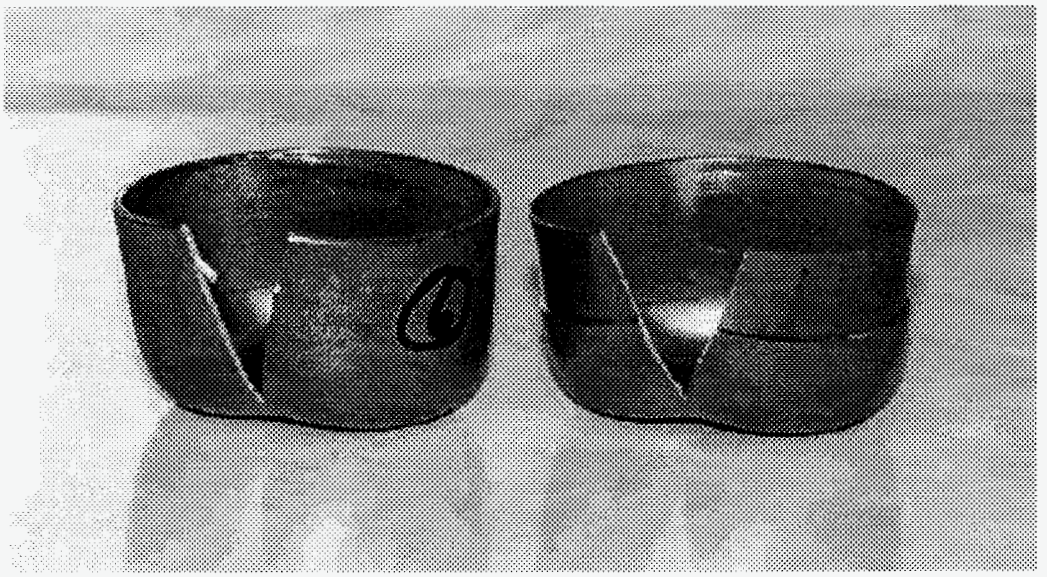

Figure 32. As-drawn and reduced-wall cups after trimming.

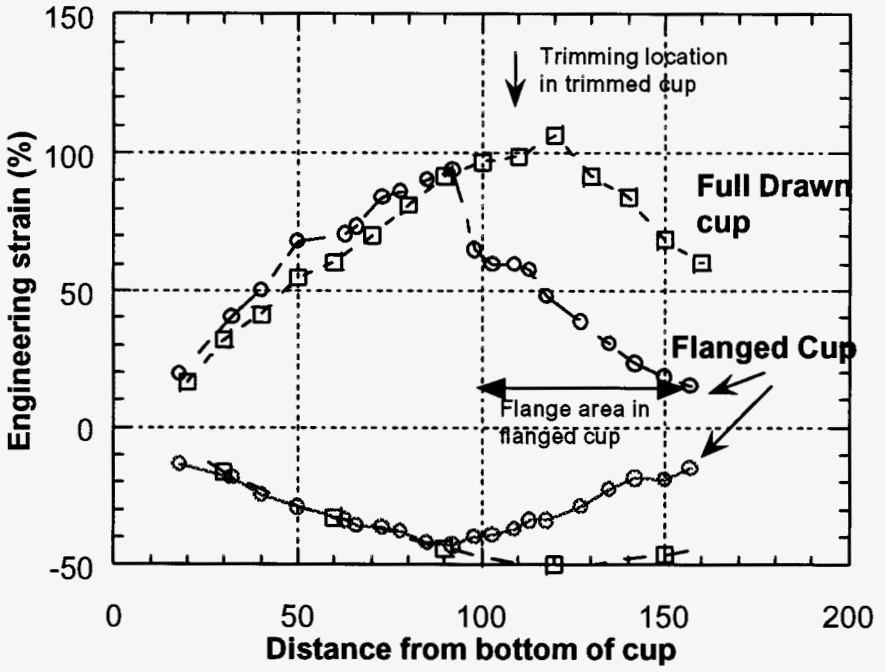

(a) Draw Ratio 2.3, flange width of 40 mm

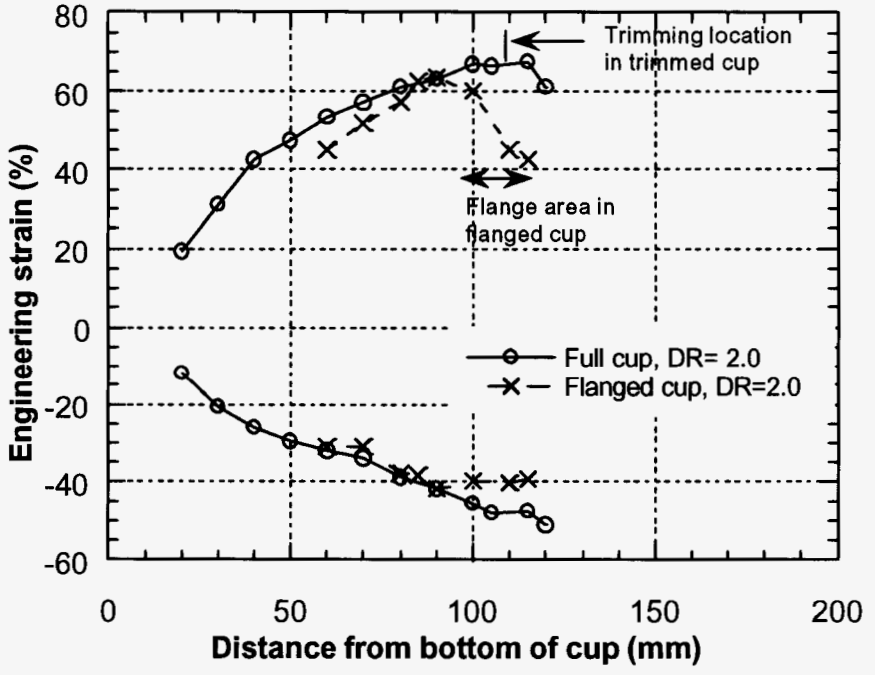

(b) Draw ratio 2.0, flange width 15-20 mm

Figure 33. Strain distribution in full drawn and flanged cups

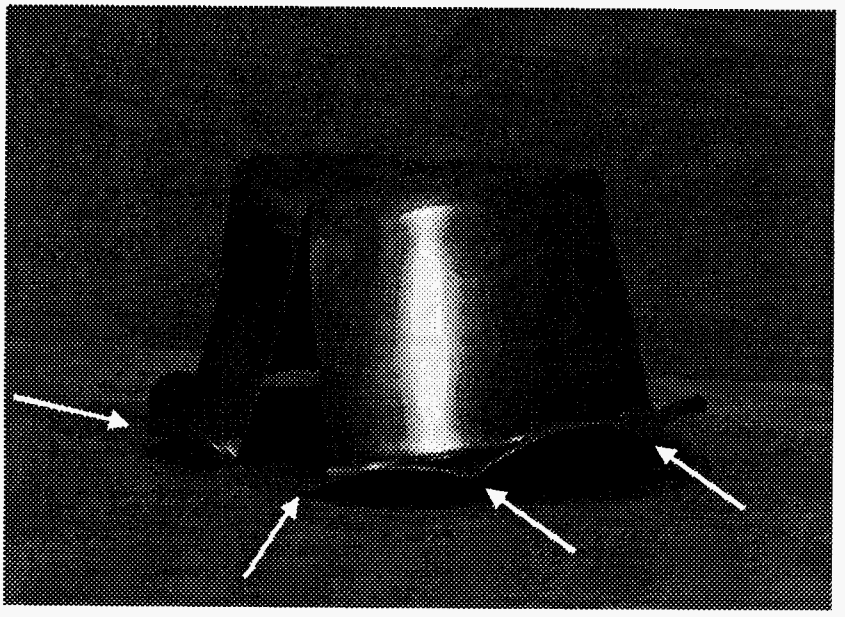

Figure 34. Flanged cup using a draw ratio of 2.0 showing bending of the flange as indicated by the arrows

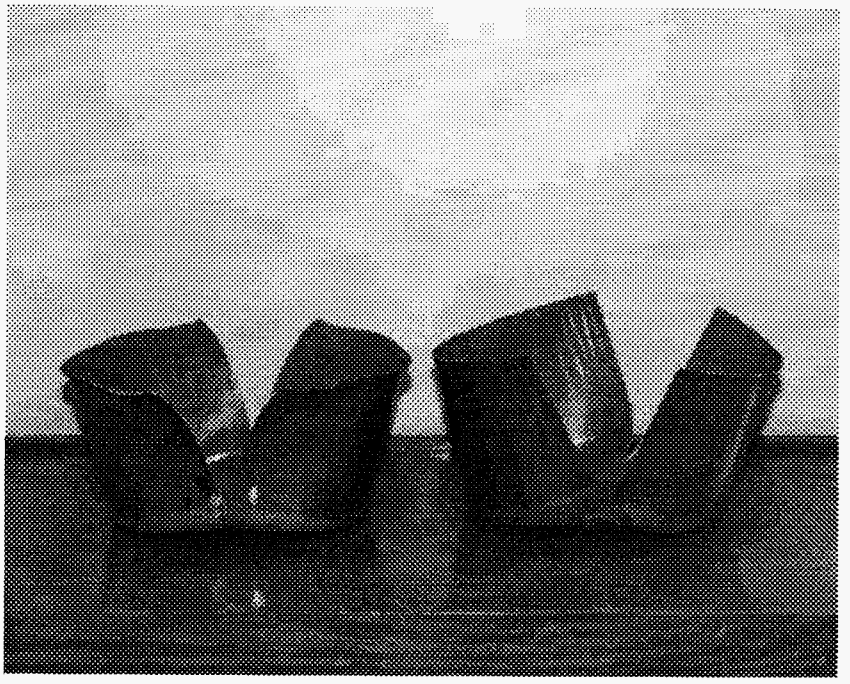

Figure 35. Notched cups tested at 0°C showing a ductile fracture on the left and a brittle one on the right

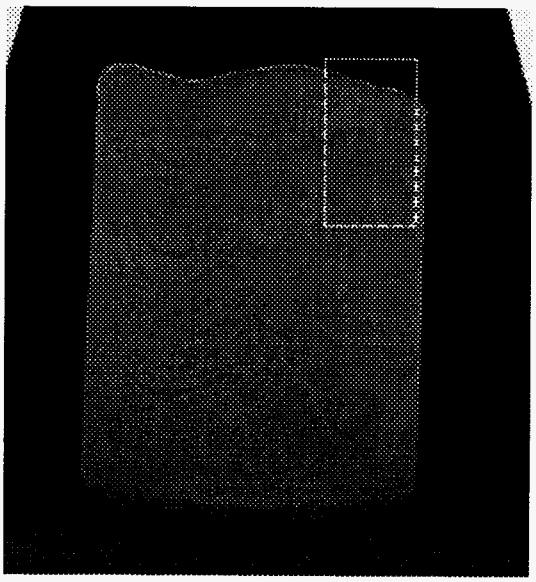

Figure 36(a). Crack at the edge of an as-drawn 6-inch cup.

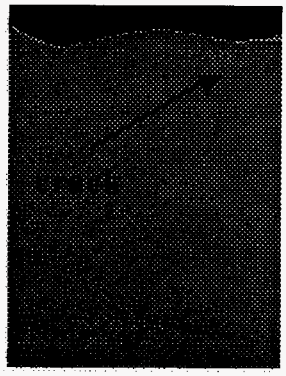

Figure 36(b). Larger magnification of the area indicated in Fig. 36(a).

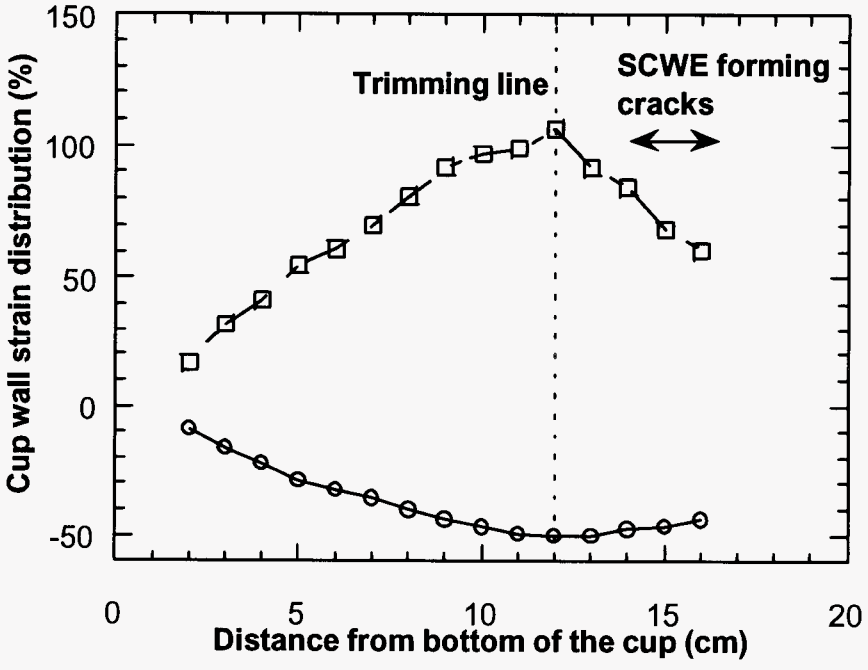

Figure 37. Strain in region of the cup with SCWE forming cracks.

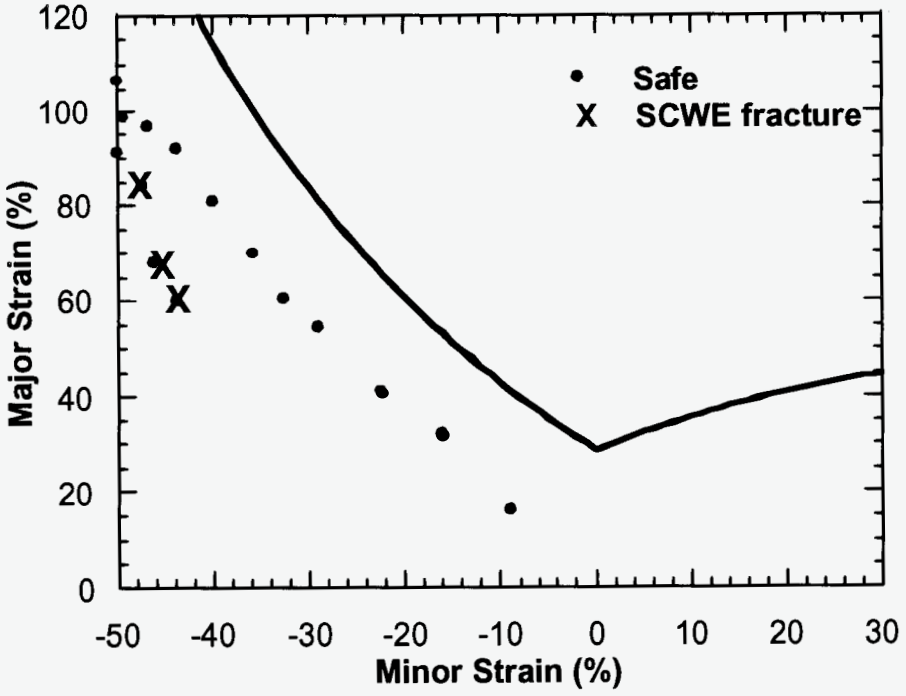

Figure 38. Strain distribution in 6- inch cups with 2.3 draw ratio.

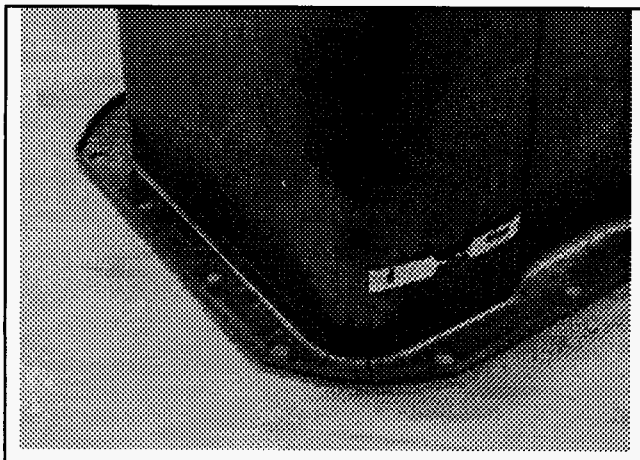

Figure 39(a). Cracks in the draw corner of an a V-8 engine oil pan made with steel S6b.

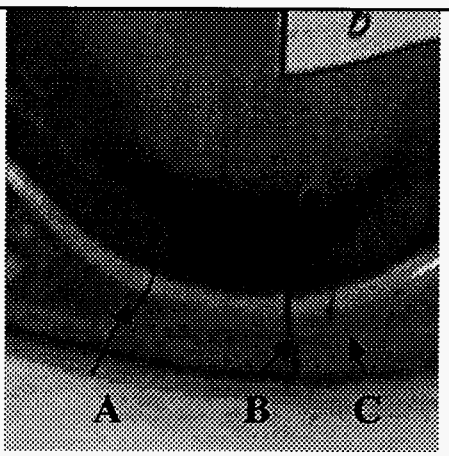

Figure 39(b). Same as 39(a) at higher magnification.

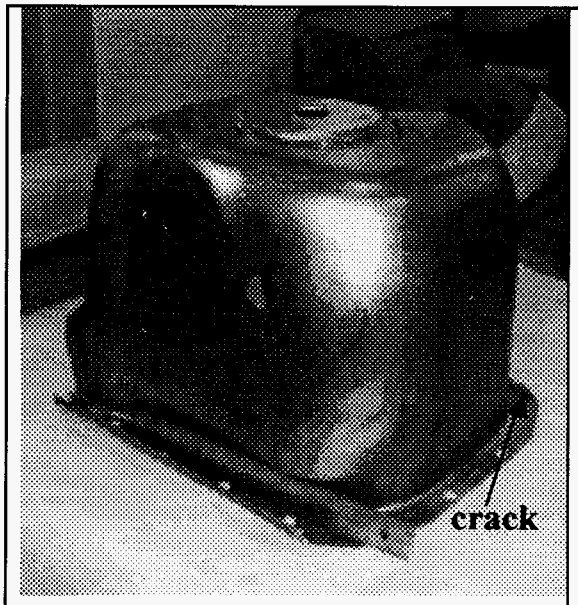

Figure 39 (c). Large diesel engine oil pan.

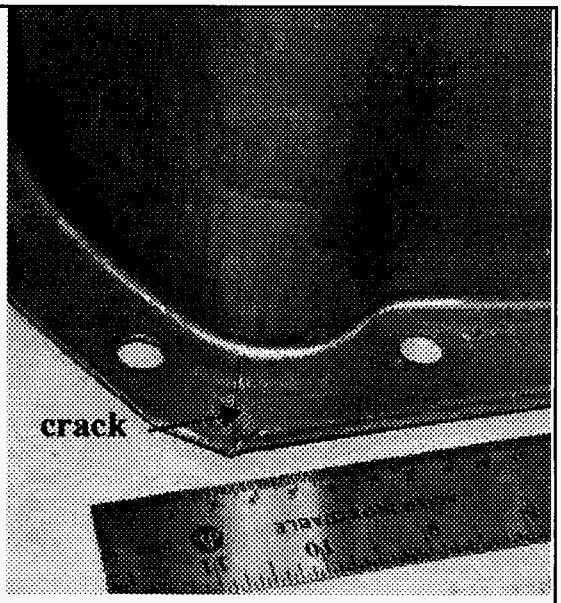

Figure 39 (d). Crack in a corner of a large diesel engine oil pan shown in Fig. 39(c).

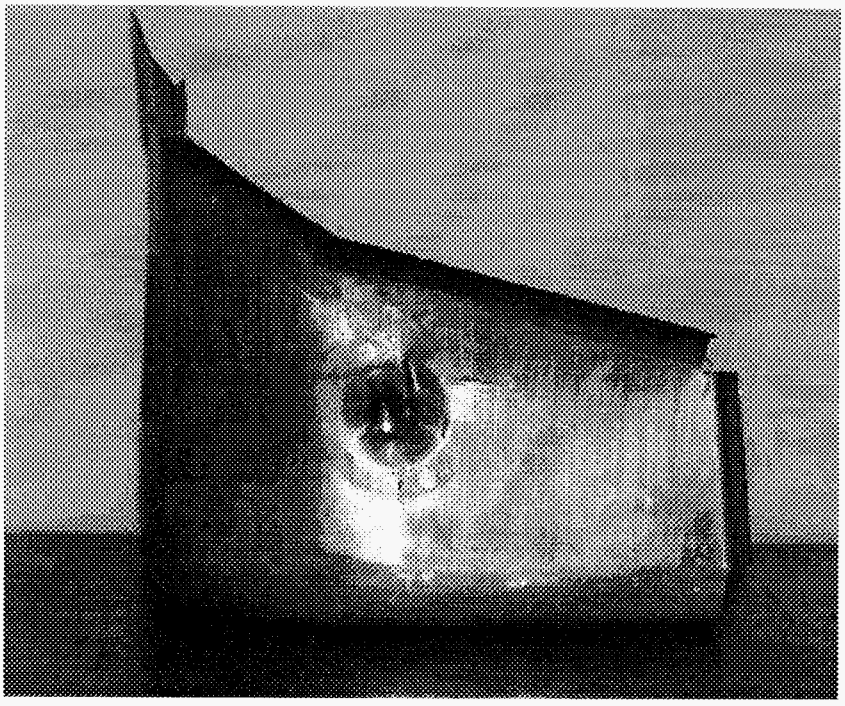

Figure 40. Shock tower part after localized testing showing plastic deformation

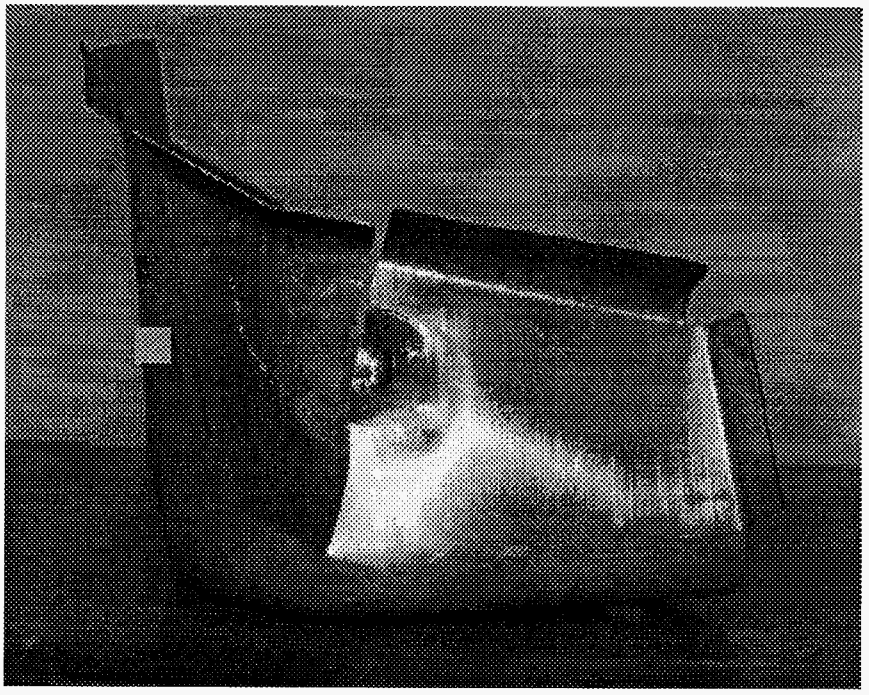

Figure 41. Shock tower part after localized impact testing showing brittle fracture

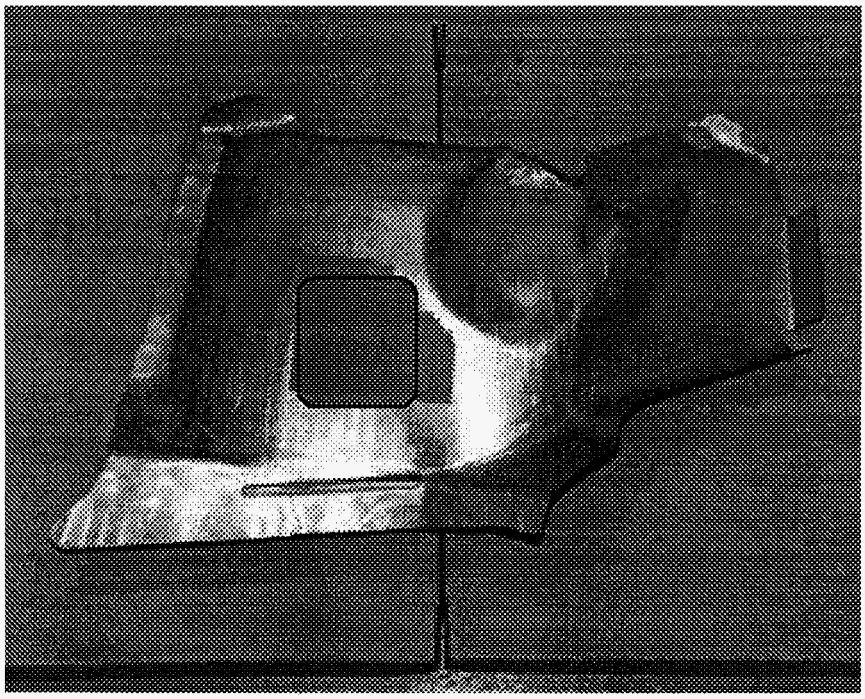

Figure 42. Shock tower part showing plastic collapse after general impact testing

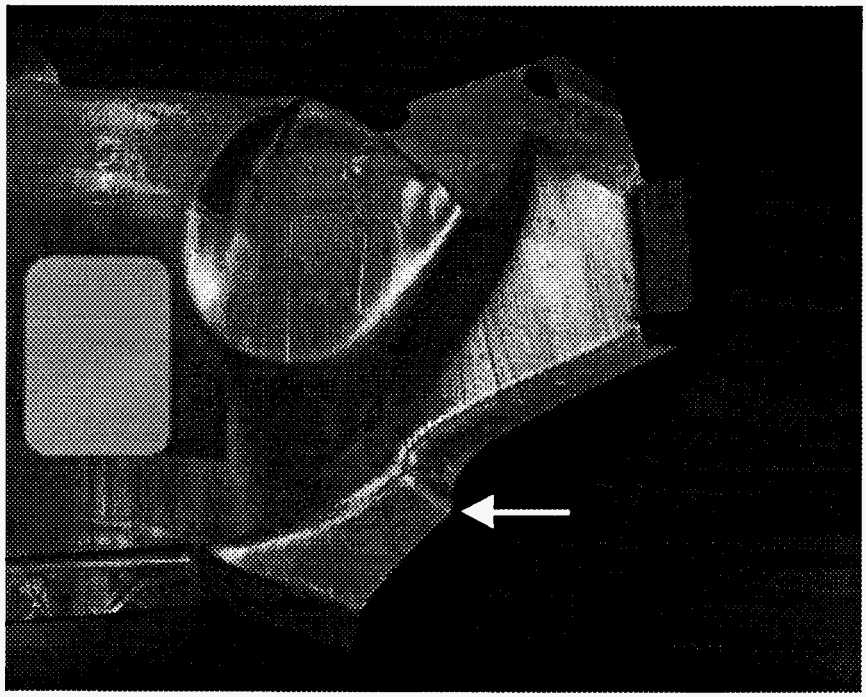

Figure 43. Shock tower part after general impact testing showing buckling at the flange indicated by the arrow

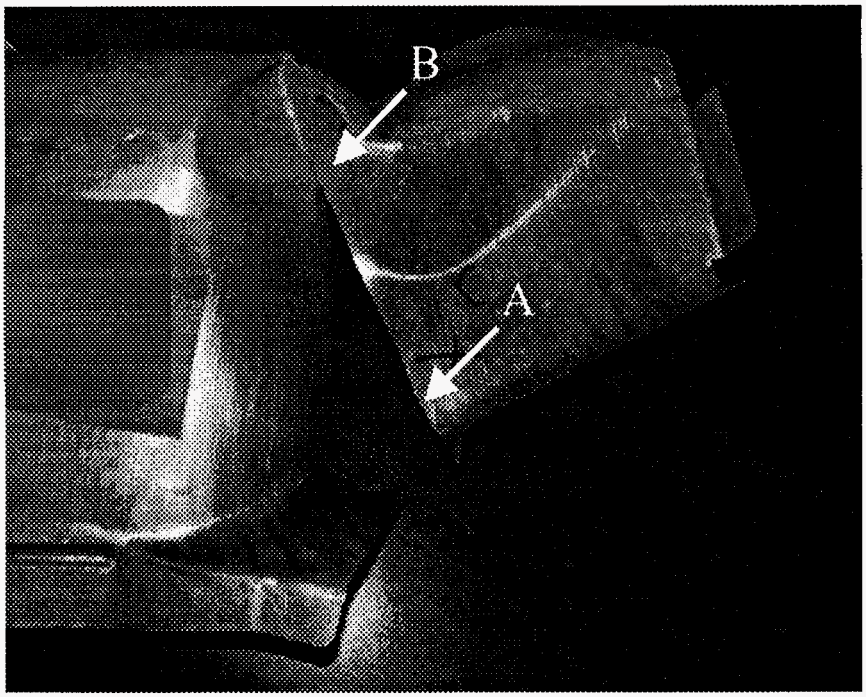

Figure 44. Shock tower part after general impact testing showing brittle fracture initiating at A and arresting at point B.

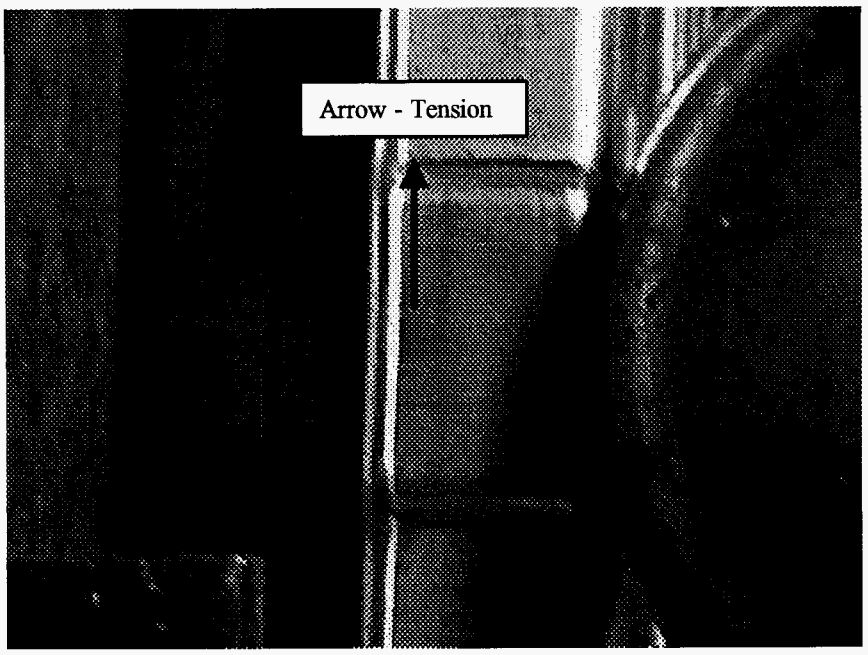

Figure 45(a) Floor suspension panel using test configuration shown in figure 14 at test location immediately prior to impact

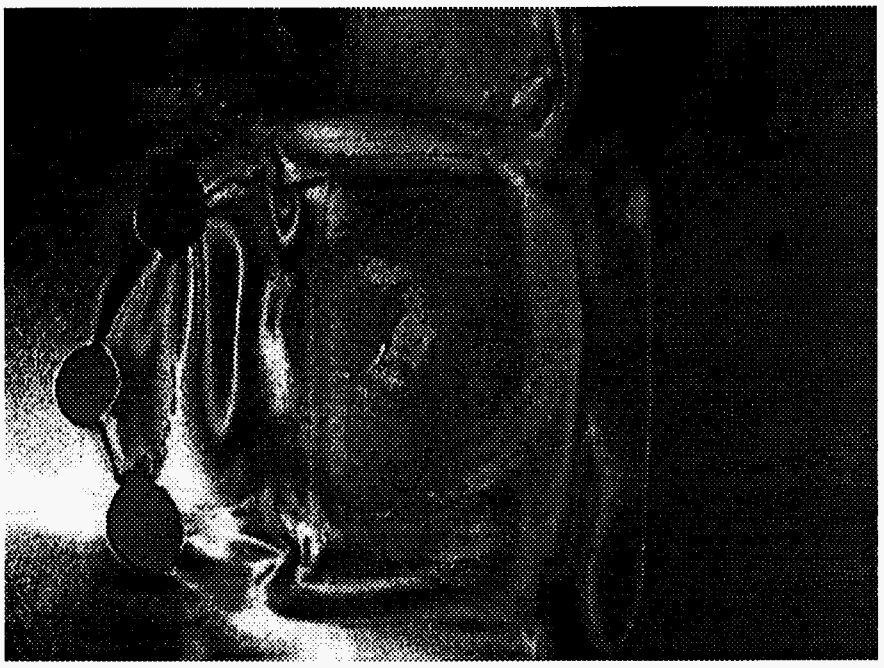

Figure 45(b). Test location shown in figure 45(a) after impact

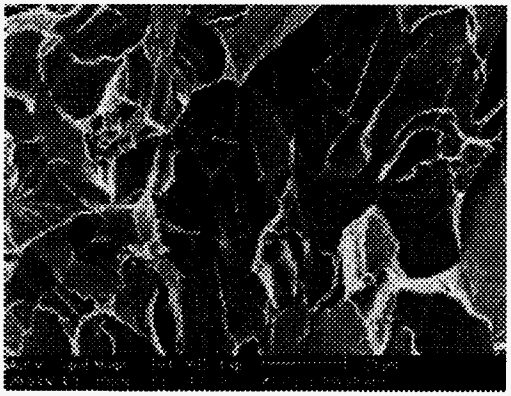

a) Steel S1, DBTT: -55°C; 4% IG

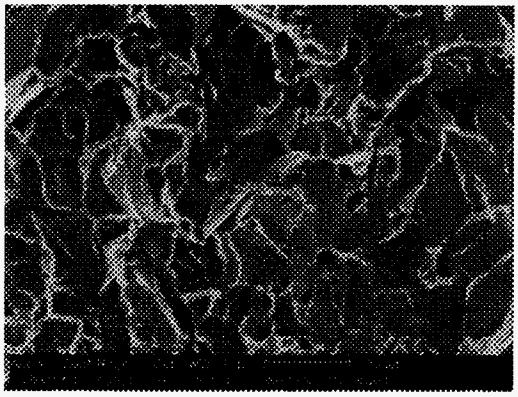

b) Steel S2, DBTT: -30°C; 20% IG

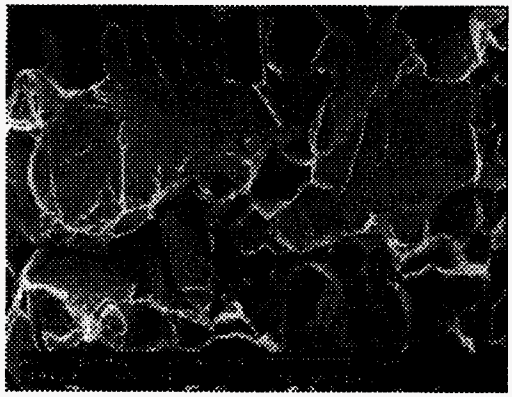

c) Steel S4a , DBTT: -15°C; 63% IG

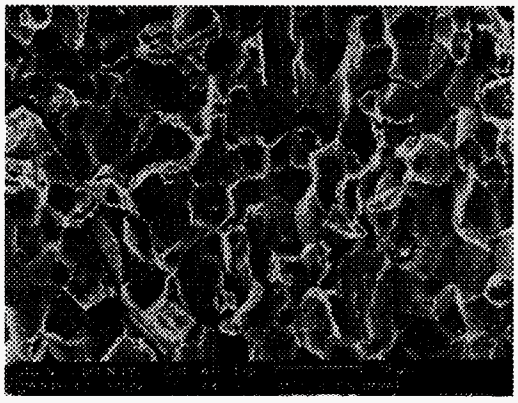

d) Steel S3, DBTT: +10°C; 82% IG

Figure 54. Unstrained steels notched and fractured in liquid nitrogen.

a) Steel S1, 12 % IG

b) Steel S2, 67% IG

c) Steel S4a, 72% IG

d) Steel S3, 80% IG

Figure 55. Prestrained steels notched and fractured in liquid nitrogen (LN orientation).

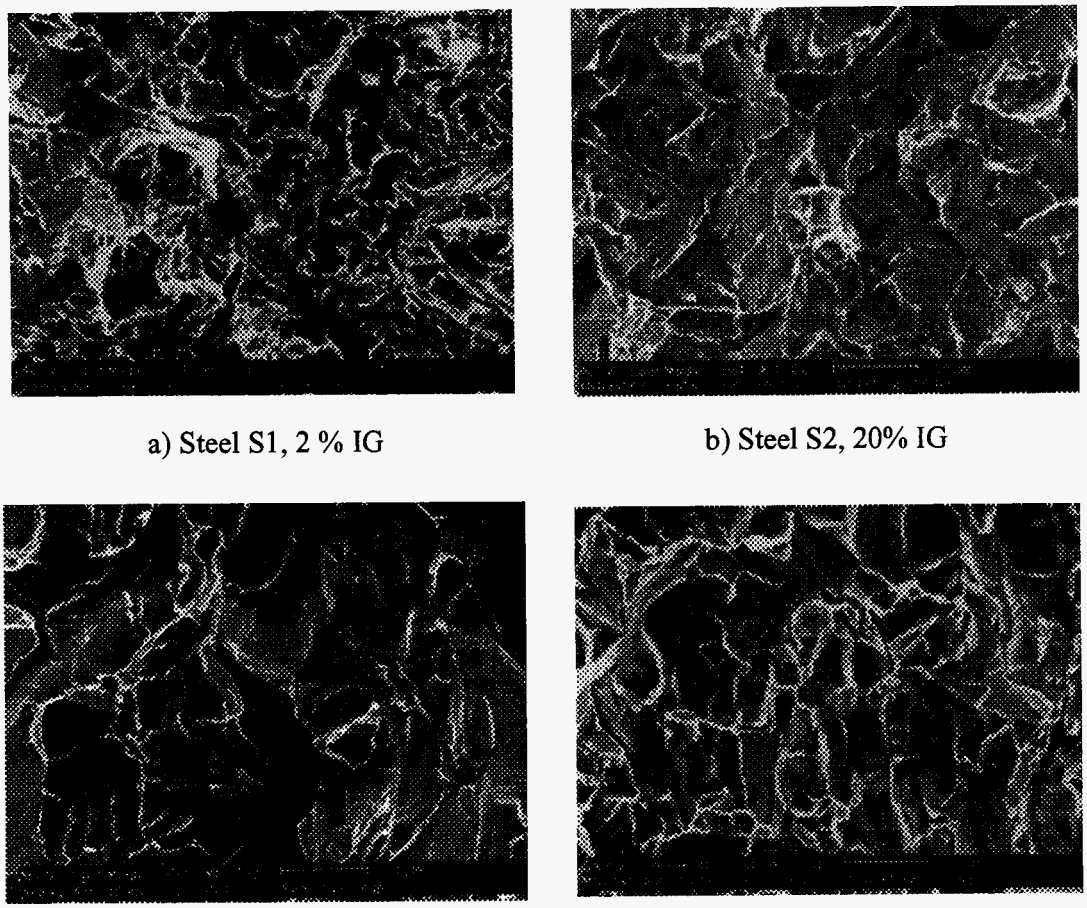

a) Steel S1, 2 % IG

b) Steel S2, 20% IG

c) Steel S4a, 44% IG

d) Steel S3, 78% IG

Figure 56. Prestrained steels notched and fractured in liquid nitrogen (TN orientation).

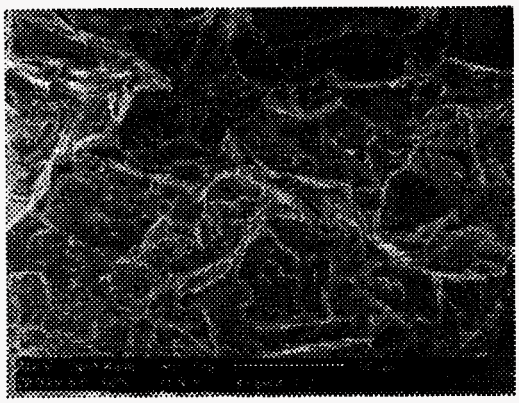

a) Steel S1, DBTT: -10°C

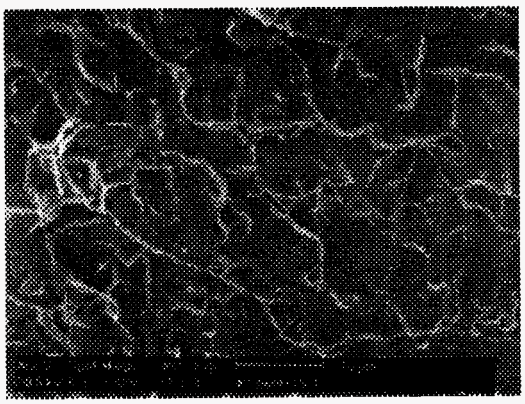

b) Steel S2, DBTT: +15°C

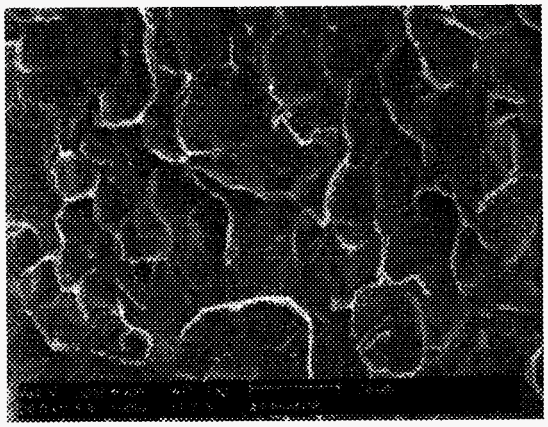

c) Steel S3, DBTT: +95°C

Figure 57. Fracture surface of bend specimens

a) Steel S3, DR=1.8, 25% major strain, fractured at –10°C

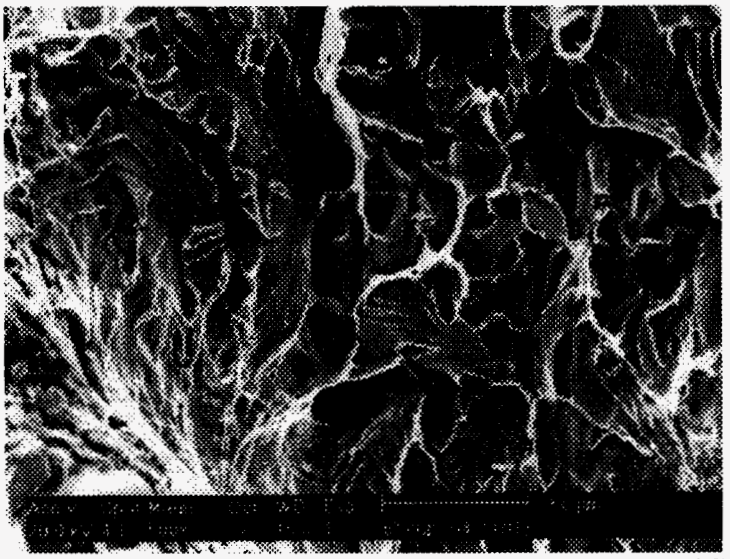

b) Steel S4a, DR=2.0, 42% major strain, fractured at –15°C

Figure 58. Fracture surface of steel S3 and S4(a) near the brittle to ductile transition area along the cup wall (cup/expansion specimens fractured at the transition temperature).

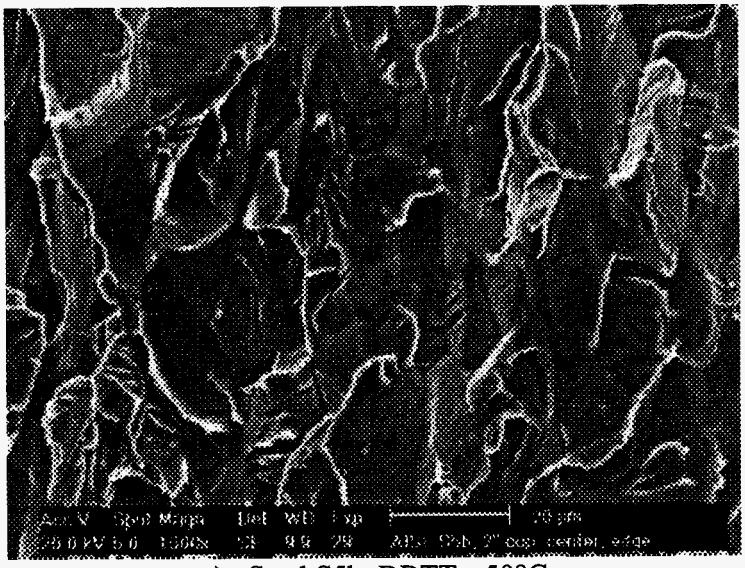

a) Steel S5b, DBTT: -50°C

b) Steel S6a, DBTT: -10°C

Figure 59. Fracture surfaces of 2-inch cups from steels S5b and S6a (fracture surface at edge corresponding to 55% major strain).

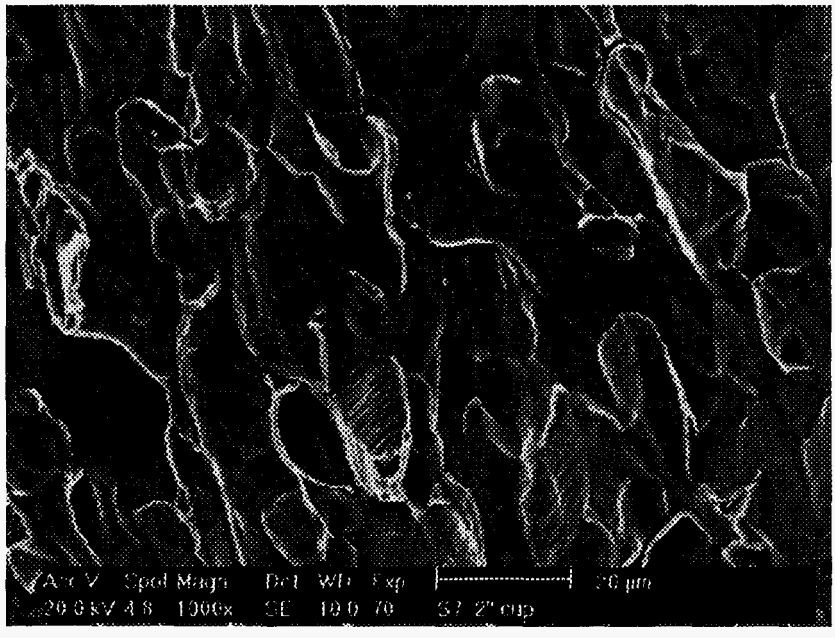

S7 Steel, specimen fractured at -35°C

Figure 60. Fracture surface at the edge of the 2-inch cup for steel S7

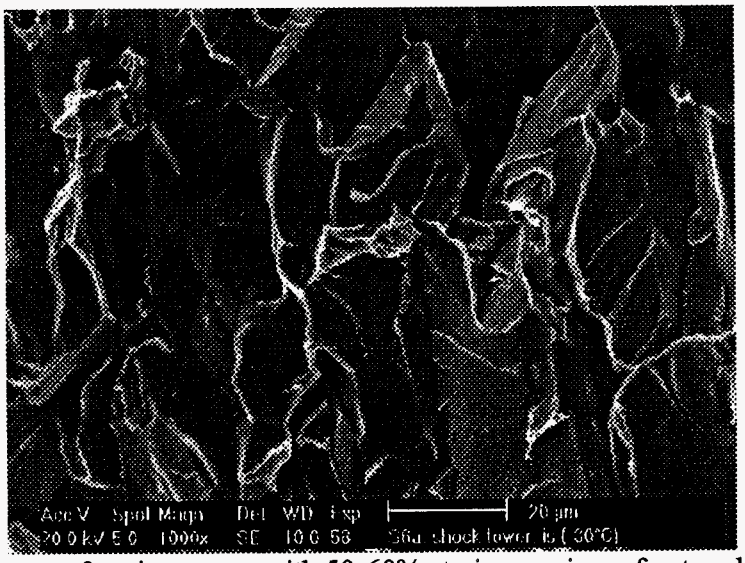

a) Fracture surface in an area with 50-60% strain, specimen fractured at -30°C

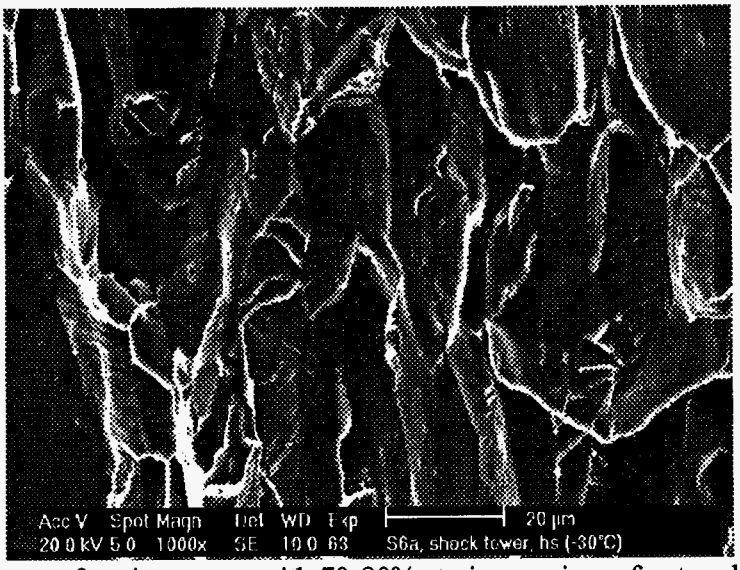

b) Fracture surface in an area with 70-80% strain, specimen fractured at -30°C

Figure 61. Fracture surface of shock tower parts after localized testing of steel S6a

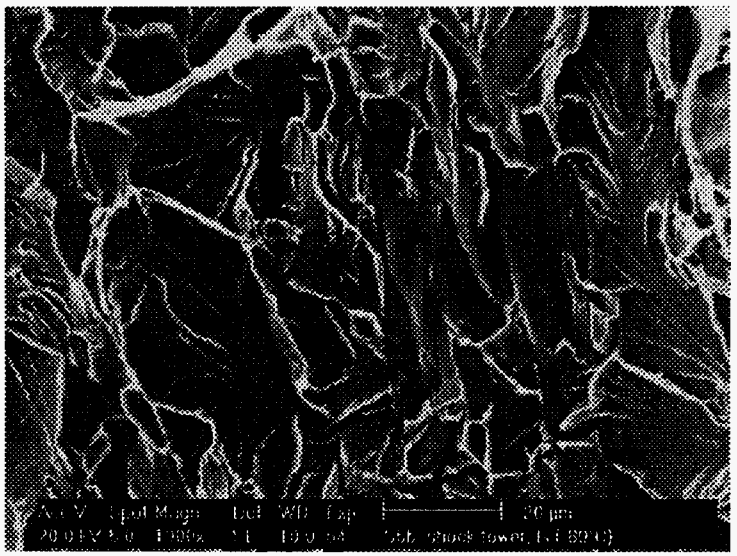

a) Fracture surface in an area with 50-60% strain, specimen fractured at -80°C

b) Fracture surface in an area with 70-80% strain, specimen fractured at -65°C

Figure 62. Fracture surface of shock tower parts after localized testing of steel S5b.